Spring 5-9-2016

Genetic and Epigenetic Mechanisms Underlying Stress-Induced Behavioral Change

Katharine E. McCann
Georgia State University

GENETIC AND EPIGENETIC MECHANISMS UNDERLYING STRESS-INDUCED BEHAVIORAL CHANGE

by

KATHARINE E. MCCANN

Under the Direction of Kim Levy Huhman, PhD

ABSTRACT

Social stress is the most common stressor experienced by humans and exposure to social stress is thought to cause or exacerbate neuropsychiatric illness. Social stress also leads to behavioral and physiological responses in many animal models that closely mirror the symptoms of fear and anxiety in humans. Our laboratory uses Syrian hamsters to study behavioral responses to social stress. Hamsters are highly territorial, but after losing an agonistic encounter, hamsters exhibit a striking behavioral change, abandoning all territorial aggression and instead becoming highly submissive. This behavioral shift is termed conditioned defeat. Epigenetic modifications, such as changes in histone acetylation, are a possible molecular mechanism underlying such behavioral shifts. Histone deacetylase (HDAC) inhibitors have been shown to enhance fear learning and conditioned place preference for drugs of abuse, while suppressing histone acetylation with histone acetyltransferase (HAT) inhibitors impairs long-term memory

formation. The first goal of this study was to test the hypothesis that histone acetylation is a molecular mechanism underlying conditioned defeat. We found that animals given an HDAC inhibitor systemically before social defeat later exhibited increased conditioned defeat. This treatment also suppressed defeat-induced immediate-early gene activity in the infralimbic cortex but not the basolateral amygdala. Next, we demonstrated that administration of an HDAC inhibitor in the infralimbic cortex before defeat enhanced stress-induced behavioral responses while HAT inhibition blocked these behavioral changes. Although both males and females exhibit conditioned defeat, the behavioral expression is more pronounced in males. We next used transcriptomic analysis to investigate potential genetic mechanisms leading to this sexually dimorphic expression and to further delineate the role of acetylation in stress-induced behavioral changes. We sequenced the whole brain transcriptome of male and female hamsters as well as the transcriptome of basolateral amygdala, a nucleus necessary for the acquisition and expression of conditioned defeat, of dominant, subordinate, and control animals. Our analysis revealed that numerous genes relating to histone acetylation, including several HDACs, were differentially expressed in animals of different social status and between sexes. Together, these data support the hypotheses that histone modifications underlie behavioral responses to social stress and that some of these modifications are sexually dimorphic.

INDEX WORDS: Conditioned defeat, Transcriptomics, Histone acetylation, Sex differences, Social stress

GENETIC AND EPIGENETIC MECHANISMS UNDERLYING STRESS-INDUCED BEHAVIORAL CHANGE

by

KATHARINE E. MCCANN

A Dissertation Submitted in Partial Fulfillment of the Requirements for the Degree of

Doctor of Philosophy

in the College of Arts and Sciences

Georgia State University

2016

GENETIC AND EPIGENETIC MECHANISMS UNDERLYING STRESS-INDUCED BEHAVIORAL CHANGE

by

KATHARINE E. MCCANN

Committee Chair: Kim L. Huhman

Committee: H. Elliot Albers

Laura L. Carruth

Kerry J. Ressler

Walter Wilczynski

Electronic Version Approved:

Office of Graduate Studies

College of Arts and Sciences

Georgia State University

May 2016

Dedication

For my husband, my parents, and my brother for never letting me forget why I came back to school and why this research is important.

Acknowledgements

First and foremost I want to thank my advisor, Dr. Kim Huhman. Kim, you have been an amazing mentor, role model, and friend. I could not have asked for a better graduate school experience or a better advisor to help get me here. You have taught me so much about how to be a good scientist and how to keep a balanced life without sacrificing success. I am incredibly grateful that you took that chance on me all those years ago! I also want to thank the members of my committee, Dr. Elliott Albers, Dr. Laura Carruth, Dr. Kerry Ressler, and Dr. Walt Wilczynski. Thank you Elliott for being a second mentor to me all through graduate school. I am excited for the opportunity to continue to work with and learn from you over the next year. To Laura, thank you for teaching me the importance of being a well-rounded scientist. I am a better scientist because of your mentorship. To Walt and Kerry, I would not have made it this far without your support and guidance. I dove in head first to the world of epigenetics and transcriptomics, and I may have drowned had it not been for you both. I also want to thank all of the members of both the Huhman and Albers labs who have supported and helped me throughout this entire process, especially Alisa. Alisa – you know we would all be lost without you. Your help and guidance in the lab is invaluable, but more importantly, I am happy to have found a life-long friend. Furthermore, this work would not have been possible without the support of my friends and family, the GSU DAR staff, the NI administration, and GSU IS&T. Lastly, I would like to thank Ken and Georganne Honeycutt. Knowing that I had people as genuine and supportive as the Honeycutts rooting for me has made reaching the finish line so much easier.

TABLE OF CONTENTS

List of tables

List of figures

1 Introduction

1.1 Animal models of human psychopathology: Using hamsters in a translational model of social stress-induced behavioral change

Animal models are crucial to understanding the mechanisms underlying neuropsychiatric disorders as well as to the development of novel treatments for clinical populations. Stress, especially unexpected, prolonged, or traumatic stress, can lead to the development of neuropsychiatric illness, including anxiety disorders, depression, and posttraumatic stress disorder (PTSD) (Agid et al., 2000; Ehlers et al., 2000; Kelleher et al., 2008). There are many animal models used to study stress responses, and most employ a physical stressor such as foot or tail shock, restraint stress, or forced swimming. Social stress, however, is the most common stressor experienced by humans (Bjorkqvist, 2001), and social stress in humans is thought to cause or exacerbate mental illness (Tamashiro et al., 2005; Borghans and Homberg, 2015). Thus, animal models focused on the behavioral and physiological concomitants of social stress have the potential to help us to understand better how this social experience promotes the development of anxiety- and depressive-like symptoms and allow us to develop treatment strategies to prevent or reverse these changes.

Social defeat models are proposed to have particular relevance to human social stress (Huhman, 2006; Chaouloff, 2013; Hollis and Kabbaj, 2014; Borghans and Homberg, 2015). These models use a variety of species, including rats, mice, hamsters, and non-human primates and, in each model, social stress provokes similar behavioral and physiological changes to those observed in humans with neuropsychiatric disorders, including social avoidance, altered feeding behavior, enhanced startle responsiveness, sleep disruptions, and altered hormone and neurotransmitter function (Sapolsky, 1990;

Blanchard et al., 1995; Virgin and Sapolsky, 1997; Shively, 1998; Berton et al., 2006; Foster et al., 2006; Solomon et al., 2007b; Pulliam et al., 2010; McCann and Huhman, 2012). For example, rats housed in the visible burrow system, a model of chronic social stress, quickly develop a stable social hierarchy. Subordinate animals in this model of chronic stress exhibit elevated levels of corticosterone, depleted levels of testosterone, and decreased body weight when compared with controls (Blanchard et al., 1995). Likewise, baboons living in social groups also develop and maintain lasting social hierarchies, and the subordinate males in these groups also exhibit increased basal cortisol, a blunted cortisol response to stress and decreased testosterone during stress (Sapolsky, 1990; Virgin and Sapolsky, 1997). Subordinate animals in both of these models can be identified through marked changes in behavior. These behavioral and physiological markers of social stress are not unique to mammals. Rainbow trout also develop dominant-subordinate relationships when paired, and the subordinate animals exhibit elevated cortisol and melatonin (Larson et al., 2004).

Hamsters are a particularly useful species for studying social stress because, unlike some other rodents that are used in social defeat models, hamsters do not require complex housing conditions in the laboratory to elicit conspecific aggression or behavioral responses to defeat. In addition, both male and female hamsters will readily attack intruding conspecifics, even in the laboratory (Huhman et al., 2003; Solomon et al., 2007a). Furthermore, agonistic interactions in hamsters are highly ritualized so that they rarely result in physical injury; thus, it is possible to examine the behavioral and physiological effects of social stress in the absence of physical injury or trauma and the concomitant inflammatory response. While hamsters are normally aggressive, after losing one agonistic encounter, typically a 15min inescapable defeat, subordinate

hamsters display a striking change in behavior, abandoning all aggression and instead displaying submission and social avoidance, even if the opponent is a non-threatening stimulus animal (Potegal et al., 1993; Huhman et al., 2003; McCann and Huhman, 2012; McCann et al., 2014). This behavioral change has been termed conditioned defeat, and it persists for up to one month in the majority of hamsters (Huhman et al., 2003). Many models of social stress, as outlined above, require a chronic or repeated stressor to elicit behavioral and physiological changes in subordinate animals. Hamsters, however, exhibit many of the same responses observed after chronic stress in other species, including elevated cortisol and social avoidance, after only one agonistic encounter (Huhman et al., 1991; Huhman et al., 2003; McCann and Huhman, 2012).

Our laboratory has made significant progress in delineating the neural circuitry and many of the neurochemical correlates of this long-term, social stress-induced change in behavior. It is well established that the amygdala is a crucial site of plasticity necessary for processing and responding to emotional and fearful stimuli (Davis, 1992; Fanselow and Gale, 2003; McGaugh, 2004). We have also demonstrated that the basolateral amygdala (BLA) is a critical component of the neural circuit mediating conditioned defeat. Synaptic transmission in this region is necessary for both acquisition and expression of defeat-induced behavioral changes (Jasnow and Huhman, 2001; Markham et al., 2010). In addition, protein synthesis in the BLA is necessary for conditioned defeat (Markham and Huhman, 2008), and acquisition of conditioned defeat can be enhanced following viral vector-mediated overexpression of cyclic AMP response element binding protein (CREB) in the BLA (Jasnow et al., 2005). Recently, we have also established the importance of the medial prefrontal cortex (PFC) in the conditioned defeat circuitry (Markham et al., 2012). Administration of a GABA-A

agonist to temporarily inactivate this nucleus enhances the acquisition of conditioned defeat, while a GABA-A antagonist blocks conditioned defeat.

We are now beginning to explore molecular and genetic markers of conditioned defeat. The persistence of the behavioral changes observed after a single social defeat suggests a potential role of epigenetic mechanisms. A better understanding of the molecular mechanisms within the nuclei mediating conditioned defeat (e.g., BLA, PFC) may lead us to a clearer understanding of how social stress impacts future social behavior. **The overarching goal of this project is to test the hypothesis that epigenetic changes within the neural circuit that mediates conditioned defeat contribute to the observed behavioral changes after acute social stress.**

1.2 Epigenetic mechanisms underlying conditioned defeat: The potential role of histone deacetylases

Many processes play a role in the development and maintenance of the long-term memories that lead to changes in behavior. Transcription is necessary for the formation of these memories (Agranoff et al., 1967), and transcription in the amygdala encodes the memories of a fearful or stressful event (for review, see (White and Wood, 2014)). The acetylation of histones, proteins around which DNA is coiled, is one regulator of transcription, wherein adding acetyl groups to histone tails increases the likelihood of transcription. Histone deacetylases (HDACs), a class of enzymes that remove acetyl groups from histones, cause DNA to wrap more tightly around histones, which leads to a repression in the transcription of targeted genes (for review, see (Whittle and Singewald, 2014)). HDACs can interfere with memory processing (Kilgore et al., 2010;

Reolon et al., 2011) and are densely located in the amygdala (Broide et al., 2007). Recent advances using animal models of neuropsychiatric disorders suggest that inhibiting Class I HDACs can enhance long-term memory at each stage of memory processing (e.g., acquisition, consolidation, extinction). Specifically, acquisition of conditioned fear is enhanced following the administration of a Class I HDAC inhibitor, as is reconsolidation of that memory (Bredy and Barad, 2008). Many studies have focused on the extinction of a fear memory for the translational value that extinction may have in cognitive-behavioral and exposure therapies, and administering an HDAC inhibitor during the extinction process enhances extinction of that memory (Lattal et al., 2007; Itzhak et al., 2012; Stafford et al., 2012). Likewise, in a predator model of PTSD, chronic administration of an HDAC inhibitor reduces PTSD-like symptoms during the recovery period (Wilson et al., 2014). HDAC inhibition also leads to more persistent long-term memory in an object discrimination test (White and Wood, 2014), and some studies have shown that HDAC inhibition can alter sensitization and context memory for drugs of abuse (e.g., cocaine, morphine) (Jing et al., 2011; Itzhak et al., 2013; Wang et al., 2015). These data demonstrate that HDACs are critical components regulating a wide range of tasks related to learning and memory and, by further defining their role in the behavioral responses to acute social stress, we can pinpoint specific targets underlying neuropsychiatric disorders associated with aberrant fear learning (e.g., PTSD).

On the other hand, histone acetyltransferases (HATs) are enzymes that add acetyl groups to histones, loosening the DNA around the histone complex and making transcription more likely. Considerably less data exist regarding the role of HATs in regulating behavior, however, recent work has shown that interfering with HATs during stressful events also results in marked changes in behavior. In contrast to the behavioral

changes observed after HDAC inhibition, inhibition of HATs during fear conditioning blocks the acquisition and consolidation of that fear memory (Maddox et al., 2013b; Maddox et al., 2013a; Monsey et al., 2015). HAT activity also increases in response to ethanol exposure (Pascual et al., 2012) and HAT inhibition reverses cocaine-induced conditioned place preference (Hui et al., 2010). The data available on HATs further solidifies the importance of histone acetylation in regulating learning and memory. A stronger understanding of these mechanisms, and the additional genes they regulate, as they relate to social stress and the subsequent behavioral changes is critical to developing novel interventions for the clinical population.

Most of the current studies that have investigated the behavioral effects of altering histone acetylation in response to an aversive stimulus have used non-social stressors, and those using models of social stress have focused on repeated or chronic exposure to the stressor. While the study of chronic social stress is important, not all social stressors that humans experience are chronic in nature. Acute social stress or trauma can also lead to sudden and discernable changes in behavior, sometimes leading to psychopathology (e.g., PTSD). Furthermore, using an acute model of social stress we can much more precisely determine when acquisition and consolidation are occurring, therefore we can test hypotheses about these processes in a way that is not possible in chronic models. Thus, it is critical to investigate the underlying mechanisms leading to changes in behavior and physiology after exposure to an acute stressor rather than solely focusing on chronic stress.

Furthermore, we are constantly discovering new mechanisms of action for drugs that are already in use in the clinical population for various neuropsychiatric disorders. For example, the drug valproic acid has been used in the clinical population for decades for

epilepsy and bipolar disorder for its pharmacodynamic effect on GABA neurotransmission (Nau and Loscher, 1982; Tunnicliff, 1999). We now know that inhibition of Class I HDACs (HDACs 1, 2, 3, and 8) is another primary mechanism of action for this drug (Gottlicher et al., 2001; Phiel et al., 2001; Tremolizzo et al., 2002). Further investigation into how this drug, and others, impacts long-term behavioral and physiological reactions to social stress may lead us down new paths for more targeted treatments and interventions that could become immediately available for clinical populations. **Thus, the first aim of this project was to pharmacologically test the role of HDACs and HATs in the long-term behavioral changes associated with acute social defeat in Syrian hamsters.**

1.3 Genetic resources for non-traditional animal models using transcriptomics

In order to study the underlying molecular, genetic, and epigenetic mechanisms that lead to changes in behavior after stress exposure, many laboratories use mouse models because of the extensive resources available for genetic work in mice (i.e., transgenic lines, fully annotated genome available for designing species-specific primers and probes for specific genes). Mice, however, do not provide a one-size-fits-all model for behavior, and it has, in fact, been proposed that the social behavior of laboratory mice, particularly in many inbred, genetic models, may be somewhat impoverished (Crawley et al., 1997; Moy et al., 2007). For example, many strains of mice exhibit virtually no aggressive behavior while other strains are so aggressive that it puts the welfare of the animals at risk when paired (Kessler et al., 1977; Crawley et al., 1997; Van Loo et al., 2003). Most mouse models of social stress employ relatively severe chronic or repeated defeat procedures to elicit changes in behavior, and the aggressor used to

defeat the subjects is a mouse of a different strain (often a CD-1 mouse, which is one of the few strains that are highly aggressive). Furthermore, outside of maternal defense of pups, female mice do not spontaneously exhibit conspecific aggression. Thus, most research exploring the effects of social stress has solely relied on information gained from testing male subjects. As described above, hamsters are uniquely suited to study the effects of social stress in both males and females without any physical injury and the associated inflammatory response. Unfortunately, however, the tools available for genetic and molecular research in hamsters are limited. There are not currently transgenic lines of hamsters available, and the hamster genome is not fully sequenced and annotated, making it difficult to develop primers and probes to target specific genes.

Transcriptomics is a rapidly growing field of research in which one can sequence the complete set of RNA transcripts present in specific tissue samples. This technique has recently become more widely available and enables investigators to characterize active genes in traditional and non-traditional model organisms. These sequences can then be used to ask more specific molecular and genetic questions using species-specific sequences. **Thus, the second aim of this project was to sequence the brain transcriptome of Syrian hamsters and to create a usable database for all researchers using hamsters. Finally, we wanted to use that database to answer specific questions about conditioned defeat and the underlying genetic and epigenetic markers associated with social stress-induced behavioral change.**

1.4 Specific aims overview

1.4.1 Specific Aim 1: Does inhibition of HDACs or HATs increase or decrease, respectively, social avoidance and submissive behavior after acute social defeat?

We first tested the impact of inhibiting HDACs and HATs on the acquisition of conditioned defeat. Using both systemic injections and site-specific microinjections into the BLA and PFC, we tested the hypothesis that histone acetylation enhances the acquisition of conditioned defeat while deacetylation reduces social-stress induced submission and avoidance (Chapter 2).

1.4.2 Specific Aim 2: Does systemic HDAC inhibition during social defeat increase subsequent neuronal activity (as measured by Fos-immunoreactivity) in specific nodes of the neural circuit that mediates conditioned defeat?

We next measured the effect of systemic HDAC inhibition on immediate-early gene activity in several nuclei of the neural circuit that mediates conditioned defeat. *C-fos*, an immediate-early gene in the Fos family, is a marker for neural activity and a transcription factor modulated by the acetylation and deacetylation of histone proteins (Pascual et al., 2012; Hendrickx et al., 2014). The purpose of this aim was to discover where within the conditioned defeat circuitry HDAC inhibition might be acting to promote behavioral responses to social stress. We tested the hypothesis that inhibition of HDACs increases neural activity within specific nodes of the conditioned defeat neural circuit, specifically the BLA and PFC, thereby enhancing the acquisition of conditioned defeat (Chapter 2).

1.4.3 Specific Aim 3: Are Class I HDACs highly expressed in the hamster amygdala and is their expression altered by social defeat?

In order to continue to use hamsters as a model of social stress, we needed to improve the resources available to answer questions about specific genes and epigenetic modifications. To this end, we sequenced the entire brain transcriptome of male and female Syrian hamsters (Chapter 3). We also sequenced the transcriptome of amygdalae taken from dominant, subordinate, and home-cage control male and female hamsters to compare transcript expression after a single agonistic encounter (Chapter 4). The primary goal of this aim was to determine if Class I HDACs, or other genes involved in the epigenetic regulation of histones, are highly expressed in the amygdala of control animals and whether their expression levels are altered after exposure to social stress.

2 Pharmacological manipulation of histone acetylation modulates behavioral responses to acute social stress

2.1 Introduction

DNA transcription is necessary for development and maintenance of experience-dependent, long-term memories that elicit subsequent changes in behavior. The removal or addition of acetyl groups to histones by histone deacetylases (HDACs) or histone acetyltransferases (HATs) alters the likelihood of transcription. Inhibition of Class I HDACs enhances long-term memory at each stage of memory processing (e.g., acquisition, consolidation, reconsolidation, extinction) (Kilgore et al., 2010; Reolon et al., 2011), while HAT inhibition impairs memory (Maddox et al., 2013b; Monsey et al., 2015). For example, the HDAC inhibitor valproic acid (VPA) enhances the acquisition of

cued fear (Bredy and Barad, 2008). Consistent with the idea that HDAC inhibition promotes a broad range of learning processes, administration of an HDAC inhibitor during extinction training enhances extinction of a variety of cued and contextual fear memories (Lattal et al., 2007; Bredy and Barad, 2008; Itzhak et al., 2012; Stafford et al., 2012). Likewise, in a predator model of posttraumatic stress disorder (PTSD), HDAC inhibition reduces PTSD-like symptoms during recovery (Wilson et al., 2014). Finally, HDAC inhibitors alter sensitization to, as well as memory for contextual cues associated with, drugs of abuse (Jing et al., 2011; Itzhak et al., 2013; Wang et al., 2015). Consistent with their opposite effect on histone acetylation, HAT inhibitors interfere with the acquisition and consolidation of new or reactivated fear memories (Maddox et al., 2013b; Monsey et al., 2015).

HDAC inhibitors, including VPA, are already being used clinically to treat a variety of illnesses such as epilepsy and bipolar disorder, but their effects on learning suggest that they may also be useful in a range of neuropsychiatric illnesses, such as PTSD or specific phobia, wherein fear learning is potentially aberrant (Bredy and Barad, 2008; Parsons and Ressler, 2013). While the initial data are encouraging, most studies have used physical stressors (e.g., foot/tail shock) and only a few studies have examined the role of histone acetylation in more ethologically relevant models of stress-induced behavioral change (Hollis et al., 2011; Espallergues et al., 2012; Covington et al., 2015). Social defeat models have strong face and construct validity for human anxiety and depressive behavior (Huhman, 2006; Toth and Neumann, 2013; Hollis and Kabbaj, 2014), but the majority of these models use relatively severe, repeated exposure to social defeat in male mice. Our laboratory studies acute social defeat stress in Syrian hamsters. Hamsters offer a unique social stress model because both males and females are highly

territorial, and home cage animals of both sexes will readily attack an intruding conspecific. Additionally, after losing one agonistic encounter, hamsters abandon all territorial aggression and, instead, become highly submissive and socially avoidant (Huhman, 2006; McCann and Huhman, 2012; McCann et al., 2014), a behavioral change termed conditioned defeat. The conditioned defeat model is unique among social defeat models for several reasons. First, unlike models using rats or mice, conditioned defeat in hamsters allows examination of defeat-induced behavior in both sexes. In addition, no complex housing arrangements are necessary, and finally, striking behavioral changes are observed after even a *single*, relatively mild defeat that results in *no physical injury*. Thus, our model provides an excellent opportunity to study the behavioral and physiological responses specific to acute social stress.

We have made significant progress in delineating the neural circuitry mediating conditioned defeat, in particular the roles of the prefrontal cortex (PFC) and basolateral amygdala (BLA) (Jasnow and Huhman, 2001; Jasnow et al., 2005; Markham et al., 2010; Markham et al., 2012), however we have only begun to characterize molecular mechanisms contributing to its development. The purpose of the present study was to test for the first time whether epigenetic mechanisms mediate, at least in part, behavioral responses to acute social stress.

2.2 Materials and Methods

2.2.1 Animals

Adult male and female Syrian hamsters (*Mesocricetus auratus*) were obtained from Charles River Laboratories (Wilmington, MA) or bred in-house from animals obtained from Charles River. Subjects (approximately 12 weeks, 120-130g) were

individually housed in a polycarbonate cage (23 x 43 x 20 cm) and were handled daily for at least one week before any behavioral manipulations began. The colony room was temperature-controlled, and animals were kept on a 14:10 light/dark cycle. All cages contained corncob bedding and cotton nesting material, and food and water were available *ad libitum*. Same sex resident aggressors (RAs) were used for social defeat training and for social avoidance testing. RAs are larger, individually-housed hamsters that readily attack an intruder placed in their home cage. Female subjects were paired with ovariectomized female RAs. Behavioral manipulations were done in a dedicated testing suite within the vivarium during the first 3 hours of the dark phase of the daily light/dark cycle. All procedures and protocols were approved by the Georgia State University Institutional Animal Care and Use Committee and are in accordance with the standards outlined in the National Institutes of Health Guide for Care and Use of Laboratory Animals.

2.2.2 Social defeat training

For social defeat training, subjects were placed into the home cage of a same-sex RA as described previously (McCann and Huhman, 2012; McCann et al., 2014). Estrous cycles of female subjects were monitored via vaginal swabs for at least two cycles before the experiment, and females were defeated on Diestrus 1 (D1) and tested on Diestrus 2 (D2) because we have previously shown this results in the most pronounced avoidance after social defeat (unpublished observations). A clear cage top was placed on top of the RA's cage to prevent either animal from escaping the cage during a 5min (suboptimal) or 15min defeat session. The holding box used for social avoidance testing, described below, was placed in the RA's cage during training. At the end of the defeat, subjects

were returned to their home cages. Animals were monitored during defeat to ensure that no injury occurred to either animal. No-defeat controls were placed in a novel cage with soiled RA bedding and a holding box for the same amount of time as the defeat group and were subsequently returned to their home cage until social avoidance testing. Behavior emitted by RAs and by subjects during defeat training was recorded and scored by trained observers that were blind to experimental condition to ensure that pre-training drug infusions did not alter either the amount of aggression displayed by the RAs toward the subjects or the amount of submission shown by the subjects during defeat training.

2.2.3 Social avoidance testing

Social avoidance testing was conducted as described previously (McCann and Huhman, 2012; McCann et al., 2014) and was recorded for later analysis. In brief, 24hr after social defeat training, subjects were placed in a clean, novel testing arena (23 x 40 x 20cm) with an unfamiliar RA placed inside a smaller holding box on one end of the arena. The holding box for the unfamiliar RA was constructed of perforated plastic that allowed the subject to see, hear, and smell the unfamiliar stimulus animal but not to come into direct contact with it. For scoring purposes, the testing arena was divided into eight sections (Figure 2.1). Time spent in the far half of the testing arena (operationally defined as avoidance) as well as total number of line crosses (a measure of locomotor behavior) were scored. A line cross was counted when the subject's head and both front paws crossed over a line. Frequencies of specific submissive behaviors (i.e., flees, risk assessments), as defined previously (McCann and Huhman, 2012), were also counted.

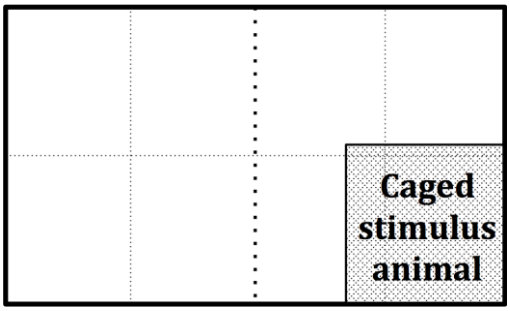

Figure 2.1 Schematic of testing arena
Dotted lines represent line markers for scoring subjects' movements during the 5min testing period.

2.2.4 Cannulation and microinjections

For site-specific injections, subjects were implanted with bilateral cannulae targeting the BLA or with a unilateral cannula primarily targeting the infralimbic (IL) region of the PFC. Coordinates for guide cannulae used to target the BLA and PFC were measured from bregma and were as follows for BLA: +0.0AP, ±4.0ML, -3.0DV from dura perpendicular, and for PFC: +3.0AP, ±1.6ML, -3.2DV from dura at a 20° angle toward the midline to avoid the central sinus. Anesthesia was induced with 5% isoflurane, and animals were maintained at 3-5% isoflurane in a stereotaxic apparatus for the entire surgical procedure. Animals were handled for 1 week after surgery before any experimental manipulations. The compounds and concentrations listed below were injected directly into the site of interest using an infusion pump (Harvard Apparatus) and a Hamilton syringe connected to an injection needle by 50-gauge polyethylene tubing. In order to minimize damage to the area being injected, a shorter guide cannula (26-gauge) was used, and the final depth was reached with a smaller (33-gauge) injection needle that projected from the guide cannula (BLA: 3.3mm below the guide; PFC: 1.2mm below the guide). The injection needle was left in the cannula guide for 1min post-injection to ensure diffusion of the pharmacological agent from the needle tip. Successful injections were inferred if solution flowed easily from the needle before

and after injection and a small air bubble placed between the drug and the saline solution in the tubing moved during microinjection.

2.2.5 Pharmacological agents

VPA (Sigma-Aldrich, St. Louis, MO) was dissolved in physiological saline. Intraperitoneal (IP; 100mg/kg, 200mg/kg, 300mg/kg) as well as site-specific (100µg/0.2µl) injections of VPA were given (Nau and Loscher, 1982; Bredy and Barad, 2008; Kim et al., 2008; Kilgore et al., 2010; Heinrichs et al., 2013). IP injections were administered 2hr before defeat training because peak brain histone acetylation occurs 2hr after peripheral administration (Tremolizzo et al., 2002), and behavioral changes in this time window have previously been observed (Bredy et al., 2007; Bredy and Barad, 2008; Arent et al., 2011; Ploense et al., 2013). To test the temporal specificity of peripherally administered VPA in our model, we also completed two control experiments in which we administered VPA 1hr before defeat training or 2hr before avoidance testing. Sodium butyrate (NAB; Alfa Aesar, Ward Hill, MA) was given IP (600mg/kg, 1200mg/kg in physiological saline) to a small subset of animals, but because this drug induced a temporary, but extreme, ataxia, its systemic use was discontinued, and it was only tested site-specifically (1.32µg/0.2µl) (Lattal et al., 2007; Kilgore et al., 2010; Mahan et al., 2012; Heinrichs et al., 2013; Blank et al., 2014; Simon-O'Brien et al., 2015). Finally, Curcumin (Cur, Epigentek, Farmingdale, NY, 1.1µg/0.2µl) was dissolved in 55% DMSO. This drug appears to be one of the few, if not only, HAT inhibitors that is currently commercially available that does not have to be dissolved in 100% DMSO. All site-specific injections were given 30min before social defeat (Xing et

al., 2011; Simon-O'Brien et al., 2015) at a total volume of 0.2µl to limit the spread of the injection.

2.2.6 Histology

After social avoidance testing, cannulated animals were given an overdose of sodium pentobarbital, and 0.2µl of ink, to match the volume of drug administration, was injected through the guide cannulae for the purpose of site verification. Brains were sectioned on a cryostat and stained with neutral red for microscopic analysis of cannula placement. Placements more than 300µm from the target nucleus were used as anatomical, or "miss", controls to assess site specificity of the drug effects.

2.2.7 Immunohistochemistry for immediate-early gene c-fos

Animals were given IP injections of either saline or VPA (200mg/kg) 2hr before a suboptimal defeat and were perfused 1hr after the defeat. Postfixed brains were sectioned on a cryostat into cryoprotectant and were stored at -20°C until processing. On Day 1, sections were washed 3x5min with potassium phosphate buffered saline (KPBS) and incubated in 0.3% hydrogen peroxide in KPBS for 30min. Sections were washed again 3x5min in KPBS and incubated with primary c-fos antibody (rabbit polyclonal IgG, 1:5000, Santa Cruz Biotechnology, Dallas, TX) in KPBS with 1% TritonX-100 and 1% normal goat serum overnight at room temperature. On Day 2, sections were washed 3x5min with KPBS and incubated with 0.4% secondary (biotin-SP-conjugated AffiniPure goat anti-rabbit IgG, Jackson ImmunoResearch, West Grove, PA) in KPBS-T for 90min at room temperature. Sections were again washed 3x5min in KPBS and then incubated in pre-prepared avidin/biotin blocking solution (Vector Laboratories, Burlingame, CA) at room temperature for 1hr. After incubation, sections

were washed 3x5min with KPBS and then incubated in 3,3-diaminobenzidine (Vector Laboratories, Burlingame, CA) for 2-5min. Sections were rinsed 2x5min in KPBS, mounted using 0.15% gelatin in dH2O and allowed to dry overnight. Sections were then dehydrated for 2min each in EtOH 50%, 70%, 95%, and 10min in 100% EtOH, followed by 30min in Citrosolv and then coverslipped with DPX. For analysis, a template was created for each region of interest and immunoreactive-positive cells within this area were counted using NIH ImageJ software (Figure 2.5). Bilateral counts from two or three sections per animal were averaged for each brain area.

2.2.8 Statistical analysis

Statistics for group comparisons were completed using SPSS for Windows (PASW Statistics 22.0). Student's t-tests or ANOVA with LSD post-hoc analysis were used for all analyses. All significant results reported here had a p-value of less than 0.05. Following statistical analysis, all avoidance data were graphed as percent of control for each experiment because baseline avoidance among the experiments was somewhat variable. This variability among experiments is to be expected, particularly given that some experiments involved a 5min and others a 15min defeat.

2.3 Results

2.3.1 Systemic administration of an HDAC inhibitor before social stress enhances the acquisition of conditioned defeat

VPA or saline was administered IP 2hr before defeat training, and we subsequently measured social avoidance and submission in response to a caged stimulus animal 24hr later. Following a 15min defeat, there was no difference in social avoidance during testing among animals given VPA (regardless of dose) and those given

saline (Figure 2.2a); however, animals receiving 200mg/kg of VPA displayed a significant increase in the number of risk assessments (Figure 2.2b). VPA did not alter avoidance ($p=0.517$) or number of risk assessments ($p=0.264$) in no-defeat controls, suggesting that the increase in risk assessments observed in defeated animals given VPA was not a non-specific effect of the drug on agonistic or anxiety-like behavior. Animals given VPA 1hr before social defeat training also did not differ in social avoidance (Supplemental Figure 1) or risk assessment during testing compared with animals given saline.

In the first experiment, all defeated animals, regardless of group, exhibited social avoidance when compared with no-defeat controls. It is possible, therefore, that there was a ceiling effect on avoidance following a 15min defeat. To test this possibility, animals were given 200mg/kg VPA (the dosage shown to increase risk assessment in the first experiment) or saline IP 2hr before a suboptimal, 5min defeat. Animals given VPA before a suboptimal defeat exhibited both increased social avoidance (Figure 2.2c) and increased risk assessments (Figure 2.2d) during testing compared with animals given saline. Again, there was no effect of VPA on behavior of no-defeat controls during testing ($p=0.482$).

To further determine if VPA-enhanced conditioned defeat was specific to the acquisition of the memory of defeat, we also tested defeat-induced social avoidance in animals given VPA 2hr before social avoidance testing to examine whether VPA had an effect on the expression of conditioned defeat. There was no difference in avoidance displayed by animals given VPA or saline (Supplemental Figure 2).

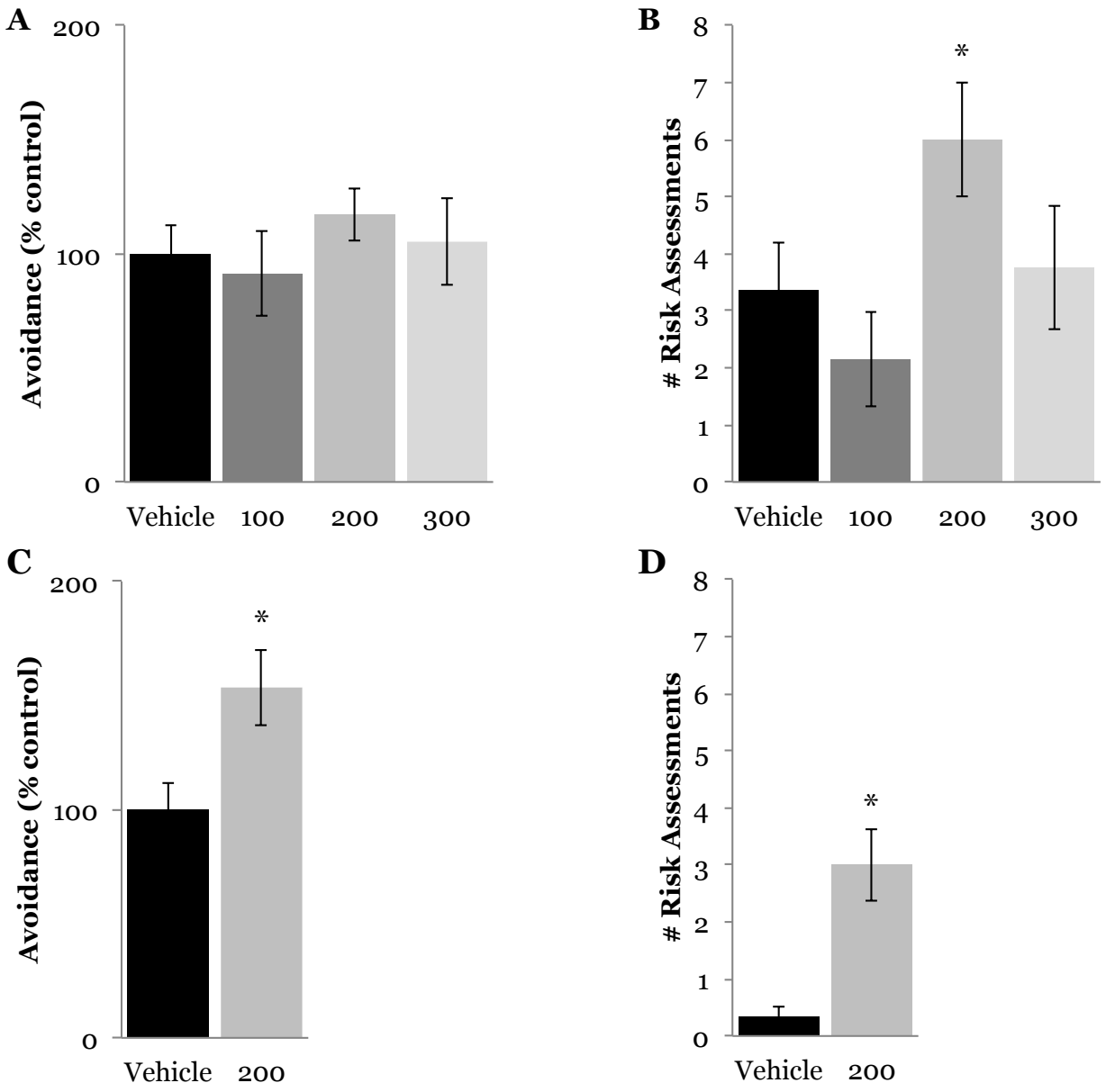

Figure 2.2 Systemic administration of VPA enhances the acquisition of conditioned defeat
Systemic VPA did not increase (A) social avoidance when given before a 15min defeat regardless of drug dose (0mg/kg (n=11), 100mg/kg (n=7), 200mg/kg (n=11), 300mg/kg (n=8); $F(3,33)=0.527$, $p=0.667$); however, animals given 200mg/kg VPA exhibited an increase during testing in the number of (B) risk assessments ($F(3,33)=2.883$, $p=0.05$; post-hoc $p=0.041$ compared with saline). When given before suboptimal (5min) defeat training, systemic VPA (200mg/kg (n=10), saline (n=9)) increased both (C) social avoidance ($t(17)=-2.569$, $p=0.02$) and (D) number of risk assessments ($t(17)=-3.882$, $p=0.001$) observed during testing 24hr later. *$p<0.05$ compared with vehicle

2.3.2 Systemic administration of VPA also enhances acquisition of conditioned defeat in female hamsters

Subjects in the above experiments were male hamsters, and the purpose of the next experiment was to test if systemic VPA administration also enhances the acquisition of conditioned defeat in females. Like males, females given VPA (200mg/kg) 2hr before a suboptimal defeat displayed increased social avoidance (Figure 2.3a) and risk assessments (Figure 2.3b) compared with females given saline. VPA also significantly decreased flank marking exhibited by defeated females (Figure 2.3c). One animal receiving vehicle was removed from analysis because its avoidance score during testing was an outlier (z-score = 2.24). Again, there was no effect on behavior of no-defeat controls during testing ($p=0.883$), indicating that the behavioral effects of systemic HDAC inhibition were specific to the expression of agonistic behavior in defeated females.

2.3.3 Site-specific HDAC inhibition in the IL, but not in the BLA, alters behavioral responses to social defeat

To test if HDAC inhibition in the BLA enhances the acquisition of conditioned defeat, we next administered an HDAC inhibitor (either VPA or NAB) directly into the BLA. Surprisingly, animals given drug before a suboptimal defeat exhibited the same amount of avoidance (Figure 2.4a) as did animals given saline, suggesting the role of the BLA in the acquisition of conditioned defeat may be independent of HDAC activity. In contrast, we found that administration of an HDAC inhibitor in the PFC before defeat training enhanced the behavioral response to social defeat. VPA given in the IL appeared to have a more robust effect on social avoidance (220.2s ± 22.28s, n=5) than

did VPA given in the prelimbic (PL) (159s ± 30.57s, n=3), but because this was not statistically significant (p=0.151), these groups were collapsed for analysis. There was a main effect of HDAC inhibition in the PFC on seconds of social avoidance exhibited during testing (Figure 2.4b). Animals given VPA displayed significantly more avoidance than did animals given saline (p=0.006). Animals given NAB exhibited a trend towards increased avoidance over those given saline (p=0.063) and did not differ from those given VPA (p=0.218).

There was no effect of central HDAC inhibition on avoidance of no-defeat controls (BLA, p=0.341; PFC, p=0.768). Furthermore, HDAC inhibition in the anatomical ("miss") controls (n=3) for PFC, located in the cingulate cortex more than 300μm from the IL, did not cause significant increases in social avoidance compared with controls (t(5)=-0.810, p=0.455), supporting anatomical specificity of the drug effect.

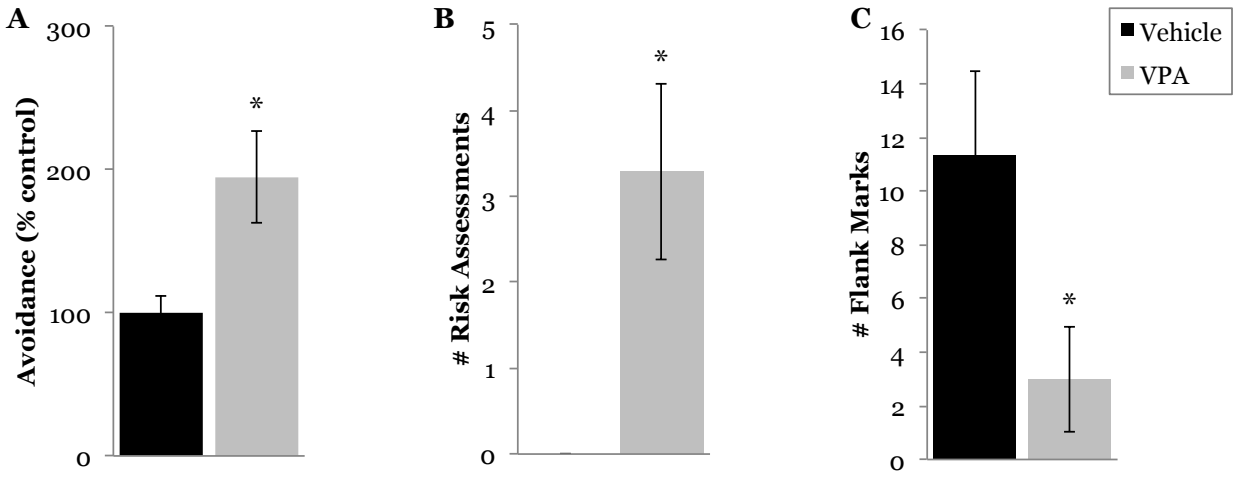

Figure 2.3 Systemic administration of VPA enhances acquisition of conditioned defeat in females
VPA (200mg/kg (n=7)) increased defeat-induced (A) social avoidance (t(11)=-2.609, p=0.02) and (B) risk assessments (t(11)=-2.972, p=0.01) and decreased (C) flank marking (t(11)=2.328, p=0.04) in females compared with females given saline (n=6). *p<0.05

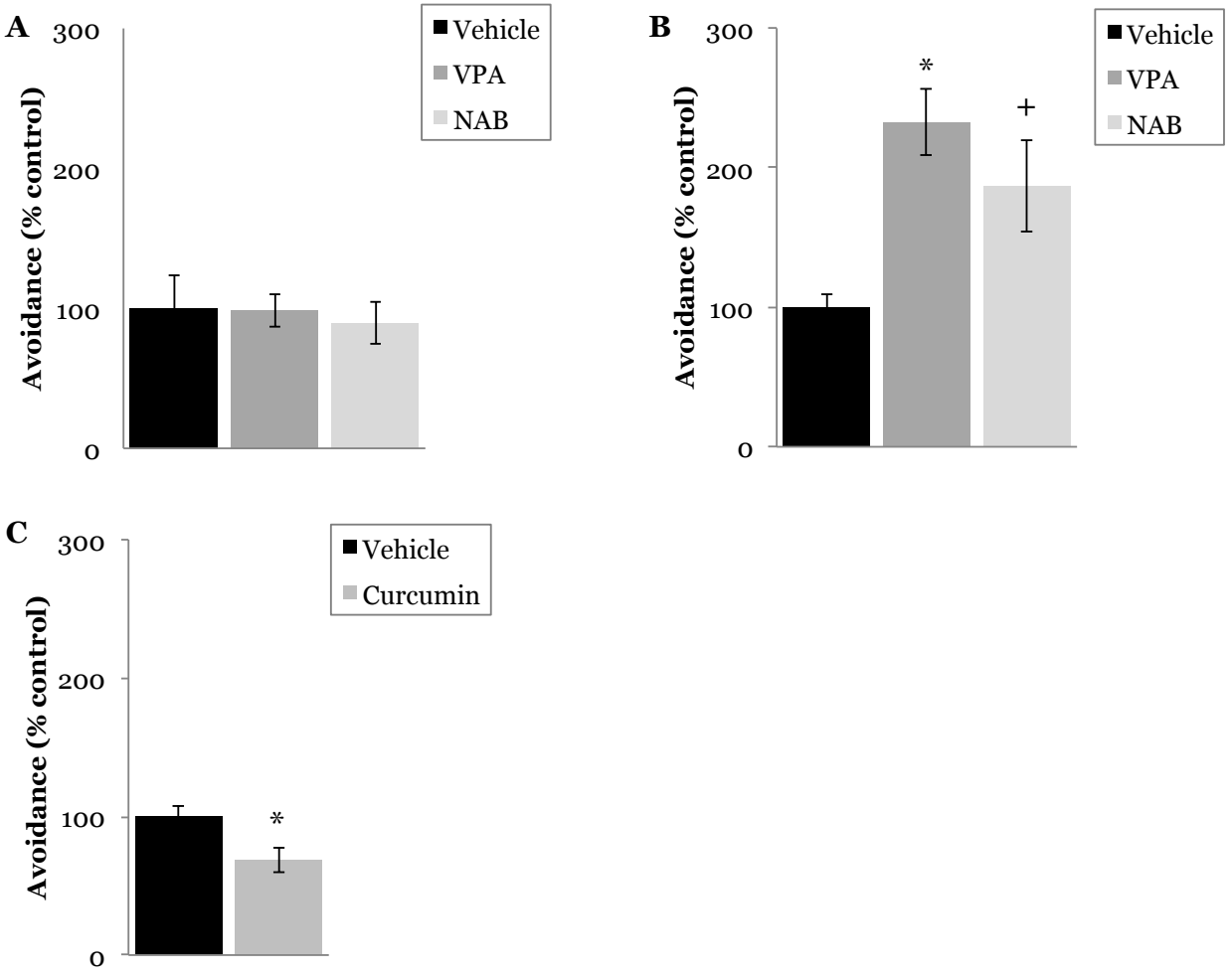

Figure 2.4 HDAC and HAT inhibition in the PFC, but not the BLA, modulate behavioral responses to social defeat
HDAC inhibition in the (A) BLA (VPA (n=11), NAB (n=6), saline (n=7)) before social defeat training did not alter social avoidance ($F(2,21)=0.095$, $p=0.91$) during testing 24hr later. HDAC inhibition in the (B) PFC (VPA (n=8), NAB (n=7), saline (n=4)) during social defeat training significantly increased social avoidance during testing ($F(2,16)=4.897$, $p=0.022$), while (C) HAT inhibition (Cur (n=8), vehicle (n=4)), specifically in the IL, decreased social avoidance ($t(10)=2.328$, $p=0.042$). *$p<0.05$, +$p=0.06$ compared with vehicle

2.3.4 HAT inhibition in the IL blocks the acquisition of conditioned defeat

To test whether histone acetylation in the IL is necessary for behavioral responses to social defeat, we administered the HAT inhibitor Cur (Balasubramanyam et al., 2004; Kang et al., 2005) to determine if this treatment would decrease the acquisition of conditioned defeat (i.e., have the opposite effect of HDAC inhibition). Cur

administration resulted in decreased avoidance when compared with vehicle (Figure 2.4c). HAT inhibition in "miss" controls (n=6) did not cause a significant decrease in avoidance when compared with animals receiving vehicle ($t(8)=1.795$, $p=0.11$).

2.3.5 Systemic administration of VPA decreases suboptimal defeat-induced immediate-early gene activation in the IL

Lastly, we used immunohistochemistry for c-fos to suggest where systemically administered VPA might be acting within the neural circuit mediating conditioned defeat to enhance behavioral responses to suboptimal defeat. Fos-immunoreactive cells were counted in several nuclei of the amygdala (basolateral, central, medial) and PFC (prelimbic, infralimbic) (Figure 2.5). Not surprisingly, given our lack of a behavioral effect after HDAC inhibition in the BLA, no differences from control were observed in the number of fos-positive cells in amygdala following HDAC inhibition (Figure 2.6). Consistent with our behavioral data after intra-PFC injections, however, there was a significant decrease in the number of Fos-positive cells in the PFC of defeated animals that received systemic VPA (Figure 2.6). There was a main effect of HDAC inhibition in the IL and a trend for suboptimal defeat, alone, to increase Fos activation. No main effects were observed in the PL.

2.3.6 Overall behavioral effects of HDAC and HAT inhibition

Pharmacological manipulation of histone acetylation did not affect the amount of aggression shown by RAs during training nor the amount of submission shown by the subjects (Table 2.1) in any experiment described above. With the exception of animals given the highest dose of VPA in Experiment 1, drug manipulations did not affect locomotor activity during testing, as measured by number of line crosses (Table 2.2).

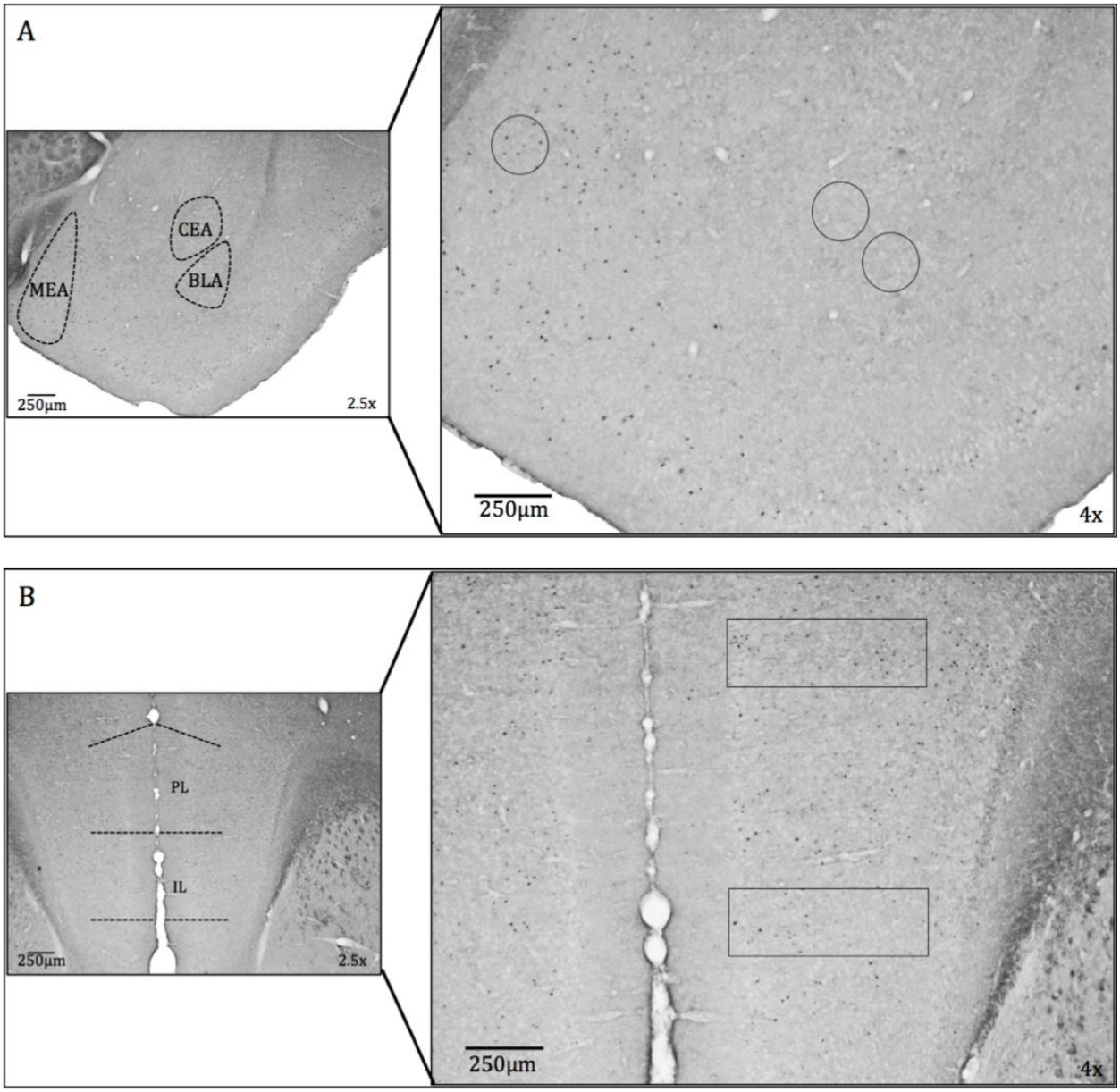

Figure 2.5 Representative sections where fos-positive cells were counted
Cells were counted in sub-regions of the (A) amygdala (BLA: basolateral, CEA: central, MEA: medial) and (B) PFC (PL: prelimbic, IL: infralimbic) (n=6 per group)

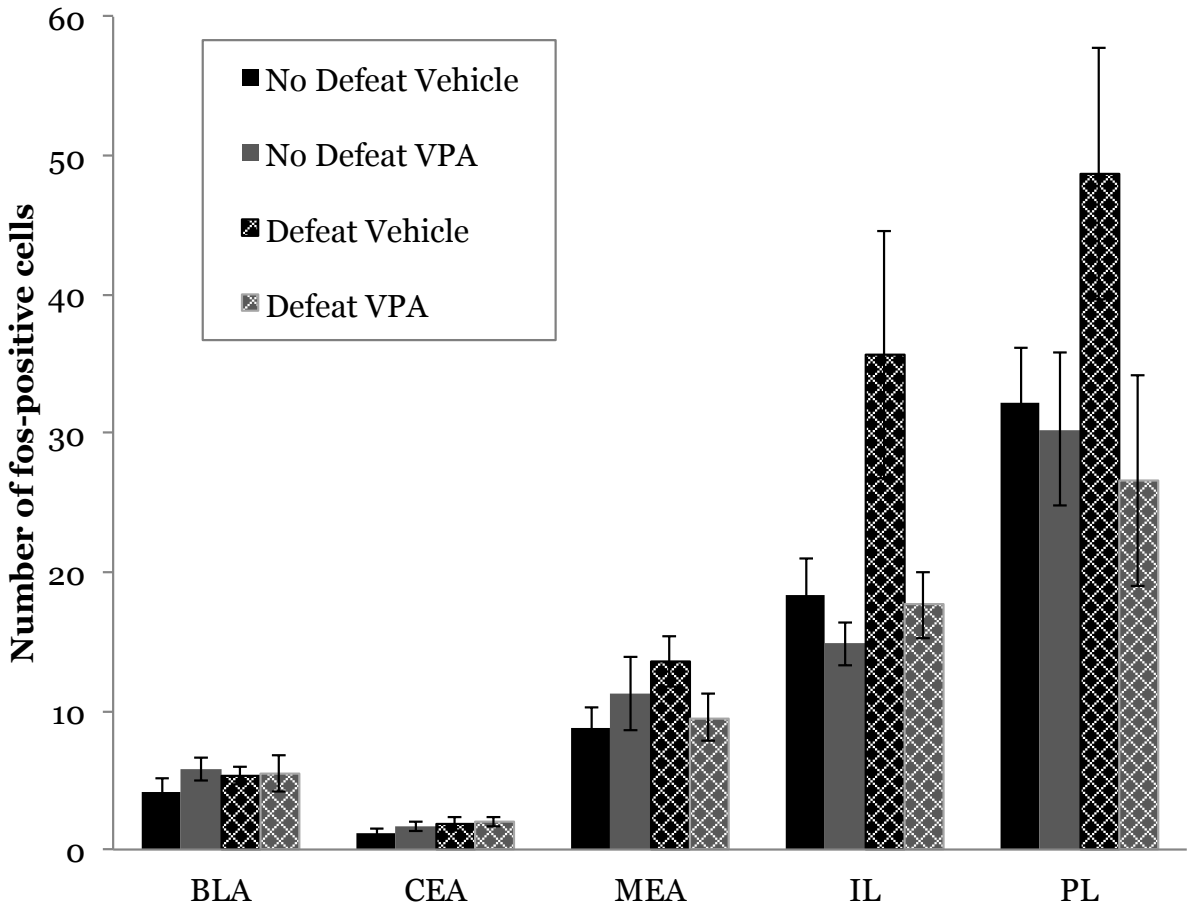

Figure 2.6 Systemic HDAC inhibition modulates neural activity in the IL
Animals were given VPA (200mg/kg) 2hr before a suboptimal (5min) defeat and sacrificed 1hr after defeat. Fos-positive cells were counted in the amygdala (BLA, CEA, MEA) and in the PFC (IL, PL). No differences were found in the amygdala (HDAC inhibition: BLA: $F(1,20)=0.946$, $p=0.342$; CEA: $F(1,20)=0.556$, $p=0.465$; MEA: $F(1,20)=0.154$, $p=0.699$; defeat: BLA: $F(1,20)=0.191$, $p=0.667$; CEA: $F(1,20)=1.774$, $p=0.198$; MEA: $F(1,20)=0.591$, $p=0.451$) or PL (HDAC inhibition $F(1,20)=3.075$, $p=0.095$; defeat: $F(1,20)=0.882$, $p=0.359$). Animals given vehicle before a suboptimal defeat had significantly higher fos counts in the IL than all other groups in the IL, while animals given VPA showed fos counts comparable to no-defeat controls (HDAC inhibition: $F(1,20)=4.897$, $p=0.039$; defeat: $F(1,20)=4.27$, $p=0.052$). *$p<0.05$

2.4 Discussion

In summary, the data presented here suggest that manipulation of histone acetylation, even with systemically administered drugs, may offer a novel way to alter behavioral responses to social stress in both males and females. The data further suggest that these treatments act, at least in part, via their action in the IL and emphasize the importance of prefrontal epigenetic regulation in mediating behavioral changes observed after exposure to acute social stress. Systemic administration of VPA before a

single social defeat experience intensified subsequent behavioral responses to defeat. Our customary defeat procedure uses a 15min, inescapable defeat. This is a relatively mild social stressor, but it is sufficient to lead to robust and quantifiable behavioral changes observed during subsequent testing (Jasnow and Huhman, 2001; McCann and Huhman, 2012; Gray et al., 2015b). In our original experiment, we did not observe a change in social avoidance in animals given VPA, but this could be due to a ceiling effect. We did, however, observe a significant increase in risk assessment, which is a defensive/submissive behavior in which subjects cautiously stretch forward to investigate a potential threat. This increase in risk assessments suggests that there indeed was an increase in submission after systemic HDAC administration that was not captured by measuring seconds of avoidance. Suboptimal defeats produce lower levels of submission and avoidance; therefore, we reasoned that a suboptimal defeat might provide a better starting point with which to discern possible effects. Using a suboptimal defeat, we were able to demonstrate that hamsters given systemic VPA exhibit significant increases in social avoidance. Overall, these data demonstrate that a systemically administered HDAC inhibitor can enhance behavioral responses to social stress.

We next wanted to test if systemic VPA had the same effect in females. Females are often overlooked in other translational models of social stress because of the difficulty in eliciting spontaneous female aggression in rats and mice. Female hamsters typically exhibit more aggression during agonistic encounters than do males, and their expression of conditioned defeat after losing a fight appear to be less marked than that observed in males (Huhman et al., 2003). Using the caged-opponent avoidance test described herein, however, we found that VPA causes a similar increase in avoidance

and risk assessments in females as it does in males. Interestingly, VPA also reduces the number of flank marks in defeated females. Flank marking is a mode of social communication in which a hamster rubs its flank glands along the wall of the cage. This behavior is produced more often by dominant animals and is thought to communicate information about social status (Albers and Prishkolnik, 1992). There are also significant sex differences in flank marking, with females flank marking more often than do males. Not surprisingly, males exhibited very little flank marking (mean of less than 1 flank mark per animal during a 5min test), while most females marked during testing. The decrease in flank marking observed in defeated females given VPA is thus an additional measure of submission or loss of territoriality. Together, these data are the first to show that HDAC inhibition in both males and females enhances the acquisition of stress-induced behavioral changes following acute social defeat. Further, our data have potential translational value not only because the effect is found in both sexes, but also because the drug used here is already being used in the clinical population for other purposes (as described above).

Peripheral VPA crosses the blood brain barrier quickly, with peak concentrations of the drug found in the brain 15min after administration, dropping to non-detectable levels at 8hr post-administration (Nau and Loscher, 1982). VPA is an HDAC inhibitor (Gottlicher et al., 2001; Phiel et al., 2001) and peak acetylation occurs in brain 2hr after systemic administration (Tremolizzo et al., 2002), coinciding with our main behavioral effect. VPA did not affect behavior when given 1hr before defeat, a time when the drug has entered the brain but before peak brain acetylation occurs, nor when given before avoidance testing. There was also no effect of the drugs on no-defeat controls or on the behavior observed during training when the drug was on board. Together, these findings

indicate that systemic VPA time-specifically enhances the acquisition of the memory of a mild social defeat stressor and that this effect coincides with peak brain acetylation. Our site-specific microinjections offer further support for a role of histone acetylation in the behavioral changes observed in response to acute social defeat. We have previously demonstrated that the PFC is a critical component of the neural circuit for conditioned defeat. Microinjection of a GABA-A agonist into the PFC enhances acquisition of conditioned defeat, while activation with a GABA-A receptor antagonist blocks its acquisition (Markham et al., 2012). Previous reports also indicate that ventricular and intra-PFC administration of VPA or NAB decreases HDAC activity in the PFC (Arent et al., 2011). Here, we demonstrate that HDAC inhibition in the PFC enhances the acquisition of conditioned defeat while HAT inhibition impairs it.

Contrary to our data, a recent study reported that administration of an HDAC inhibitor into the PFC following chronic social defeat stress reduces social avoidance (Covington et al., 2015). There are several important differences in the experimental design of the two studies that may help to explain the difference in outcomes. In addition to the species used (mouse versus hamster), the Covington study used a chronic social defeat model that lasted 10 days, whereas we used an acute model of defeat that lasted at most 15min. In addition, they chronically administered the HDAC inhibitor via a minipump into the PFC, including both the IL and PL, rather than a by single injection primarily targeting the IL. Lastly, our study measured the effect of acute HDAC inhibition on the acquisition of conditioned defeat whereas the previous study tested the behavioral effects of HDAC inhibition only after cessation of the chronic stressor. Together, however, both studies highlight an important role for epigenetic regulation in the PFC in modifying behavioral responses to social stress.

We have previously demonstrated that the BLA is critical for acquisition and expression of conditioned defeat (Jasnow and Huhman, 2001; Markham et al., 2010). Temporary inactivation of this nucleus with a GABA-A receptor agonist blocks the acquisition and expression of defeat-induced behavioral changes (Jasnow and Huhman, 2001; Markham et al., 2010) as does an NMDA glutamate receptor antagonist (Jasnow et al., 2004), and *de novo* protein synthesis in this nucleus is necessary for the behavioral changes characterizing conditioned defeat (Markham and Huhman, 2008). We were thus surprised to find that acute HDAC inhibition within the BLA did not effect the acquisition of conditioned defeat. There are data, however, showing that HDAC activity in the amygdala is not decreased following ventricular administration of VPA or NAB, and that HDAC activity is not reduced following intra-amygdalar administration of VPA (Arent et al., 2011). Thus, it is entirely possible that our drug treatment did not alter acetylation in the BLA.

Another prominent use for VPA is as an anticonvulsant or a mood stabilizer because of the drug's pharmacodynamic effect of increasing GABAergic neurotransmission (Nau and Loscher, 1982; Tunnicliff, 1999). While some of the observed behavioral effects in this study might result from an increase in GABA signaling, it is important to note that the enhanced avoidance and submission observed after acute systemic HDAC inhibition is specific to the time point of peak brain histone acetylation. Acetylation (specifically at H3) reaches a peak 2hr after systemic administration, corresponding with our main behavioral effect, whereas increased GABA signaling in the brain is observed within 15min after systemic VPA and remains elevated for up to 8hr (Nau and Loscher, 1982). We demonstrated that there was no effect of VPA on behavior when the drug was given 1hr before social defeat, a time when

GABA signaling in the brain is enhanced, nor when it was given before avoidance testing, a time when GABAergic receptor agonists potently inhibit the expression of conditioned defeat. Similarly, in the BLA, if VPA were acting primarily via a GABAergic mechanism, then we would certainly expect to see a decrease in the acquisition of conditioned defeat as seen when a GABA-A agonist is administered (Jasnow and Huhman, 2001). Together, these data argue strongly against the observed behavioral changes resulting from an effect of VPA on GABAergic signaling.

Further support for the hypothesis that the behavioral effects observed in this study are primarily due to changes in acetylation is the finding that PFC administration of VPA does, in fact, decrease HDAC activity (Arent et al., 2011). In addition, NAB administration, which does not directly affect GABA signaling, caused a similar enhancement of defeat-induced behavior to VPA, while HAT inhibition in the IL, which reduces histone acetylation, reduced the acquisition of conditioned defeat. The opposing behavioral effects observed following enhancement versus reduction of histone acetylation support the hypothesis that epigenetic regulation in the PFC is a critical mediator of behavioral responses to acute social stress.

Finally, we also observed less cellular activation, as measured by Fos-immunoreactivity, in the IL after systemic VPA administration compared with saline. No other brain region analyzed exhibited differential Fos-immunoreactivity after HDAC inhibition or suboptimal defeat. We have shown previously that Fos-immunoreactivity increases in the BLA after a 15min social defeat (Markham et al., 2010); here, we show that a suboptimal (5min) defeat is not sufficient to increase immediate-early gene activation in the amygdala. It is perhaps notable that there was a trend for defeat to increase Fos activation in the IL, suggesting that the IL is sensitive even to an extremely

mild, 5min social defeat stressor. The IL has strong inhibitory connections to the BLA and, although we do not see a corresponding increase in Fos-immunoreactivity in the BLA, it is possible that disinhibition of specific BLA neurons via descending connections from the IL is the mechanism by which the acquisition of conditioned defeat is enhanced after systemic or central HDAC inhibition. This model is consistent with our previous reports showing the importance of the BLA in the acquisition of conditioned defeat, but also highlights the importance of the IL as a site where epigenetic modifications may underlie behavioral responses to social stress. Furthermore, the BLA neurons that we are targeting may contain both stress/fear-driving as well as stress-inhibiting populations of neurons (for review see (Herry et al., 2008; Duvarci and Pare, 2014)). Thus, future studies will be required to further elucidate the roles of these potential subpopulations of neurons in regulating social defeat learning with improved sub-region or cell-type specificity.

These data, together with our drug manipulations in the PFC, suggest changes in histone acetylation in the PFC, perhaps specifically in IL, are important for generating behavioral responses to acute social stress. Experiments are currently underway in our laboratory to measure acetylation of specific histone targets (e.g., H3K14) known to be involved in learning and memory (Zhong et al., 2014; Wang et al., 2015) and determine how these specific markers may mediate behavioral changes after exposure to acute social stress. Future experiments will also look specifically at which cell types in the IL are being affected after systemic HDAC inhibition as well as which specific histone targets are altered.

2.5 Conclusion

The current study focused on the effect of acute HDAC or HAT inhibition during the experience of a mild social stressor. Social stress is particularly relevant in that it is argued to be the most common stressor experienced by humans (Bjorkqvist, 2001), and perceptions of social defeat are strongly associated with depression, anxiety, social withdrawal, and submissiveness (Nemeroff, 1998; Agid et al., 2000; Heim and Nemeroff, 2001). Understanding the role that histone acetylation plays in the acquisition of socially relevant fear memories could be an important step in elucidating the molecular mechanisms underlying stress-related neuropsychiatric diseases such as mood and anxiety disorders and in potentially developing better treatments to alter maladaptive behavioral responses to stressful events. It is especially important from a translational standpoint to examine the effects of HDAC inhibitors such as VPA because many of these drugs are already on the market, and we may find new uses for them in the treatment of stress-related mental health disorders.

2.6 Acknowledgements

Authors of manuscript submitted for publication: Katharine E. McCann, Anna M. Rosenhauer, Genna MF Jones, Alisa Norvelle, Dennis C. Choi, Kim L. Huhman

Research reported here was supported by the National Institute of Mental Health of the National Institutes of Health under Award Number R01MH062044 awarded to KLH. The content is solely the responsibility of the authors and does not necessarily represent the official views of the National Institutes of Health. The authors would like to acknowledge AD Guzman Bambaren, BM Thompson, KA Partrick, and TM Kahl for their assistance with this project.

Table 2.1 Behavior during defeat training
No differences in seconds of aggression produced by the RA or seconds of submission exhibited by the subject were observed between groups in any experiment. All data are shown as mean ± standard error of the mean.

		Aggression by RA (s)	Submission by Subject (s)
Experiment 1: Systemic VPA Aggression: F(3,33)=1.772, p=0.172 Submission: F(3,33)=0.912, p=0.446	Vehicle	304.45 ± 53.75	513.73 ± 58.41
	100mg/kg	155.86 ± 26.43	448.57 ± 60.78
	200mg/kg	190.64 ± 43.1	381.36 ± 56.27
	300mg/kg	259.13 ± 61.58	421.25 ± 77.57
Experiment 2: Systemic VPA (suboptimal defeat) Aggression: t(17)=0.475, p=0.641 Submission: t(17)=-0.163, p=0.873	Vehicle	72.78 ± 15.02	120.33 ± 26.64
	VPA	64.80 ± 7.75	125.40 ± 17.27
Experiment 3: Systemic VPA in females Aggression: t(11)=0.521, p=0.612 Submission: t(11)=-0.887, p=0.394	Vehicle	85 ± 20.54	87 ± 24.92
	VPA	70.86 ± 17.91	122 ± 29.57
Experiment 4: Systemic VPA (1hr) Aggression: t(23)=-1.338, p=0.194 Submission: t(23)=-0.319, p=0.753	Vehicle	173 ± 33.66	323.08 ± 57.36
	VPA	241.46 ± 37.45	354.31 ± 77.76
Experiment 5: Intra-BLA HDAC inhibition Aggression: F(2,21)=1.046, p=0.369 Submission: F(2,21)=0.107, p=0.899	Vehicle	104 ± 22.57	161 ± 23.03
	VPA	136.36 ± 22.31	152.27 ± 18.93
	NAB	93 ± 19.69	144.33 ± 29.96
Experiment 6: Intra-PFC HDAC inhibition Aggression: F(2,14)=1.25 p=0.317 Submission: F(2,14)=2.564, p=0.113	Vehicle	289.75 ± 101.50	519.25 ± 83.53
	VPA	224.71 ± 35.31	561.71 ± 105.4
	NAB	165.67 ± 33.16	318.17 ± 21.44
Experiment 7: Intra-PFC HAT inhibition Aggression: t(9)=1.782, p=0.108 Submission: t(9)=0.877, p=0.403	Vehicle	253.25 ± 27.2	386.25 ± 56.73
	Cur	153 ± 38.9	302 ± 64.18

Table 2.2 Number of line crosses during social avoidance testing
Animals exhibited no difference in locomotor activity, as measured by the number of line crosses, during social avoidance testing with the exception of animals given the highest dose of VPA in Experiment 1. While there were no obvious signs of ataxia, animals given 300mg/kg VPA exhibited significantly fewer line crosses than all other groups in that experiment (*p<0.05). All data are shown as mean ± standard error of the mean. See Figure 1 for schematic of testing arena and scoring markers.

		# Line Crosses
Experiment 1: Systemic VPA F(3,33)=5.437, p=0.004	Vehicle	88.55 ± 6.28
	100mg/kg	96.86 ± 7.95
	200mg/kg	87.45 ± 5.04
	300mg/kg	63.25 ± 2.05*
Experiment 2: Systemic VPA (suboptimal defeat) t(17)=-0.999, p=0.332	Vehicle	86.89 ± 3.9
	VPA	94.2 ± 5.98
Experiment 3: Systemic VPA in females t(11)=1.688, p=0.12	Vehicle	79 ± 6
	VPA	67.57 ± 3.62
Experiment 4a: Systemic VPA (1hr) t(23)=1.816, p=0.082	Vehicle	91.92 ± 4.98
	VPA	79.69 ± 4.55
Experiment 4b: Systemic VPA (expression) t(10)=0.77, p=0.459	Vehicle	81.83 ± 9.05
	VPA	71.83 ± 9.31
Experiment 5: Intra-BLA HDAC inhibition F(2,21)=2.678, p=0.092	Vehicle	63.71 ± 5.22
	VPA	76.73 ± 4.78
	NAB	80.67 ± 4.52
Experiment 6: Intra-PFC HDAC inhibition F(2,15)=0.375, p=0.694	Vehicle	65.25 ± 14.03
	VPA	79.43 ± 13.01
	NAB	67.71 ± 10.3
Experiment 7: Intra-PFC HAT inhibition t(10)=0.743, p=0.475	Vehicle	93.25 ± 7.35
	Cur	80.5 ± 11.35

3 Sequencing the whole brain transcriptome of male and female Syrian hamsters

3.1 Introduction

Syrian hamsters (*Mesocricetus auratus*) have been used in biomedical research for decades because they are uniquely suited for the study of a wide variety of behaviors and diseases. In recent years, however, the use of hamsters has declined (Gao et al., 2014). A PubMed search of 'Syrian hamster' yields 2,280 publications before 1995, 856 publications from 1995-2004, and only 463 publications from 2005-2015. This decline is likely due to the advancement in genetic and molecular tools for other rodents, namely mice, and is not due to a general decline in the utility of hamsters in biomedical research. For example, hamsters provide an excellent model with which to study many types of cancer (Vairaktaris et al., 2008; LaRocca et al., 2015), a variety of tumors (Li and Li, 1984; Gimenez-Conti and Slaga, 1993), and even pathogens such as Ebola viruses (Wahl-Jensen et al., 2012; Prescott et al., 2015). The hypothalamic-pituitary-adrenal (HPA) axis, the so-called stress axis, in humans is more similar to that of hamsters than it is to that of other rodents, making hamsters a valuable model for studying behavioral and neurochemical responses to stress (Potegal et al., 1993; Kollack-Walker et al., 1997; Wommack and Delville, 2003). In addition, hamsters display robust circadian rhythms (Albers and Ferris, 1984; Antle and Mistlberger, 2000), which make them an ideal subject for the study of the neurobiological basis of circadian rhythmicity. Finally, both male and female hamsters display a rich array of social and communicative behaviors, including intraspecific aggression and striking behavioral responses to social defeat stress (Kollack-Walker and Newman, 1995; Albers

et al., 2002; Huhman et al., 2003; Huhman, 2006; Bell and Sisk, 2013), allowing for the study of sex differences in a wide variety of endpoints using this species.

Historically, the vast majority of research has used primarily male subjects. This is the case with humans but has also been prevalent in research using rodent models (Beery and Zucker, 2011). This bias towards males has historically been attributed to the complexity introduced by working with females that have pronounced fluctuations in hormonal state, but it is also the case that, among mammals, some behaviors are not prominently produced by females (e.g., territorial aggression). Female rats and mice, for example, rarely produce any aggression outside of maternal defense of pups (St John and Corning, 1973). It is clearly the case, however, that female humans can be highly aggressive even outside of defense of offspring, thus rats and mice do not represent a good choice with which to model human agonistic behavior. Female hamsters, on the other hand, readily display a range of social and agonistic behaviors (Hennessey et al., 1994; Huhman et al., 2003; Taravosh-Lahn and Delville, 2004; Faruzzi et al., 2005; Solomon et al., 2007a) presenting the opportunity to study social behavior in both sexes rather than trying to generalize findings from males to females.

Social defeat models have become prominent because they are thought to represent an ethologically relevant model of the anxiety- and depression-like changes that are observed in humans exposed to social stressors (Kudryavtseva et al., 1991; Huhman, 2006; Toth and Neumann, 2013; Krishnan, 2014). Although these models have used a variety of rodent species, they have concentrated mainly on males and on behavioral responses to chronic social defeat stress. Our lab established a model of social stress-induced behavioral change in Syrian hamsters that we have termed conditioned defeat. Conditioned defeat is the dramatic shift from territorial aggression

to submission and social avoidance that can be observed in both males and females after losing even a single agonistic encounter (Potegal et al., 1993; Huhman et al., 2003; McCann and Huhman, 2012). We have begun to study some of the genetic and epigenetic markers of conditioned defeat but have been limited in some cases by a lack of specific probes and primers that are selective for hamsters. To generate improved genetic tools for hamsters used in biomedical research, we sequenced the entire brain transcriptome of males and females. In addition, this process also provided an overview of the baseline sex differences in gene expression in the brains of male and female hamsters and highlighted some specific genes that may be of particular interest to those studying neuropsychiatric disorders that result from or are exacerbated by social stress.

3.2 Materials and Methods

3.2.1 Animals and tissue collection

Six adult male and six adult female Syrian hamsters were obtained from Charles River Laboratories (Danvers, MA). Animals were approximately 10 weeks old upon arrival and weighed between 120-130g. Subjects were singly housed and handled daily. During handling, estrous cycles of females were monitored for at least two cycles via vaginal swabs to confirm estrous cycle stage and stability. All females were killed on Diestrus 2 to minimize variation in gene expression based on day of the estrous cycle. This day of the cycle was chosen because we know that females will produce robust social avoidance following social defeat when tested on Diestrus 2, most closely resembling the behavior of males after social defeat (unpublished observations). An equal number of males were killed at the same time. Animals were rapidly anesthetized via isoflurane exposure and then decapitated. Brains were quickly extracted, frozen

immediately in isopentane on dry ice, and stored at -80°C until processing. All procedures and protocols were approved by the Georgia State University Institutional Animal Care and Use Committee and are in accordance with the standards outlined in the National Institutes of Health Guide for Care and Use of Laboratory Animals.

3.2.2 RNA extraction

Two brains from same-sex animals were pooled together for each RNA extraction in order to minimize the effect of individual variability. We used Trizol (Life Technologies, Grand Island, NY) for extractions, following a modified version of the manufacturer's protocol. In brief, frozen brains were cut into large pieces and placed in 50mL conical tubes on ice. Brains were homogenized on ice with 20mL Trizol. After full homogenization, the sample was allowed to settle at room temperature for 5min. The homogenate was then mixed with 4mL of chloroform, allowed to stand at room temperature for 2-3min and centrifuged at 5,250g for 45min at 4°C to separate the phases. The aqueous RNA phase was removed and dispensed into a new conical tube. The aqueous phase was washed with 200µL/mL of chloroform, mixed well, allowed to stand 2-3min and then centrifuged at 12,000g for 10min at 4°C. For enhanced visualization of the pellet, 3µL/mL of GlycoBlue (Life Technologies, Grand Island, NY) was added and mixed gently. For RNA precipitation, 500µL/mL of 100% isopropanol was added, mixed gently and allowed to stand at room temperature for 10min. To obtain an RNA pellet, the solution was centrifuged at 12,000g for 20min at 4°C. The remaining liquid was carefully removed and the pellet was washed twice in 75% ethanol in RNase-free water and centrifuged at 7,500g for 5min at 4°C. The pellet was allowed to air dry

for approximately 5min and was then re-suspended in 125µL of ultrapure water and immediately stored at -80°C.

3.2.3 RNA quality assurance and RNA-seq

RNA quality was assessed using the Agilent RNA 6000 Nano Kit (Agilent Technologies, Santa Clara, CA) on the Agilent Bioanalyzer, following the manufacturer's instructions. RNA integrity numbers (minimum standard of 6) and concentration (ng/µl) were recorded and sent with the samples for sequencing. Samples (n=6) were sent on dry ice to Beckman Coulter Genomics (Danvers, MA) for Illumina Automated RNA sequencing and were sequenced in paired-end 100bp reads, averaging 110M reads per sample.

3.2.4 Transcriptome assembly and optimization

In order to produce a comprehensive brain transcriptome, we completed a *de novo* transcriptome assembly with Trinity (Grabherr et al., 2011; Haas et al., 2013) (https://github.com/trinityrnaseq/trinityrnaseq/wiki) using the jaccard clip parameter to minimize potential fusion transcripts. After assembly, TransDecoder (Haas et al., 2013) (https://transdecoder.github.io) was used to identify coding domain sequences with a minimum cut-off of 50 amino acids (Feng et al., 2015). Assembled transcripts were also run through NCBI's BLASTx (Altschul et al., 1990) (http://blast.ncbi.nlm.nih.gov/Blast.cgi) using the Uniprot-rodent database from January 21, 2016 (UniProt, 2015) (http://www.uniprot.org) to match *de novo* sequences to known genes.

Annotation of the assembly was accomplished with Trinotate, an annotation platform designed for use with the Trinity platform (https://trinotate.github.io). Trinotate is a series of annotation steps specific for *de novo* assemblies, encompassing

the use of NCBI's BLAST to match sequences to known genes, PFAM (Punta et al., 2012) and HMMR (Finn et al., 2011) to identify protein domains, tmHMM (Krogh et al., 2001) to predict transmembrane regions, signalP (Petersen et al., 2011) to predict signal peptides, and RNAMMER (Lagesen et al., 2007) to identify rRNA transcripts. Finally, we compared our annotated assembly to a database of highly conserved orthologs using the BUSCO (Benchmarking Universal Single Copy Orthologs, http://busco.ezlab.org) database to add an additional quality measure to our optimized assembly (Simao et al., 2015; Theissinger et al., 2016).

We further identified gene ontology terms associated with our annotated transcripts using PANTHER (Protein Analysis Through Evolutionary Relationships, http://www.pantherdb.org) (Ashburner et al., 2000; Mi and Thomas, 2009; Mi et al., 2013; Mi et al., 2016). We compared all genes using *Mus musculus* as the reference organism in PANTHER and identified the molecular functions, biological processes, protein classes, and pathways associated with the fully annotated transcriptome and the subsets of differentially expressed genes, described below.

3.2.5 Differential expression analysis

Differential gene expression in male and female hamster brains was calculated using an exact test in the Bioconductor package edgeR (Robinson et al., 2010) (https://bioconductor.org/packages/release/bioc/html/edgeR.html) in R (Team, 2014) (https://www.R-project.org). We used RSEM (RNA-Seq by Expectation-Maximization, http://deweylab.github.io/RSEM) (Li and Dewey, 2011) to generate read counts matching the optimized assembled transcriptome for the recommended input into edgeR. Transcripts with artificially low counts (<1 across all samples) were excluded

before differential expression analysis was completed. Transcripts were considered to significantly differ in expression between males and females if the log2 fold change was >1.5 and the false discovery rate (FDR) was <0.05.

3.3 Results and Discussion

3.3.1 Sample quality and description of raw reads

All RNA samples (n=3 male, 2 brains per sample and n=3 female, 2 brains per sample) were measured with the Agilent Bioanalyzer before sequencing. The RNA integrity numbers (a measure of sample quality) of all samples were good, falling between 7-8 (maximum value of 10), and all above the standard cutoff of 6. Table 3.1 shows the RNA quality and concentration of each sample. Final raw sequence data was run through a quality assurance test (FastQC, http://www.bioinformatics.babraham.ac.uk/projects/fastqc) to ensure minimal bias in sequencing and to confirm quality of starting library material. This test provides confidence in the quality of the sequence output before proceeding to assembly and annotation. Per base sequence quality scores all fell in the "very good" range (above 28, green section in Figure 3.1) giving us the confidence to move forward with transcriptome assembly.

Table 3.1 Individual sample quality and concentration

Sample	RNA integrity number (RIN)	Concentration (ng/µl)
Female A	7.7	802
Female B	7.3	1286
Female C	7.3	848
Male A	7.4	1231
Male B	7.7	915
Male C	7.4	992

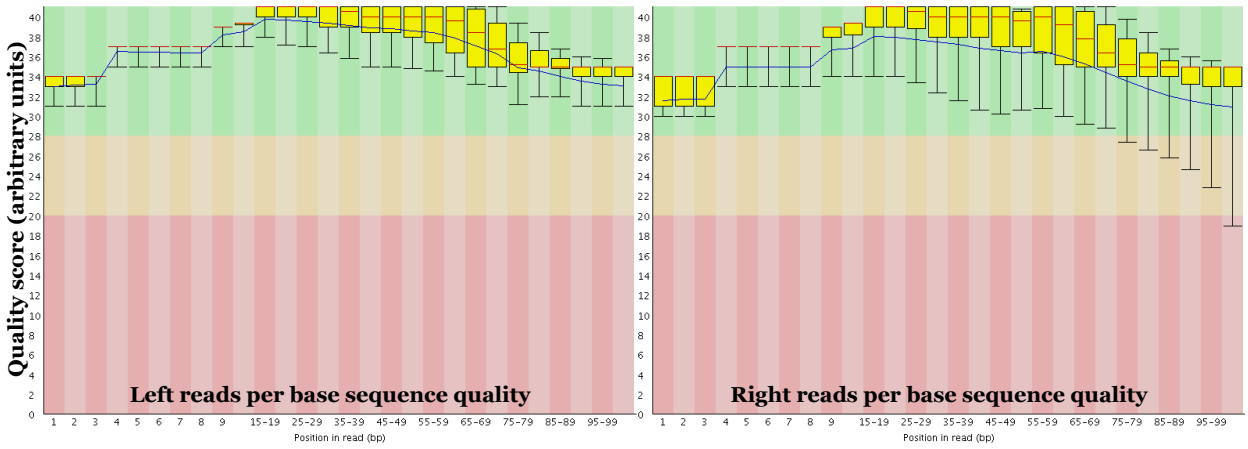

Figure 3.1 FastQC Analysis of raw reads of whole brain samples
All scores for each base fell in the "very good" (green) range after FastQC analysis was completed.

3.3.2 Transcriptome assembly

We assembled the Syrian hamster brain transcriptome using *de novo* techniques because, while there is a partially annotated Syrian hamster genome available (NCBI NW_00401604.1), we were unable to reliably use this for a genome-guided assembly for several reasons. First, the genome currently available was sequenced from a single female hamster, thus eliminating the sequences of any Y-linked genes. One of the purposes of this project was to compare males and females, so having Y-linked sequences would not only provide a positive control when looking at sex differences but would also lead to a more complete and representative transcriptome. In addition, the incomplete annotation of the current hamster genome leads to a number of problems when trying to build a transcriptome. The software currently available for building genome-guided assemblies assumes complete, or near-complete, annotation, and therefore returns error messages for any sequence that is not already annotated. Thus, we moved forward with a *de novo* assembly for more accurate and complete results.

The *de novo* assembly using Trinity revealed 1,002,166 total Trinity genes and 1,147,108 transcripts from 973,648,406 total assembled bases. The average contig,

overlapping sequences to be mapped, was 848.79 bases (median 440) with a percent GC content of 45.62. After completing the *de novo* assembly, raw reads were aligned back to the assembly. Proper pairs (both left and right reads aligned to same contig) accounted for 80.83% (539,735,450) of the 667,738,987 total aligned reads. Of the remaining pairs, left-only reads accounted for 9.68% (64,655,456) and right-only for 7.85% (52,410,243). Improper pairs, in which left and right reads align but to different contigs due to fragmentation, accounted for only 1.64% (10,937,838) of the total reads. These data provide an excellent starting point with which to build a usable transcriptomic database for Syrian hamster brain.

3.3.3 Assembly optimization and annotation

Trinity genes are transcripts that may or may not code for a specific gene. Trinity *de novo* sequencing builds transcripts from sequence patterns that are *likely* to code for a gene. Without a genome to guide the assembly, some guesswork is involved in assembling the bases into known sequences. Thus, the approximation of the *de novo* assembly calls for several additional parameters to be put in place to build a more confident and usable transcriptome database. In order to be confident in our assembly and to minimize false positives as well as artificial sequences created by the *de novo* assembly, we ran a number of programs (see Materials and Methods) to optimize the assembly into an accurate representation of transcripts present in Syrian hamster brain, as done previously with other *de novo* assemblies in several fish and rodent species (MacManes and Lacey, 2012; Sharma et al., 2014; Albertin et al., 2015; Feng et al., 2015; Theissinger et al., 2016). See Figure 3.2 for a schematic of the assembly optimization process.

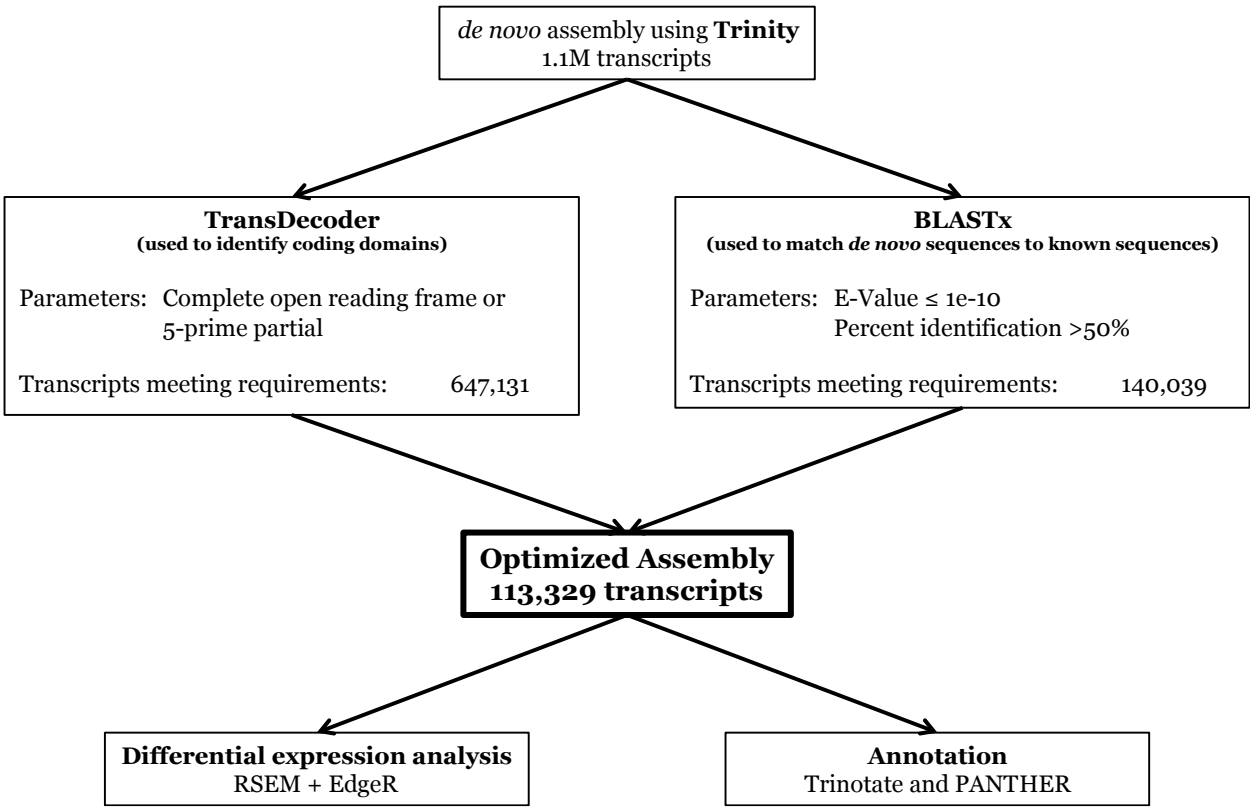

Figure 3.2 Schematic of *de novo* assembly optimization and analysis
After initial *de novo* assembly using Trinity, we optimized the assembly using several programs to omit falsely assembled sequences or sequences that were not likely to code for an actual gene. After optimization, we used RSEM to generate expected counts of each transcript from the raw reads and used those reads to calculate differential expression between males and females using edgeR. Annotation of the optimized assembly was completed using Trinotate and PANTHER.

First, TransDecoder was completed to determine the number of probable coding sequences within the assembly. Complete coding sequences accounted for 456,234 of the total number of open-reading frames (790,773). There were 108,213 3'-partial, 190,897 5'-partial, and 35,429 internal sequences. The sequencing protocol used had a 3' bias, thus we included all transcripts with 5'-partial and complete coding sequences for our initial assembly optimization (647,131), as these transcripts were most likely to code for actual genes (Senatore et al., 2015). We also filtered the assembly using data obtained from BLASTx using the Uniprot-rodent database (1/21/16) to ensure that all genes matched a known rodent sequence. BLASTx returned 1,219,140 matches, however

many of these were at very low confidence parameters, thus only those with an E-value of ≤1e-10 and a percent identification match of ≥50 were included (140,039). These stringent parameters provide enhanced confidence in the quality of our optimized and annotated transcriptome (MacManes and Lacey, 2012; Feng et al., 2015). Finally, we combined the output from TransDecoder and BLASTx, which left 113,329 transcripts meeting all the above stated criteria. While this reduction process may have eliminated some sequences that represent true genes within hamster brain, these steps were necessary in order to eliminate a large number of false positives that can occur in *de novo* sequencing. Furthermore, BUSCO analysis revealed that 80% of the highly conserved sequences among vertebrates were present in our optimized assembly, while 86% of the conserved genes across all eukaryotes were present in our assembly. These data provide enhanced confidence in the quality and adequacy of our optimized brain transcriptome.

We used the rodent database from Uniprot in order to maximize the number of transcripts in our assembly that matched a known sequence. Almost all of the transcripts matched *Mus musculus* (mouse) (75.44%) and/or *Rattus norvegicus* (rat) (22.68%). This is not surprising considering that the mouse genome is the most highly curated rodent genome available. Of the 113,329 individual transcripts in the optimized assembly, there were only 17,785 unique gene identifiers from BLAST, suggesting that there are multiple isoforms of some of genes present in our assembly. This is consistent with data in humans and mice showing that there are approximately 17,000-25,000 genes in their respective genomes, with at least 10x the number of transcripts, and that 8,000-15,000 mRNAs are expressed in any quantified sample (Hastie and Bishop, 1976; Venter et al., 2001; Su et al., 2004; Carninci et al., 2005).

3.3.4 Gene expression analyses

Using expected read counts from RSEM, we first compiled a matrix to determine which genes were most highly expressed in Syrian hamster brain. These genes are shown in Supplemental Table 1 and, not surprisingly, represent genes that are highly expressed in brain tissue of other species. We next completed differential expression analysis on our annotated transcriptome to determine what genes, if any, were differentially expressed in male and female brains. Excluding transcripts that did not meet the minimum expression cut off (see Materials and Methods), 207 transcripts were differentially regulated, the majority of which were higher in males compared with females (130 higher in males, 77 higher in females). Some of the differentially expressed transcripts matched the same BLAST entry, suggesting that there may be differential regulation of multiple isoforms of these genes. The differentially expressed genes are listed in Supplemental Table 2.

There are several important considerations regarding the differentially expressed genes that should be addressed. First, the differentially expressed genes are presented here based on which sex had higher expression. It should be noted that the differential expression could in fact be the result of a decrease in expression of the opposite sex or a combination of an increase in one and a decrease in the other. Second, 207 genes is a reasonable number of genes to expect for overall sex differences in whole brain based on data from both humans and drosophila (Catalan et al., 2012; Trabzuni et al., 2013), however this number can vary greatly depending on the statistical test and parameters used. Here, we use a stringent analysis previously used in other *de novo* assemblies and the one recommended by the Trinity package (Fraser et al., 2011; Feng et al., 2015). Lastly, the differences reported here are representative of the entire brain, thus some

sexually dimorphic genes may not be represented in our dataset due to differential regulation in different brain regions that may act to counterbalance or eliminate overall differences in expression.

Our lab is particularly interested in genes associated with neuropsychiatric disorders, such as mood and anxiety disorders, thus a few genes stood out as potential candidates to further study sex differences in behavioral responses to social stress. Specifically, several differentially expressed genes have been associated with depression and mood disorders (*Abcb10*, *Gata2*, *Hdac5*, *Mgat5*) (Iga et al., 2007; Soleimani et al., 2008; Choi et al., 2014; Kambe and Miyata, 2015; Watanabe et al., 2015). These may be of particular interest for future research because many mood disorders have sexually dimorphic features in the clinical population, including higher overall rates of unipolar depression and PTSD in women and different primary coping styles between men and women (Weissman and Klerman, 1977; Nolen-Hoeksema, 1987; Breslau et al., 1997; Altemus, 2006). Genes that control these dimorphic features may present good candidates for developing novel or more targeted interventions. Furthermore, *Hdac5* was significantly higher in male than in female brains. HDAC5 facilitates the antidepressant effect of ketamine in male rats (Choi et al., 2015) and its expression increases in the bed nucleus of the stria terminalis in male mice with PTSD-like behavior (Lebow et al., 2012). These mechanisms, however, have not yet been studied in females and the current data suggest that *Hdac5* is differentially regulated in females and therefore may no contribute to these effects in the same manner as males.

Additional subsets of the differentially expressed genes between male and female hamster brain have been associated with learning and memory or neurodevelopmental disease states, including schizophrenia (*Cdc42bpb*, *Map6*, *Rapgef2*, *Rb1cc1*) (Narayan et

al., 2008; Degenhardt et al., 2013; Daoust et al., 2014; Merenlender-Wagner et al., 2014; Levy et al., 2015), autism (*Lin7b*) (Lanktree et al., 2008; Mizuno et al., 2015), Alzheimer's (*Cfh*, *Rb1cc1*) (Chano et al., 2007; Zhang et al., 2016), and drug or alcohol dependence (*Gria3*, *Mobp*) (Bannon et al., 2005; Weng et al., 2009; Li et al., 2015; Manzardo et al., 2015). One isoform of tolloid-like protein 1 (*Tll1*) was expressed higher in females, while another isoform was higher in males. *Tll1* has been linked to sex differences in behavioral response to stress (Tamura et al., 2005) and, based on the current data, it may be of interest to further define the role of specific isoforms of this gene in both males and females. Furthermore, chromodomain-helicase-DNA-binding proteins (CHDs), which are part of a larger family of chromatin remodeling factors, show differing regulation in various fear conditioning and extinction models (Wille et al., 2015), and are therefore candidate genes mediating the epigenetic regulation ultimately leading to changes in behavior after exposure to stressful or fearful stimuli. Two of these genes (*Chd1* and *Chd5*) were differentially expressed between male and female hamster brains. *Chd1* was higher in males as was one isoform of *Chd5*. Another isoform of *Chd5* was more highly expressed in females. Previous studies showing the regulation of these genes in response to aversive stimuli have only used male subjects. Our current data suggest that further study into the regulation of these genes after exposure to fear- or stress-producing stimuli, such as social defeat, is necessary to determine if regulation in females differs from that of males.

3.3.5 Functional annotation and gene ontology analysis

In order to complete functional annotation of the full brain transcriptome, we filtered our annotated assembly from Trinotate through PANTHER analysis to

determine which gene ontology terms were highly represented in the optimized brain transcriptome. The optimized assembly accounted for 13,258 different molecular functions, 23,842 biological processes, 13,942 protein classes, and 5,141 pathways. The top hits for each of these classifications are presented in Figure 3.3. Next, we entered the subsets of differentially expressed genes to determine if any specific gene ontology terms were more highly represented in these genes as compared with the complete transcriptome. There were 84 molecular functions, 158 biological processes, 80 protein classes, and 14 pathways represented by the genes up-regulated in females, and 123 molecular functions, 212 biological processes, 130 protein classes, and 32 pathways in the genes up-regulated in males (Figure 3.4). For all genes analyzed, catalytic activity and binding were the most represented molecular functions. Likewise, the highest number of transcript matches for biological processes were cellular and metabolic processes.

Each category represented in Figures 3.3 and 3.4 has subcategories into which the genes can be further classified and several interesting trends emerge when comparing the differentially expressed genes. For example, the vast majority of genes associated with Localization up-regulated in males (85.1%) and females (81.9%) matched the highest categories for the whole brain, including Vesicle, Protein, Ion, and Lipid Transport (81.8%). In addition, the majority of Receptors classified in the optimized brain transcriptome represented G-protein Coupled Receptor Activity (42.5%) but none of the genes that were differentially expressed between males and females were classified by this subcategory. In fact, Glutamate Receptor Activity was the only subcategory of Receptor represented in the genes up-regulated in females. Perhaps the most compelling to our laboratory, however, were the subcategories represented in

Response to Stimulus. The genes in this classification for the whole brain were most widely categorized by Response to Stress (35.6%), Immune System Response (22.2%), Response to External Stimuli (19.8%), and Cellular Defense Response (11.2%). Interestingly, of the genes up-regulated in females that fell under this category, the most highly represented were categorized under Response to Stress (54.5%) and Response to Pheromones (9.1%). The genes in this category that were up-regulated in males also represented a high number of genes that respond to stress (33.3%), however, the most represented category was Response to External Stimulus (50%). These functional classifications of the differentially expressed genes may help to identify more precise targets for understanding differences sex differences in behavioral responses to stress.

3.4 Conclusion

These data represent the first comprehensive report of the Syrian hamster brain transcriptome and the first time that genes of both male and female hamsters have been sequenced and analyzed. The differential analyses presented here between male and female baseline gene expression in the brain provide a good starting point for analyzing potential genetic and epigenetic mechanisms underlying sex differences in behavior and in response to different stimuli. Ultimately, the sequences obtained from this project will permit those conducting biomedical research with Syrian hamsters to design and use hamster-specific sequences to answer important molecular and genetic questions.

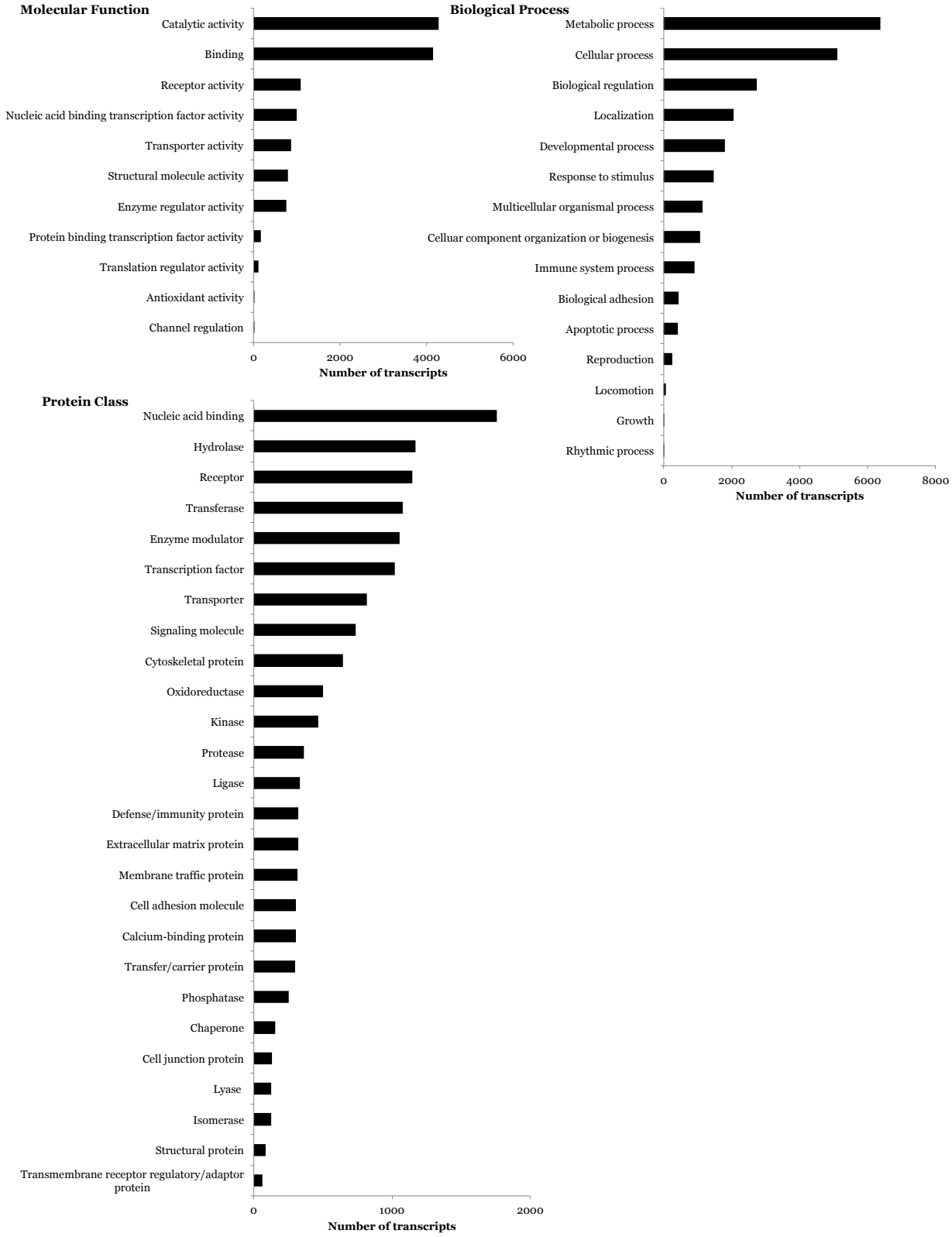

Figure 3.3 Highest represented gene ontology terms from the optimized whole brain transcriptome
We used PANTHER analysis to match the 17,785 unique genes in our optimized transcriptome to gene ontology terms for functional annotation of the assembly. These are the most represented functions in the Syrian hamster brain.

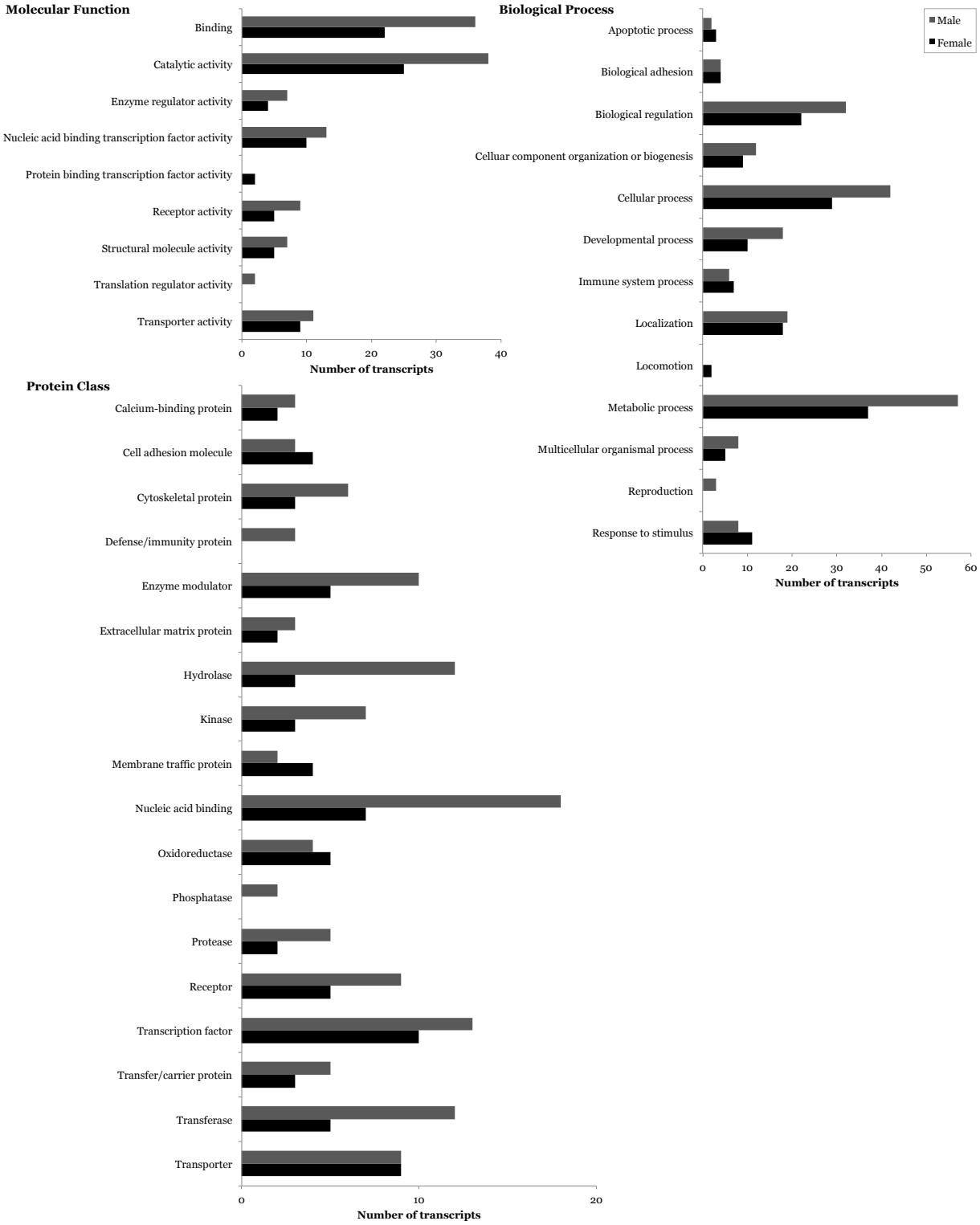

Figure 3.4 Highest represented gene ontology terms in the subsets of differentially expressed genes
Highest represented gene ontology terms from PANTHER for the 130 genes up-regulated in males (gray) and the 77 genes up-regulated in females (black) in Syrian hamster brain.

3.5 Acknowledgements

Authors for manuscript to be submitted for publication: Katharine E. McCann, David M. Sinkiewicz, Alisa Norvelle, Kim L. Huhman

Research reported here was supported by the National Institute of Mental Health of the National Institutes of Health under Award Number R01MH062044 awarded to KLH and by a Seed Grant awarded to KLH from the Brains and Behavior Program at Georgia State University. The content is solely the responsibility of the authors and does not necessarily represent the official views of the National Institutes of Health. The authors would like to acknowledge SE Pathirannehelage, AD Guzman Bambaren, BM Thompson, and GMF Jones for their assistance with this project.

4 The effect of sex and social status on gene expression in the amygdala of Syrian hamsters

4.1 Introduction

Transcriptomics, the study of all the RNA transcripts in a given sample, has become a significant investigatory tool for many branches of science, ranging from cancer research to plant biology, evolution, and behavioral neuroscience. Transcriptome sequencing gives researchers using both traditional and non-traditional model organisms the opportunity to explore genetic and epigenetic questions. Our laboratory uses Syrian hamsters to study the neurobiology of social stress-induced changes in behavior. Social stress is the most common stressor experienced by humans (Bjorkqvist, 2001) and is a risk factor for developing a number of neuropsychiatric disorders,

including anxiety and mood disorders, and posttraumatic stress disorder (Agid et al., 2000; Ehlers et al., 2000; Kelleher et al., 2008). Many labs use rats or mice to study stress, including social stress, and while these animal models are valuable and these more traditional models currently have more genetic tools available (e.g., annotated genomes and transgenic lines), hamsters provide a complementary model of social stress that offers several unique benefits.

First, both male *and* female hamsters display spontaneous agonistic behavior (Ferris et al., 1987; Harmon et al., 2002a; Huhman et al., 2003; Solomon et al., 2007a), making it possible to examine sex differences in response to social stress. In addition, hamsters do not require complex housing conditions to elicit territorial aggression; a simple pairing of two hamsters in a resident-intruder model or a novel arena will result in reliable dominant-subordinate relationships (Ferris et al., 1987; Potegal et al., 1993; Harmon et al., 2002b; Huhman et al., 2003). Of particular importance, hamsters exhibit highly ritualized behavior during agonistic encounters so that physical injury rarely occurs. This allows separation of the stress of the social encounter, which is largely psychological, from the stress of physical injury, which is more likely to occur in chronic social defeat models. Lastly, after losing *a single agonistic encounter*, hamsters abandon all territorial aggression and become highly submissive and socially avoidant. This allows the researcher to more precisely determine when the critical neurobiological mechanisms must be occurring that underlie the resulting behavioral changes. Thus, this social stress-induced change in behavior, which we have termed conditioned defeat, allows us to study the behavioral and physiological changes that occur after exposure to a mild social stressor, rather than to the repeated or chronic stressor that is often needed to elicit behavioral changes in mice and rats. Our lab has characterized much of

the neural circuitry underlying conditioned defeat in hamsters, and we have established the importance of the basolateral amygdala (BLA) in this circuit. The BLA is necessary for the acquisition and expression of conditioned defeat (Jasnow and Huhman, 2001; Markham et al., 2010) and *de novo* protein synthesis in this nucleus is required for social stress-induced behavioral change (Markham and Huhman, 2008). Furthermore, overexpression of cyclic AMP binding protein in the BLA during social defeat enhances subsequent conditioned defeat (Jasnow et al., 2005); thus, it is clear that gene regulation is promoting the behavioral responses to defeat. The purpose of this project was to determine which genes appear to be significantly up- or down-regulated in amygdala following agonistic interactions and if these genes are differentially regulated between males and females of different social status.

We previously found gene expression differences in male and female brains that directly relate to histone modifications and epigenetic regulation during or after exposure to stress. Specifically, histone deacetylase 5 (*Hdac5*) is more highly expressed in the whole brain of males compared with females (Chapter 3). HDAC5 facilitates the antidepressant effect of ketamine in hippocampal neurons of male rats (Choi et al., 2015) and its expression is enhanced in neurons of the bed nucleus of the stria terminalis in male mice displaying PTSD-like behavior (Lebow et al., 2012). Furthermore, chromatin remodeling factors, specifically chromodomain-helicase-DNA-binding proteins (CHDs), facilitate learning and memory by altering the availability of DNA for transcription, and *Chd1* and *Chd5* mediate fear conditioning in the ventral hippocampus of male mice (Wille et al., 2015). *Chd1* and *Chd5* are differentially expressed in the whole brain of male and female hamsters, however the studies described above only used male subjects, thus it is unclear as to whether these same

mechanisms hold true for females. Further investigation is needed into whether these genes, and others facilitating epigenetic regulation, including *Hdac5*, play a significant role in social stress-induced behavioral changes in males and females. Although both males and female hamsters exhibit conditioned defeat after acute social defeat, the behavioral expression is often more pronounced in males (Huhman et al., 2003). Thus, to investigate potential genetic mechanisms leading to sexually dimorphic expression of conditioned defeat, and to further delineate the role of histone acetylation in stress-induced behavioral changes, we sequenced the transcripts in the basolateral amygdalae of dominant and subordinate animals and compared gene expression to that of home cage controls.

4.2 Materials and Methods

4.2.1 Animals and social defeat training

Adult male and female Syrian hamsters were obtained from Charles River Laboratories (Danvers, MA). Animals were singly housed upon arrival and were approximately 10 weeks old, weighing between 120-130g. During handling, estrous cycles of females were monitored for at least two cycles via vaginal swab to confirm estrous cycle stage and stability. Before social defeat training, animals were weight-matched and randomly assigned as a resident, intruder, or home cage control. All females were paired on Diestrus 1 and killed on Diestrus 2 because females on Diestrus 2 show the most pronounced avoidance after defeat (unpublished observations). An equal number of males were paired and killed each day. Intruders were placed in the resident's home cage three times for 5min to ensure a stable hierarchy; each pairing was separated by an inter-trial interval of 3min. The 5min interval for the first pairing began

immediately after the first agonistic interaction wherein it was clear that one hamster displayed social dominance (characterized by side and upright attack postures as well as chasing) and the other submission (characterized by defensive postures, tail lift, and flight) (Potegal et al., 1993). Controls were left alone in their home cage during training. All procedures and protocols were approved by the Georgia State University Institutional Animal Care and Use Committee and are in accordance with the standards outlined in the National Institutes of Health Guide for Care and Use of Laboratory Animals.

4.2.2 Tissue collection, RNA isolation, and RNA-Seq

Animals were rapidly anesthetized via isoflurane exposure and then decapitated 24hr after their agonistic encounter, the time when we would normally test for the presence of conditioned defeat. Brains were quickly extracted, frozen immediately in isopentane on dry ice, and stored at -80°C until processing. Bilateral tissue punches (1mm) aimed at the basolateral amygdala were extracted from frozen brains and pooled for RNA isolation processing. RNA extractions followed a modified protocol using Trizol (Life Technologies, Grand Island, NY). Amygdalae from two animals of the same sex and social status (4 total amygdala punches) were pooled together for each RNA extraction in order to minimize the effect of individual variability. Tissue was homogenized on ice with 1mL Trizol. After full homogenization, homogenate was allowed to settle at room temperature for 5min. Homogenate was then mixed with 200µl of chloroform, allowed to stand at room temperature for 2-3min and then centrifuged at 12,000g for 15min at 4°C to separate the phases. The aqueous RNA phase was removed and dispensed into a new 2mL microcentrifuge tube. The aqueous phase

was washed with 200µL of chloroform, mixed well, allowed to stand 2-3min and then centrifuged at 12,000g for 10min at 4°C. For enhanced visualization of the pellet, 3µL of GlycoBlue (Life Technologies, Grand Island, NY) was added and mixed gently. For RNA precipitation, 500µL of 100% isopropanol was added, mixed gently and allowed to stand at room temperature for 10min. To obtain an RNA pellet, the solution was centrifuged at 12,000g for 20min at 4°C. The remaining liquid was carefully removed and the pellet was washed twice in 1mL 75% ethanol in RNase-free water and centrifuged at 7,500g for 5min at 4°C. The pellet was allowed to air dry for approximately 5min and was then re-suspended in 20µL of ultrapure water. Samples were stored at -80°C until sequencing.

RNA quality and concentration was determined as it was for whole brain analysis (Section 3.2.3) and sent for sequencing to Beckman Coulter Genomics (Danvers, MA). Amygdala sequencing was completed in paired-end 100bp reads, averaging 37M reads per sample.

4.2.3 Transcriptome assembly and optimization

The amygdala *de novo* transcriptome was assembled using Trinity (Grabherr et al., 2011; Haas et al., 2013) (https://github.com/trinityrnaseq/trinityrnaseq/wiki) with all 18 samples from both males and females, as described previously (Section 3.2.4). The assembly was optimized using TransDecoder (Haas et al., 2013) (https://transdecoder.github.io) with a minimum cut-off of 50 amino acids (Feng et al., 2015) and BLASTx (Altschul et al., 1990) (http://blast.ncbi.nlm.nih.gov/Blast.cgi), using the Uniprot-rodent database from January 21, 2016 (UniProt, 2015) (http://uniprot.org). The optimized assembly was annotated using the Trinity-recommended platform, Trinotate (https://trinotate.github.io), as described previously (Section 3.2.4). PANTHER

(Protein Analysis Through Evolutionary Relationships, http://www.pantherdb.org) was used for functional annotation of the optimized assembly, using *Mus musculus* as the reference organism.

4.2.4 Differential expression analysis and statistics

Differential expression analysis was completed using expected read counts from RNA-Seq by Expectation-Maximization (RSEM) (Li and Dewey, 2011) (http://dewey lab.github.io/RSEM) in an exact test using the Bioconductor package edgeR (Robinson et al., 2010) (https://bioconductor.org/packages/release/bioc/html/ edgeR.html), as described previously (Section 3.2.5). Transcripts were considered to significantly differ if the false discovery rate (FDR) was <0.05. In addition, we determined *a priori* to test the differential expression of HDACs using a one-way ANOVA with a p-value set at <0.05. We also used weighted coexpression analysis (WGCNA, https://labs.genetics.ucla.edu/horvath/CoexpressionNetwork/Rpackages/ WGCNA/) to cluster our individual samples by gene expression patterns in the amygdala (Langfelder and Horvath, 2008).

4.3 Results and Discussion

4.3.1 De novo transcriptome assembly

RNA samples (n=18) were measured on the Agilent Bioanalyzer before they were sent for sequencing. RNA integrity numbers (maximum value of 10) and sample concentrations are listed in Table 4.1. Sequence quality analysis (FastQC) was completed after sequencing and all base scores fell in the highest quality range (green section, Figure 4.1). The sample and sequencing quality was of a high enough standard to continue to transcriptome assembly. The *de novo* assembly using Trinity revealed

1,244,719 Trinity genes. Raw reads were then aligned back to the assembly revealing that proper pairs (left and right reads aligned to same contig) accounted for 80.78%, improper pairs (left and right reads align, but to different contigs due to fragmentation) for 13.81%, left-only reads for 3.57% and right-only reads for 1.84%.

Table 4.1 Sample quality and concentrations of amygdala samples for sequencing

Sample	RNA integrity number (RIN)	Concentration (ng/µl)
Female Control A	9.1	191
Female Control B	9.1	228
Female Control C	9.2	127
Male Control A	9.2	67
Male Control B	9.1	137
Male Control C	9.0	195
Female Subordinate A	9.2	173
Female Subordinate B	9.0	185
Female Subordinate C	9.2	101
Male Subordinate A	9.1	295
Male Subordinate B	9.0	155
Male Subordinate C	9.1	254
Female Dominant A	9.3	210
Female Dominant B	9.0	75
Female Dominant C	9.1	164
Male Dominant A	9.1	214
Male Dominant B	9.2	127
Male Dominant C	9.1	183

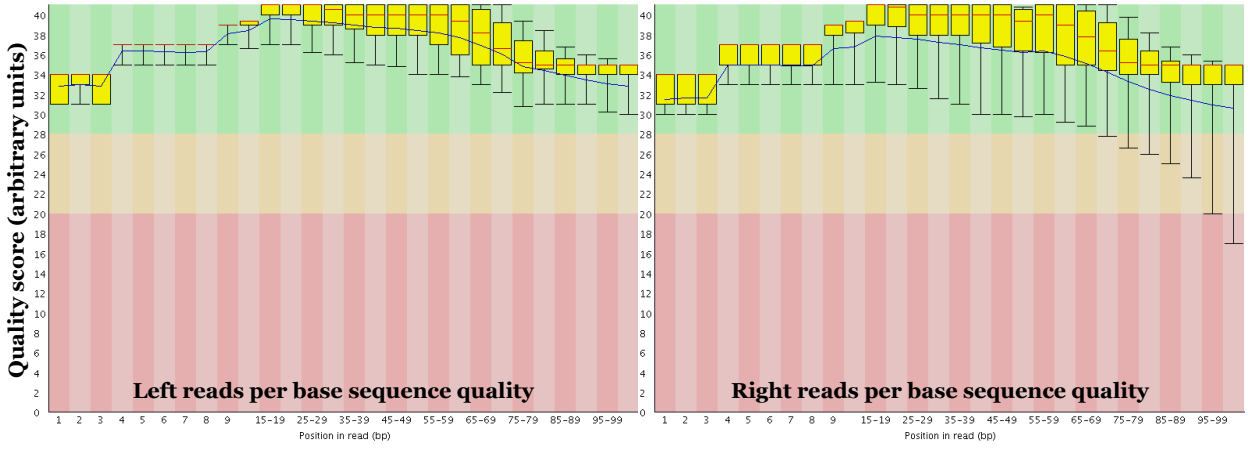

Figure 4.1 FastQC analysis of raw reads of amygdala samples
FastQC analysis revealed that all scores for each base fell in the "very good" (>28, green) range.

4.3.2 Assembly optimization and annotation

The *de novo* assembly generated 1.2M possible genes, likely many more genes than are truly represented in the hamster amygdala. To control for any sequences that were assembled incorrectly during the *de novo* assembly process, we first optimized our assembly using TransDecoder to determine the number of probable coding sequences within the assembly. A schematic of the assembly optimization process is shown in Figure 4.2. Complete coding sequences accounted for 528,193 of the 887,774 open reading frames. The remainder of the sequences were 5-prime partial (206,792), 3-prime partial (117,384), or internal (35,405). Because the sequencing protocol used had a 3-prime bias, all sequences that were either complete or 5-prime partial were retained for the optimized assembly, as these were the sequences that were most likely to code for actual genes (Senatore et al., 2015). We also filtered the full assembly through BLASTx (Uniprot-rodent database, 1/21/16) to match our sequences to known rodent gene sequences. BLASTx returned 1,319,393 matches, however many of these were at very low confidence parameters, thus only those with an E-value of ≤1e-10 and a percent identification match of ≥50 were included (148,726). These stringent parameters provide enhanced confidence in the quality of our optimized and annotated transcriptome (MacManes and Lacey, 2012; Feng et al., 2015). We then merged our data from TransDecoder and BLASTx, leaving 120,003 transcripts matching 14,493 unique BLAST identifiers. As mentioned in Chapter 3, these numbers are consistent with data in humans and mice that report there are as many as 10x the number of transcripts as compared with the number of genes, and that 8,000-15,000 mRNAs are expressed in any quantified sample (Hastie and Bishop, 1976; Venter et al., 2001; Su et al., 2004; Carninci et al., 2005).

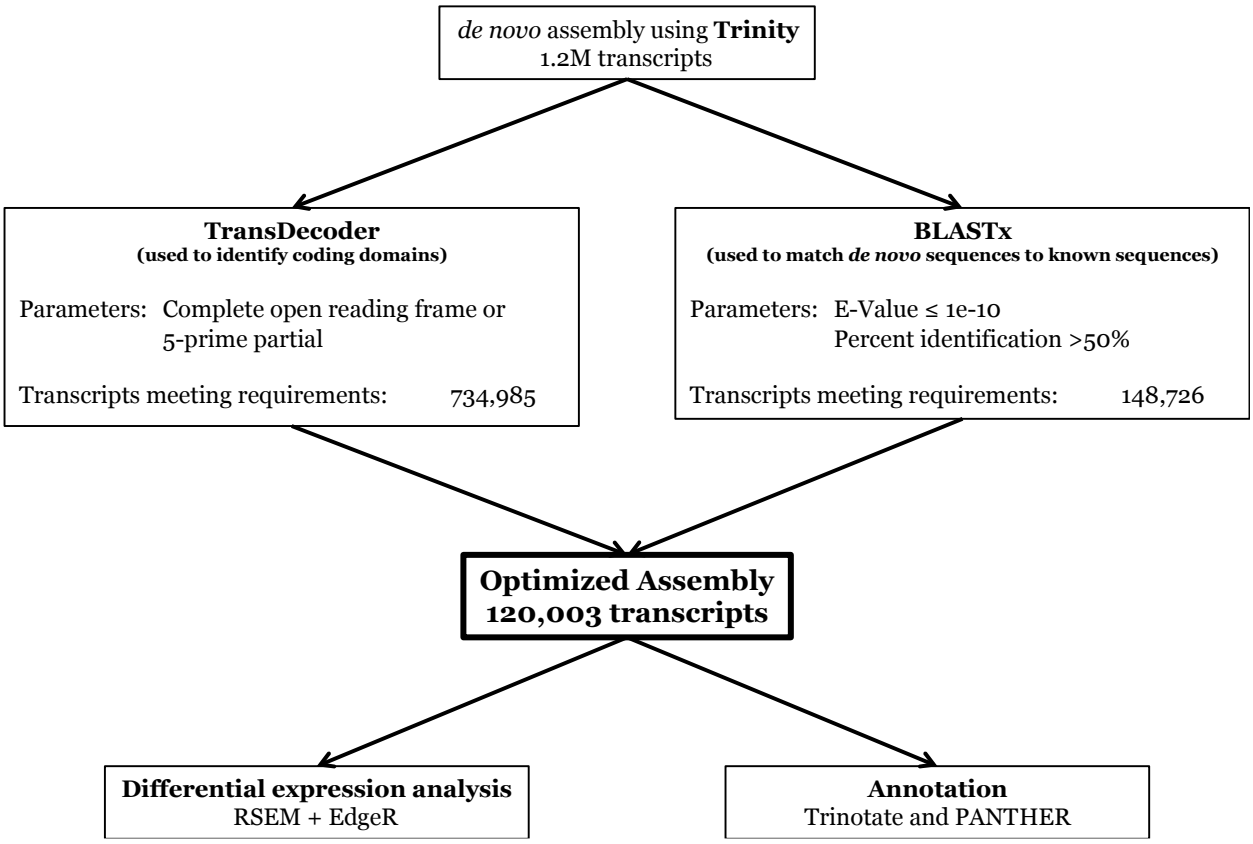

Figure 4.2 Schematic of assembly optimization
After initial *de novo* assembly using Trinity, we optimized the assembly using several programs to omit falsely assembled sequences or sequences that were not likely to code for an actual gene. After optimization, we used RSEM to generate expected counts of each transcript from the raw reads and used those reads to calculate differential expression between animals of different social status compared with home cage controls within males and females using edgeR. Annotation of the optimized assembly was completed using Trinotate and PANTHER.

4.3.3 Differential expression analyses

Expected read counts from each sample were calculated using RSEM to determine which genes were most highly expressed. The most highly expressed genes in the hamster amygdala (both male and female) are listed in Supplemental Table 3. Of the top 20 most highly expressed genes in the amygdala, 5 were also ranked in the top 20 most highly expressed genes in the whole brain of male and female hamsters (*Eef1a1*, *Scd2*, *Map1a*, *Hsp90aa1*, *Gapdh*). *Eef1a1*, an elongation factor involved in translation and cytoskeletal remodeling, is ubiquitously expressed in other species (Abbott and Proud, 2004). *Scd2* is most highly expressed in brain tissue of humans and mice

(Kaestner et al., 1989; Zhang et al., 2005) and *Map1a* reaches peak expression in mature neurons of the adult brain (Schoenfeld et al., 1989; Garner et al., 1990). *Hsp90aa1*, a highly conserved molecular chaperone, belongs to the heat-shock 90 protein family (Chen et al., 2005) and finally, *Gapdh* is found in most tissue samples and often used as a housekeeping gene for differential expression analyses (Barber et al., 2005).

We examined baseline expression of HDACs in the hamster amygdala. Previous studies show that HDAC3 is the most highly expressed HDAC in the rat brain and amygdala (Broide et al., 2007), however, we found that *Hdac2* was the most highly expressed HDAC in the hamster amygdala, consistent with the expression observed in the whole brain of male and female hamsters (Figure 4.3). There were also some observed trends for lower overall HDAC expression in males compared with females. Currently, very little data exists defining sex differences in histone acetylation in adult brains, however some developmental and neonatal studies have been completed examining the effect of acetylation on sex differences during development. For example, administration of the HDAC inhibitor, valproic acid, on the day of birth decreases volume and cell number in the bed nucleus of the stria terminalis in male mice and in females treated with testosterone (Murray et al., 2009). This nucleus is sexually dimorphic and is normally larger in volume and cell count in males compared with females. Another study found sex differences in acetylation patterns in neonatal cortex and hippocampus, but not amygdala (Tsai et al., 2009). These data suggest that histone acetylation may play an important role in the sexual differentiation of certain brain regions during development, however future studies are needed to further examine the biological relevance of potential sex differences in HDAC expression in the amygdala of adult hamsters.

Differential expression analyses were then completed on male and female samples using edgeR. Samples from dominant and subordinate hamsters were compared to samples from same-sex home cage controls. Supplemental Table 4 lists all the differentially expressed genes found in the male amygdala between animals of different social status. A higher number of genes increased in dominants (73) and subordinates (57) compared with the number of genes that decreased compared with controls (35 in dominants and 22 in subordinates) (FDR < 0.05). Fifty-three transcripts were more highly expressed in dominant females than in home-cage controls, while 30 transcripts decreased in expression. Samples from submissive females had a similar increase in expression (59), however had significantly more transcripts (63) that decreased when compared with controls (FDR < 0.05). Supplemental Table 5 is a comprehensive list of differentially expressed genes in females.

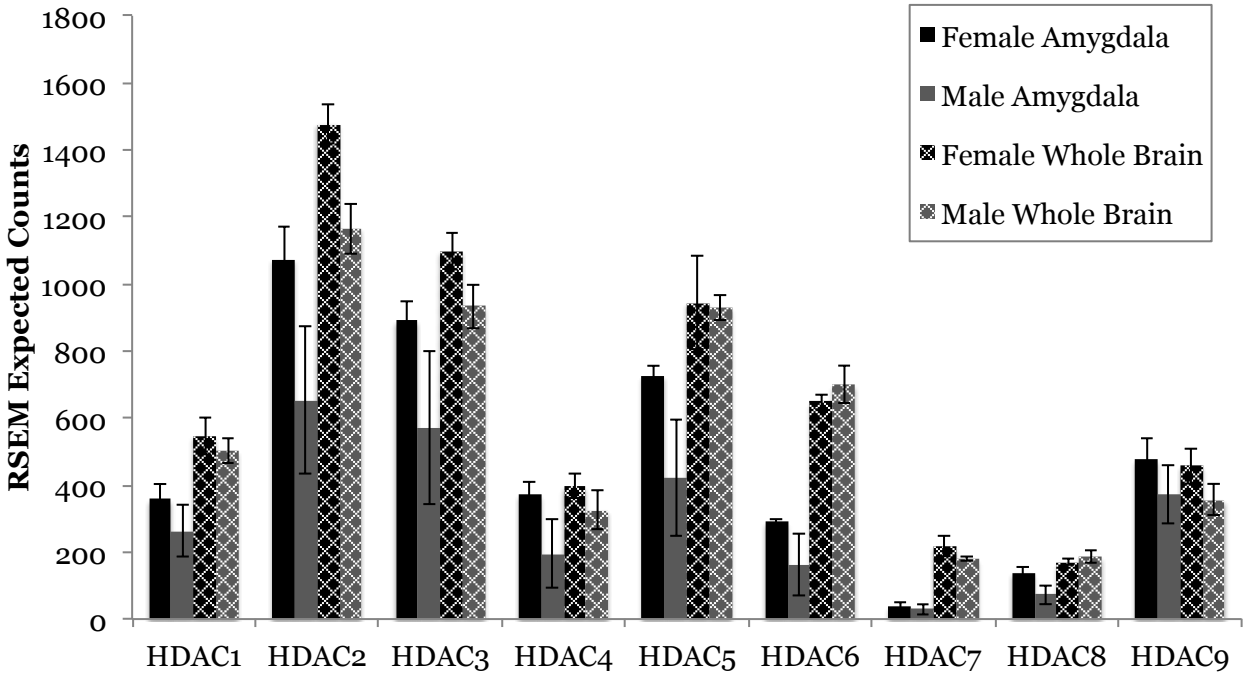

Figure 4.3 HDAC expression in the amygdala and whole brain of male and female hamsters
Expression patterns of HDACs in the amygdala and whole brain based on highest expressed isoform.

For our *a priori* analyses, we tested the differential expression of *Hdac 1-9*. We found that *Hdac4* significantly decreased ($F(2,6)=9.059$, $p=0.015$), while *Hdac6* significantly increased ($F(2,6)=24.573$, $p=0.001$) in dominant and submissive females compared with home cage controls (Figure 4.4). HDAC4 and HDAC6 have recently been linked to long-term memory formation and HDAC4 is a regulator of brain-derived neurotrophic factor (BDNF) expression (Kim et al., 2012; Sailaja et al., 2012; Fitzsimons et al., 2013; Koppel and Timmusk, 2013; Selenica et al., 2014), which has been shown to play an important role in the formation of dominant and subordinate status in male hamsters and mice (Berton et al., 2006; Taylor et al., 2011). Surprisingly, there were no significant changes in HDAC expression in male dominant or subordinate animals. However, while not reaching significance given our conservative *a priori* cutoffs for statistical analyses, *Hdacs 1*, *2*, and *3* each appear to be increasing in dominant and subordinate males compared with controls. Future experiments with larger sample sizes will reexamine HDACs following agonistic interactions using quantitative real time PCR.

Several additional differentially expressed genes are also involved in epigenetic regulation in the brain and require further investigation into the specific role they have in mediating behavioral changes after acute social defeat. Specifically, HDAC inhibition increases expression of *Abcd3*, a gene that increased in subordinate males, in a model of X-adrenoleukodystrophy, a disease state in which very long chain fatty acids accumulate in myelin in the central nervous system (Singh et al., 2011). The observed increase in subordinate males after acute social defeat offers this gene as a potential candidate in facilitating the observed increase in submission and avoidance after HDAC inhibition and suboptimal defeat (Chapter 2). Furthermore, in a model of medullablastoma, *Cul3*, which decreased in dominant males and females, interacts directly with HDACs in the

brain to regulate transcription (De Smaele et al., 2011; Nor et al., 2013). Manipulations of these genes in future experiments will further elucidate their role and test their necessity for social stress-induced behavioral changes.

In addition, *Gria2*, an ionotropic glutamate receptor, increased significantly in dominant and subordinate males compared with controls. *Gria2* is associated with stimulus-reward learning (Mead and Stephens, 2003), increases after HDAC inhibition (Nor et al., 2013), and has also been linked to sex differences in major depressive disorder (Gray et al., 2015a). *Gad2*, the gene that encodes the protein GAD65, increased in dominant males after an acute agonistic interaction. This gene is directly modulated by HDAC activity (Pan, 2012; Tao et al., 2015) and is reduced in patients with major depressive disorder (Tripp et al., 2012). Furthermore, *Cdk5*, a gene that increased in dominant and subordinate females, decreases after administration of the HDAC inhibitor, valproic acid, (Takahashi et al., 2014) and directly regulates histone acetylation in order to mediate neuronal survival (Fu et al., 2013). Finally, *Mbd1*, which decreased in dominant females, increases with the administration of fluoxetine, a selective serotonin reuptake inhibitor, or the administration of cocaine, with associated decreases in acetylated histone 3 and increases in HDAC activity (Cassel et al., 2006). Together, these genes further support a role of histone acetylation in mediating the long-term behavioral changes that are observed following social stress.

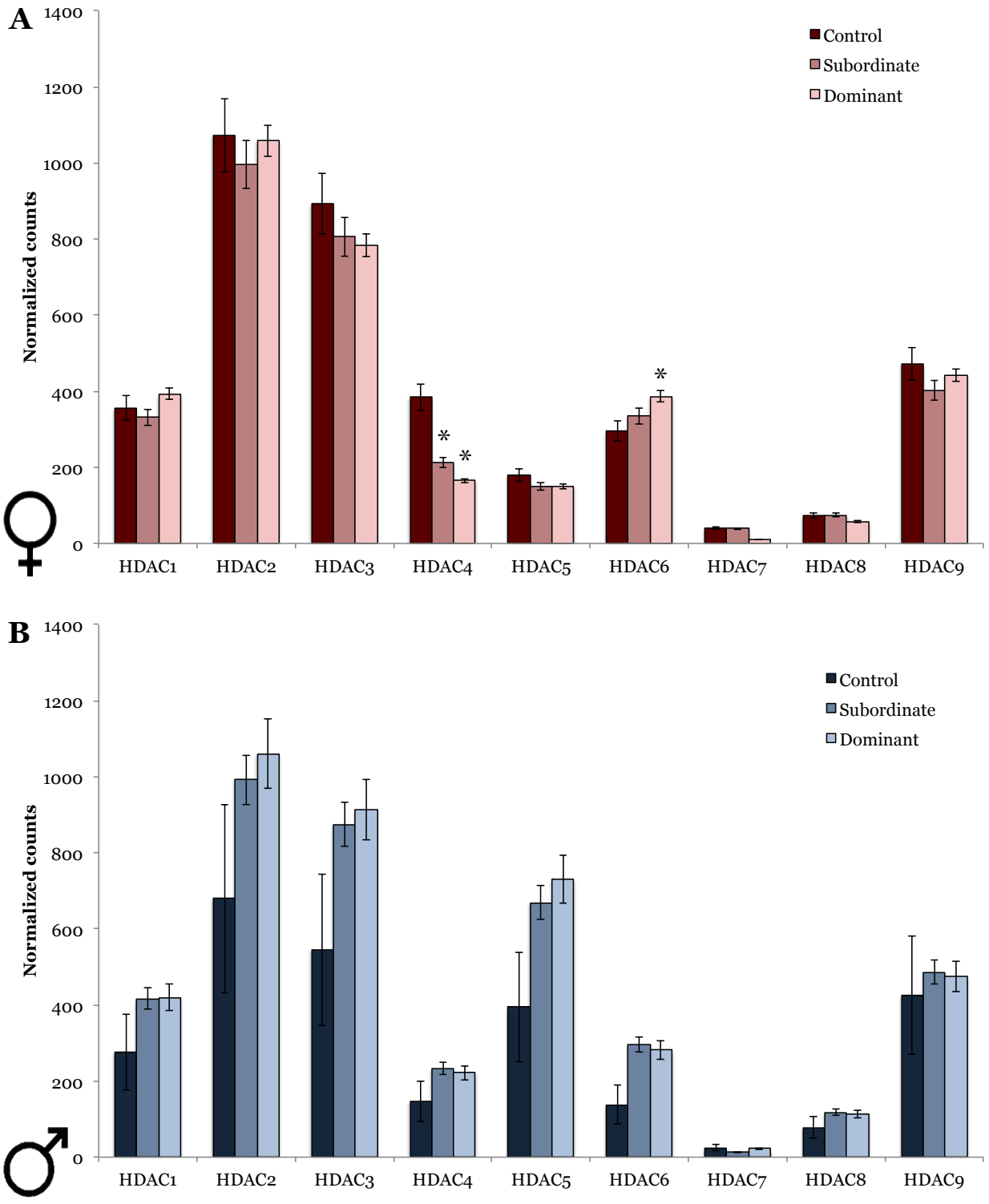

Figure 4.4 Differential expression of HDACs in the amygdala across animals of different social status
Males and females of different social status show similar expression of HDACs in the amygdala. HDAC4 was significantly reduced in the amygdala of dominant and subordinate females when compared with home cage controls. HDAC6 was significantly higher in dominant females compared with subordinates and controls. *p<0.05 compared with same-sex controls

We also examined genes associated with learning and memory, mood and anxiety disorders, and social behavior. Several genes that had lower expression in animals that experienced an agonistic encounter have been linked to bipolar disorder (*Akap5*) (Bernstein et al., 2013), general mood disorders (*Aldh1a1*) (Qi et al., 2015), anxiety (*Kif13a*) (Zhou et al., 2013), and depression (*Mgat5*) (Soleimani et al., 2008). Other genes linked to major depressive disorder (*Gad2*, *Gria2*) (Tripp et al., 2012; Gray et al., 2015a), PTSD (*Dicer1*) (Wingo et al., 2015), and anxiety (*Spock3*) (Yamamoto et al., 2014) had higher expression in dominant and/or subordinate animals when compared with controls. Specifically, *Dicer1*, a gene directly involved in the expression of other genes by regulating the production of microRNAs, increased in dominant males and, consistent with this effect, increases in this gene have been linked to stress resilience (Dias et al., 2014). On the other hand, decreases in *Dicer1* are observed in patients suffering from PTSD and depression compared with healthy controls (Wingo et al., 2015). In addition, *Uba6* decreased in subordinate males, consistent with previously observed increases in social avoidance in animals with a depletion of this gene (Lee et al., 2015).

Furthermore, *Gad2* encodes GAD65 and is associated with major depressive disorder, as described above. Glutamic acid decarboxylase (GAD) catalyzes the formation of GABA from glutamate, and GAD65, in particular, is involved in GABA synthesis specifically for neurotransmission. GAD65 increases in several nuclei after acute and chronic stressors, including specific nuclei within the bed nucleus of the stria terminalis and hypothalamus (Bowers et al., 1998), and here we demonstrate that *Gad2* increased in the amygdala of dominant males. This increase in expression suggests a potential increase in GABA stores available for neurotransmission in the numerous

GABAergic neurons in the amygdala. An increase in GABA neurotransmission in the amygdala during social defeat would suppress the conditioned defeat behavioral phenotype, thus potentially providing a protective effect in dominant animals against the stress of the encounter. Lastly, our laboratory has recently shown that BDNF modulates the acquisition, consolidation, and expression of conditioned defeat. Several differentially expressed genes in dominant males and females have been linked to the regulation of BDNF (*Eif4ebp2*, *Gad2*, *Ldlr*, *Eps8*, *Mbd1*) and at least one gene in subordinate males (*Tnr*) is regulated by BDNF (Maruyama et al., 2007; Menna et al., 2009; Tian et al., 2009; Panja et al., 2014; Tao et al., 2015; Zunino et al., 2016). Future studies will examine how manipulations of these genes, in concert with BDNF, mediate behavioral changes after acute social stress.

Finally, numerous genes that were differentially expressed in dominants and subordinates of both sexes compared with same-sex controls were genes related to dendritic growth, complexity, axon guidance, and synaptic reorganization (*Atp8a2*, *Atl1*, *Bmpr1b*, *Dcc*, *Epha10*, *Igsf11*, *Kiaa2022*, *Mdga2*, *Eps8*, *Frs2*, *Nell2*, *Slc4a10*, *Slitrk2*), and are all considered to be markers of neuroplasticity (Aruga and Mikoshiba, 2003; Joset et al., 2011; Xu et al., 2012; Gao et al., 2013; Majdazari et al., 2013; Menna et al., 2013; Van Maldergem et al., 2013; Xia et al., 2013; Xu et al., 2014; Jaworski et al., 2015; Sinning et al., 2015; Zhou et al., 2015; Antoine-Bertrand et al., 2016; Jang et al., 2016). The expression of the majority of these genes was higher in dominant animals, especially males, with some also higher in subordinate animals. Several of these genes, however, had lower expression than that seen in controls, especially in dominant females (e.g., *Nell2*, *Slc4a10*, *Slitrk2*). Together, these data provide additional evidence for increased plasticity in the amygdala after an acute agonistic encounter and future

investigation may lead to specific pathways that are being altered through the regulation of these genes.

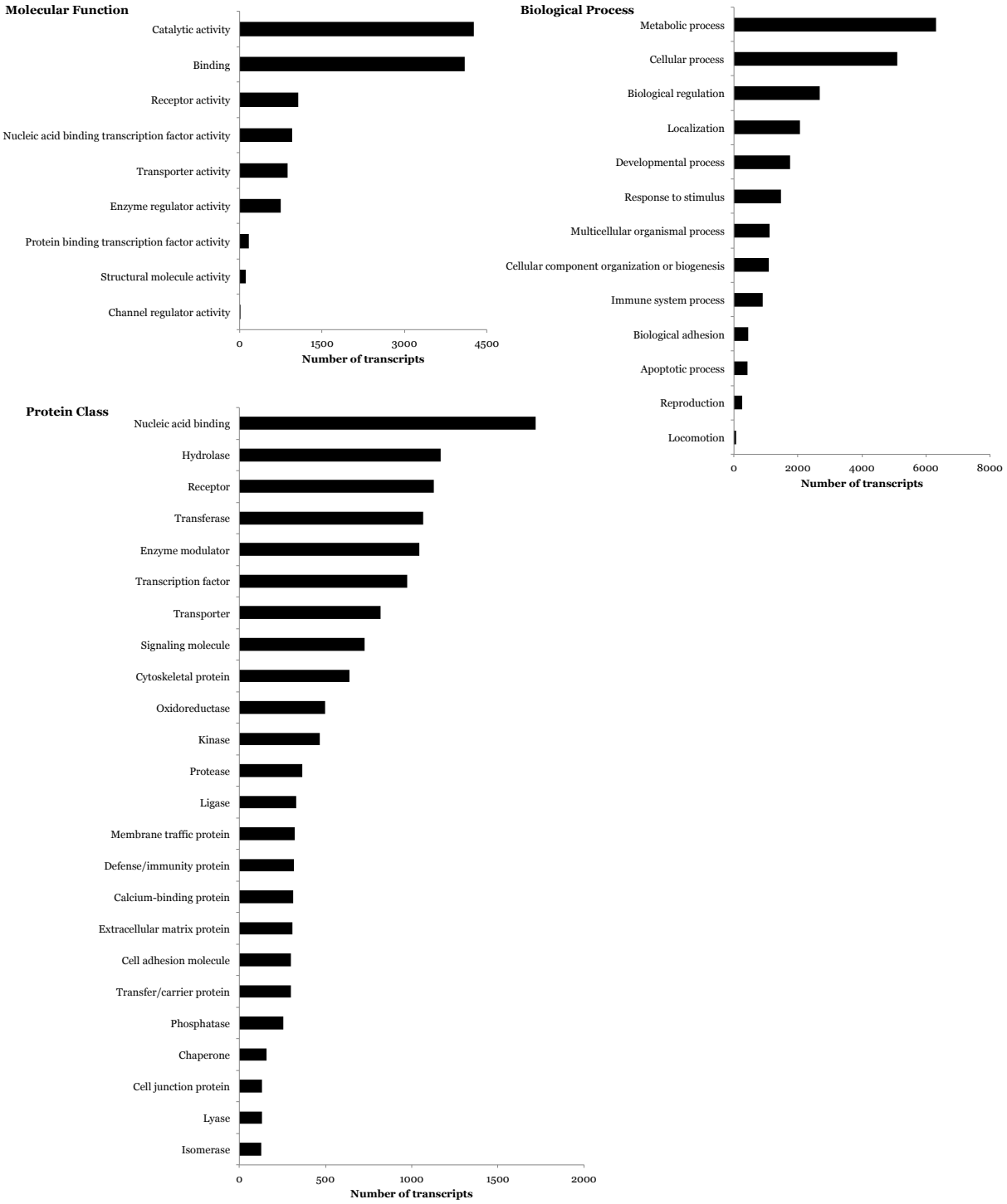

Figure 4.5 PANTHER analysis from optimized amygdala assembly
We used PANTHER analysis to match the transcripts in the optimized transcriptome (14,493 unique transcripts) to gene ontology terms for functional annotation of the assembly. These are the top hits from each category.

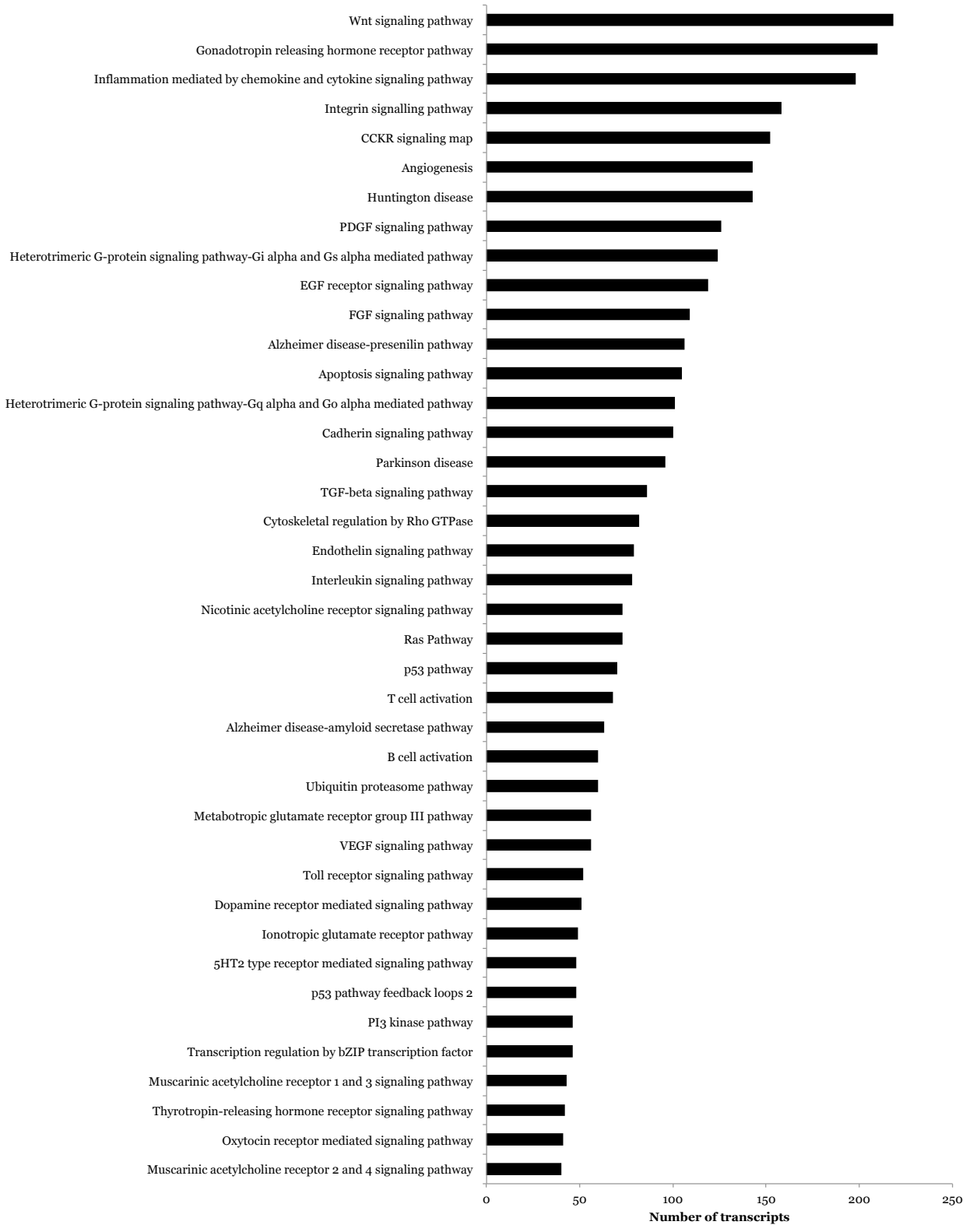

Figure 4.6 Pathways in the hamster amygdala
Top pathways represented in the optimized amygdala transcriptome of male and female hamsters

4.3.4 Gene ontology analysis and expression patterns in the amygdala

The optimized assembly and the subsets of differentially expressed genes were analyzed using PANTHER to determine which molecular functions, biological processes, protein classes, and pathways were most represented. There were a total of 13,113 molecular functions, 23,661 biological processes, 13,812 protein classes, and 5,143 pathways among the 14,493 unique genes in the optimized assembly. Catalytic activity and binding were the highest represented molecular functions, whereas metabolic and cellular processes ranked highest in biological processes. The top hits among all categories are highlighted in Figure 4.5 and Figure 4.6.

We next analyzed our subsets of differentially expressed genes to highlight specific functions and pathways that underlie the changes observed after an acute agonistic encounter. Figure 4.7 and Figure 4.8 show the top matches for each function, process, and class in females and males, respectively. The total number of classifications for each subgroup is listed in Table 4.2. In addition, some pathways were represented by multiple transcripts and may be of significance for future investigation. Three genes that increased in subordinate females represented the dopamine-mediated signaling pathway and nicotine pharmacodynamics pathway (*E41l1*, *E41l2*, *Cdk5*). We have previously shown that dopamine in the nucleus accumbens modulates the acquisition and expression of conditioned defeat (Gray et al., 2015b), thus these genes may be of further interest to determine how the dopamine signaling pathway in the amygdala is interacting with other nuclei to modulate stress-induced behavior. The gonadotropin releasing hormone pathway was represented in 4 genes that decreased in subordinate females (*Nab1*, *Nfyb*, *Bmr1a*, *Plcb1*) and 3 genes that increased in dominant males (*Bmr1b*, *Pp2ba*, *Tba1b*). We have demonstrated the roles of gonadal hormones in

agonistic behavior (Faruzzi et al., 2005; Solomon et al., 2009) and future manipulation of these specific genes may further define the role these hormones have in mediating behavior during and after agonistic encounters. Several additional pathways were represented in the differentially expressed genes, including multiple glutamate receptor pathways, beta 1 and 2 adrenergic receptor signaling pathways, 5HT2-type receptor mediated signaling pathway, oxytocin receptor mediated signaling pathway, and GABA synthesis. Assigning these functional annotations to the differentially expressed genes provides detailed information for designing future experiments to target these genes and pathways in order to more precisely determine their role in mediating social stress-induced behavior.

Finally, we used a weighted correlation network analysis to determine the similarity in gene expression patterns of the dominant, subordinate, and control samples in males and females. Analyzing gene expression in the optimized assembly (120,003 transcripts), we graphed the connectivity of our samples based on overall gene expression patterns. As seen in Figure 4.9, all six samples from subordinate animals are grouped closely together. This suggests that overall gene expression patterns in the amygdala are consistent across subordinate animals, regardless of sex. Samples from dominant and control animals, however, are intermixed, suggesting that overall expression patterns in these groups are not distinct from one another, again independent of sex. This is not surprising given that the behavioral phenotype of control animals is aggressive, closely resembling that of dominant animals. Furthermore, at first glance it appears that 'Control Male A' and 'Control Male C' are potential outliers. Males, however, are less aggressive than females during an initial agonistic encounter with a same-sex conspecific and often have a longer latency to attack. This latency discrepancy

disappears in subsequent encounters once a male has had the opportunity to win. It is therefore possible that control males are distinct from dominant animals and control females and that perhaps 'Control Male B' is the outlier within that group. Future investigation will look at the specific gene networks and how they relate across sex and social status.

4.4 Conclusion

Transcriptomic analysis of the hamster amygdala revealed the specific genes and pathways that were up- or down-regulated after a single agonistic encounter in dominant and/or subordinate hamsters. Some of these genes overlapped in males and females, but the majority did not. Furthermore, overall expression patterns of gene networks did not differ between males and females, suggesting that while individual gene expression may differ between males and females of different social status, overall network changes in response to social stress within the amygdala are similar. This is consistent with previous data and theories describing sex differences, in that specific differences between the sexes may be attributed to sex-specific pathways to reach the same ultimate goal (De Vries, 2004; de Vries and Forger, 2015). Within the individual gene differences, we found a sizable number of differentially expressed genes in both males and females that were directly involved in the acetylation and deacetylation of histones, including specific HDACs. We have previously shown that decreasing histone acetylation impairs social stress-induced behavioral changes while increasing acetylation enhances these behavioral effects. Our current data contribute to the hypothesis that histone acetylation is an underlying mechanism contributing to the acquisition of conditioned defeat and also highlight other potential factors contributing

to the epigenetic regulation of conditioned defeat, including genes that epigenetically regulate GABA and glutamate neurotransmission. Together, these data support the hypothesis that epigenetic regulation within the amygdala is at least one important component underlying stress-induced behavioral change in both males and females.

4.5 Acknowledgements

Authors of manuscript to be submitted for publication: Katharine E. McCann, David M. Sinkiewicz, Kim L. Huhman

Research reported here was supported by the National Institute of Mental Health of the National Institutes of Health under Award Number R01MH062044 awarded to KLH and by a Seed Grant awarded to KLH from the Brains and Behavior Program at Georgia State University. The content is solely the responsibility of the authors and does not necessarily represent the official views of the National Institutes of Health. The authors would like to acknowledge SE Pathirannehelage and A Norvelle for their assistance with this project.

Table 4.2 Total number of categories represented for each subgroup of differentially expressed genes

	Molecular Function	Biological Process	Protein Class	Pathway
↑Dominant Female	43	79	46	19
↓Dominant Female	36	57	38	7
↑Subordinate Female	58	94	53	29
↓Subordinate Female	62	96	70	39
↑Dominant Male	65	117	68	29
↓Dominant Male	31	36	42	16
↑Subordinate Male	57	96	54	8
↓Subordinate Male	15	30	22	13

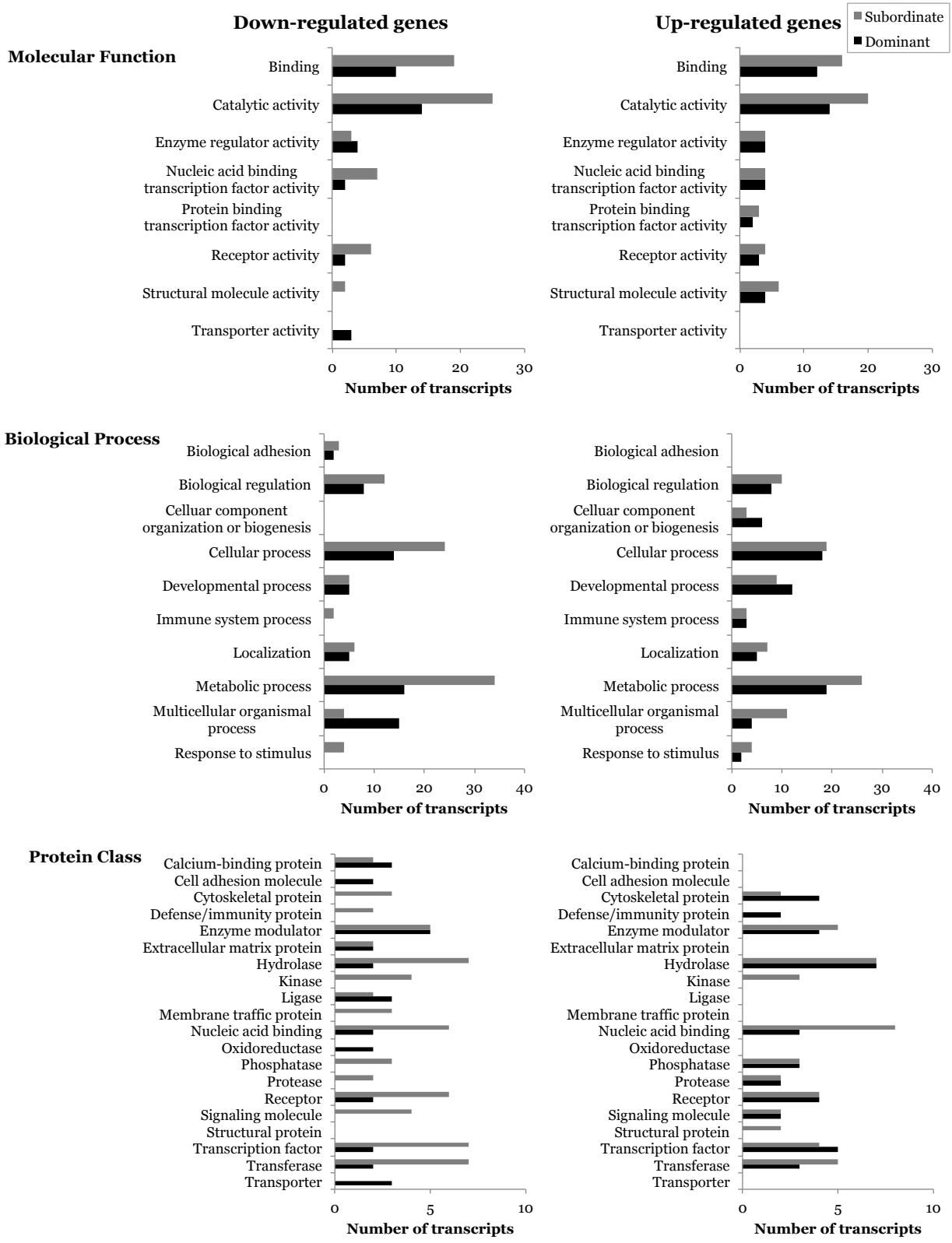

Figure 4.7 PANTHER analysis in females
Gene ontology terms most represented in genes that were differentially expressed in females of different social status (UP: 53 in dominants, 59 in subordinates; DOWN: 30 in dominants, 63 in subordinates)

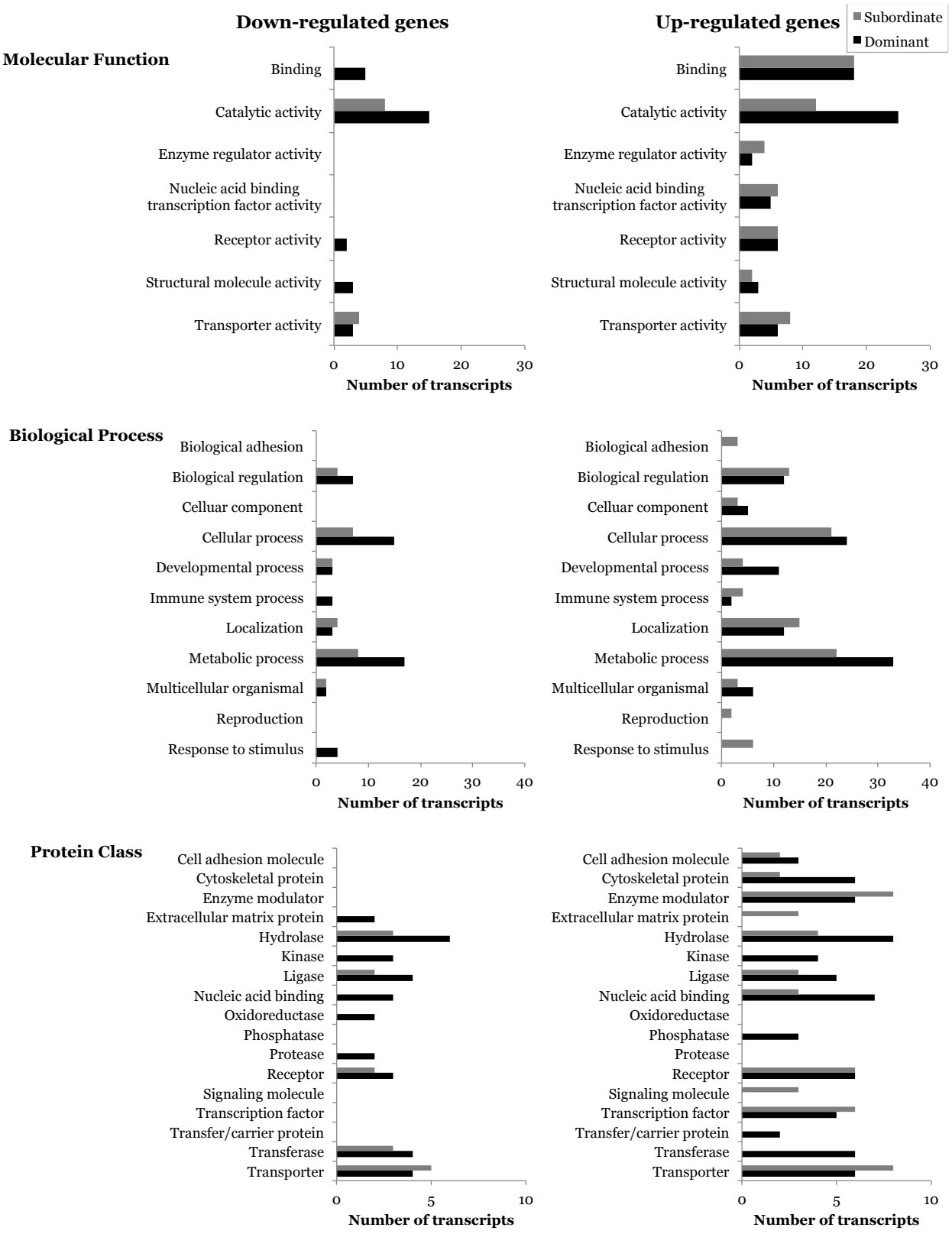

Figure 4.8 PANTHER analysis in males
Gene ontology most terms represented in genes that were differentially expressed in males of different social status (UP: 73 in dominants, 57 in subordinates; DOWN: 35 in dominants, 22 in subordinates)

Figure 4.9 Weighted co-expression network analysis
Sample clustering of all 18 amygdala samples based on gene expression patterns from optimized assembly (120,003 transcripts). All 6 samples from subordinate animals cluster together (red box) regardless of sex. Samples from dominant and control males and females are not distinct from one another.

5 Conclusions

5.1 Summary of current findings

Social stress can lead to long-term changes in mood and behavior, and it is likely that epigenetic regulation of gene expression facilitates at least some of these changes. There is a considerable amount of data supporting the role of epigenetic regulation, specifically histone acetylation, in mediating behavioral responses to stressful experiences. For example, inhibition of histone deacetylases (HDACs) enhances, while inhibition of histone acetyltransferases (HATs) impairs, conditioned fear responses

(Bredy and Barad, 2008; Maddox et al., 2013b). The majority of the available data investigating the role of histone acetylation in mediating stress-induced behavioral responses use non-social models of stress (e.g., foot or tail shock), and those that do use more ethologically relevant social stressors often employ chronic or repeated stressors. These chronic models are valuable in understanding the mechanisms underlying some stress-induced behavioral changes. There are some important gaps in the existing literature, however.

First, while social stress is the most common stressor in humans, it is not always chronic in nature. Acute social stress is also known to lead to or exacerbate mental illness (Bjorkqvist, 2001; Tamashiro et al., 2005; Borghans and Homberg, 2015). Modeling acute social stress not only contributes to an understanding of the intensity or duration of stress required to elicit changes in behavior but also allows us to more precisely determine when acquisition and consolidation are occurring. This, in turn, allows for experimental interventions that directly target individual stages of memory processing (e.g., acquisition, consolidation, extinction). This precise temporal resolution is lost in models of chronic stress. Second, and perhaps more important, the vast majority of research reporting the effects of histone acetylation on behavioral responses to social stress is done almost exclusively in males. Clinical populations exhibit sexually dimorphic trends in mental illness (e.g., females are more likely to be diagnosed with depression and to develop PTSD after a traumatic experience), coping mechanisms (e.g., males tend to develop more active coping skills), and behavioral patterns (e.g., males tend to exhibit higher rates of aggression and autism). Thus, it would appear to be a grave error to assume that results obtained using only males will necessarily explain the to underlying mechanisms of stress-induced behavioral changes in females (Weissman

and Klerman, 1977; Nolen-Hoeksema, 1987; Breslau et al., 1997; Altemus, 2006). In order to begin to fill some of these gaps in our existing knowledge on how epigenetic regulation influences behavioral responses to social stress, we used a translational model of acute social stress in male and female Syrian hamsters.

As described previously, Syrian hamsters represent a unique model of social stress in which behavioral responses to social stress are elicited in both males and females after a single agonistic encounter. The subsequent dramatic shift in behavior after losing one encounter, from territorial aggression to complete submission and social avoidance, has been termed conditioned defeat. In addition, because hamsters do not typically suffer injuries when fighting, we are able to separate the stress of physical injury, which often occurs in chronic defeat models, with the psychological stress of losing an agonistic encounter. The overarching goal of this project was to test the hypothesis that epigenetic changes within the neural circuit that mediates conditioned defeat contribute to the observed behavioral changes after acute social stress and that some of these changes are sexually dimorphic.

We first tested the effect of systemic manipulation of histone acetylation on the acquisition of conditioned defeat. Systemic administration lacks anatomical resolution to determine where the drug is acting but has valuable translational implications for the potential usefulness of the drugs for clinical populations, particularly when we use drugs that are already FDA-approved. We found that systemic administration of an HDAC inhibitor enhances the behavioral responses of both males and females to acute social stress. This treatment also suppressed defeat-induced immediate-early gene activity in the infralimbic region of the prefrontal cortex. We further tested the role of histone acetylation in the infralimbic cortex in mediating behavioral responses to acute social

stress with site-specific manipulations. Consistent with the peripheral effect of HDAC inhibitors, HDAC inhibition in this brain region also enhanced behavioral responses to acute social stress. Furthermore, HAT inhibition in the infralimbic cortex impaired the acquisition of conditioned defeat. These opposing behavioral effects of HDAC and HAT inhibition, in conjunction with the decrease in immediate-early gene activity after systemic HDAC inhibition, support a role of histone acetylation in the infralimbic cortex in mediating behavioral responses to acute social stress. Surprisingly, we did not find an effect of HDAC inhibition in the basolateral amygdala. We have demonstrated that the BLA is necessary for acquisition and expression of conditioned defeat (Jasnow et al., 2005; Markham et al., 2010), that *de novo* protein synthesis in the BLA is required for social stress-induced behavioral change and that overexpression of cyclic AMP binding protein in this nucleus during social defeat enhances conditioned defeat (Jasnow et al., 2005; Markham and Huhman, 2008). Thus, it is clear that neurobiological mechanisms including gene regulation in the BLA area a critical mediator of the behavioral responses to social defeat, however we did not alter these mechanisms by pharmacological manipulation of Class I HDACs.

To define further the role of the BLA and to determine potential underlying genetic and epigenetic mechanisms mediating conditioned defeat, we used transcriptomic analysis. Because both males and females exhibit conditioned defeat but the behavioral expression is more pronounced in males (Huhman et al., 2003), we also used transcriptomic analysis to investigate potential genetic mechanisms leading to this sexually dimorphic expression. We sequenced the whole brain transcriptome of male and female hamsters as well as the transcriptome of the BLA of dominant, subordinate, and control animals. Our analysis revealed over 200 transcripts that were differentially

expressed in the whole brain of males and females, including several that mediate histone acetylation, including *Hdac5*. In the amygdala, dominant females had 83 transcripts that were differentially expressed compared with controls and subordinates had 122 differentially expressed genes. In males, dominant animals had 108 transcripts that were differentially expressed compared with controls, while subordinates had only 79. Some overlap was present in the genes were differentially expressed in males and females, including *Cul3*, which interacts with HDACs to regulated gene transcription and several lysine-specific demethylases (*Kdm*) (De Smaele et al., 2011; Nor et al., 2013). The majority of the differentially expressed genes, however, were unique to each sex. Interestingly, when we analyzed the overall gene expression patterns to determine the unique networks within which these differentially expressed genes fell, no sex differences emerged. These data suggest the possibility that many of the unique genes differentially regulated in the amygdala of males and females may simply represent different strategies that the sexes must take to reach the same overall physiological function and similar, but not exact, behavioral outcomes.

5.2 Limitations and future directions

Several aspects of these data should also be further investigated in future experiments. First, our pharmacological data used non-specific drugs to target primarily Class I HDACs (HDACs 1, 2, 3, and 8), because this class of HDACs is known to be important in learning and memory. Our transcriptomic data suggests, however, that while targeting specific Class I HDACs in males may be of further interest, Class II HDACs, specifically HDAC 4 and 6, may be mediating some of the observed behavioral changes in females. Targeting specific HDACs may also provide a more precise picture

of the role of histone acetylation during acute social stress. In addition to targeting specific HDACs, future experiments should also examine the role of specific acetylation targets on histone tails. For example, H3K14ac (acetylation specifically on histone H3, lysine 14) increases in the nucleus accumbens after chronic social defeat in mice and is increased in this nucleus in post-mortem tissue of depressed patients (Covington et al., 2009). Consistent with our transcriptomic data highlighting specific genes involved in epigenetic regulation in the amygdala, we recently found that H3K14 acetylation increases in the BLA after social defeat (Figure 5.1). The acetylation of H3K14 is also associated with an increase in gene transcription and thus may underlie at least some of the differential gene expression observed in the amygdala 24hr after social defeat.

Another limitation of the current project is that the tissue for transcriptomic analysis was pooled based on social status (e.g., dominant or subordinate) and not by resident or intruder status. While we have consistently observed that residence does not necessarily confer dominance in weight-matched pairs, it is possible that home cage versus intruder status may still account for some of the variability observed among samples. In addition, transcriptomics measures RNA transcripts, but we know that differences in mRNA do not necessarily translate into protein differences. Future studies will measure protein expression of specific genes of interest as well as RNA expression. Finally, future studies will also include tissue from the infralimbic cortex and other nodes of the neural circuit mediating conditioned defeat to determine which genes and pathways are altered in the circuit components to result in the behavioral changes observed after social stress.

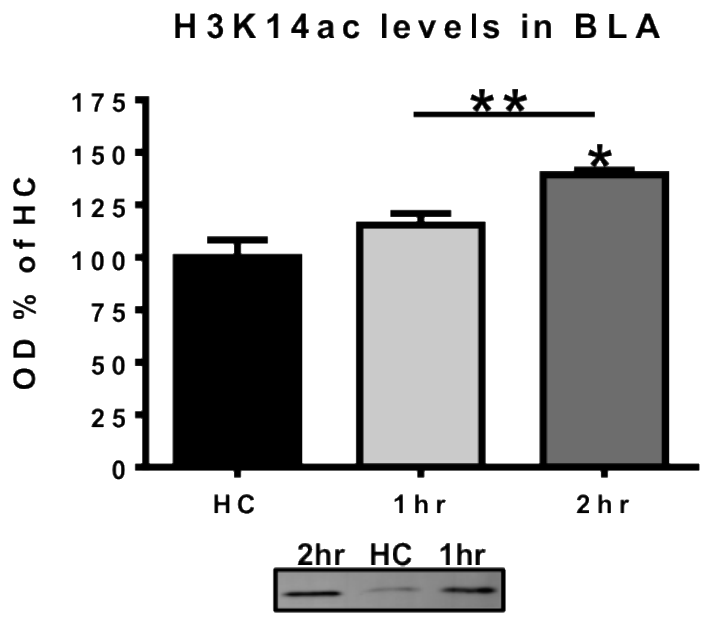

Figure 5.1 H3K14 acetylation after social defeat
H3K14 acetylation significantly increases in the BLA 2hr after social defeat

Overall, the data presented here demonstrate that histone acetylation, at least in part in the infralimbic cortex (Chapter 2) and possibly in the amygdala (Chapter 4), mediates behavioral changes observed after acute social stress in males and females. These data support the role of histone acetylation in two different nuclei of the neural circuit mediating conditioned defeat and provide potential targets for novel, sex-specific interventions in the clinical population. Finally, the fully sequenced transcriptome offers invaluable information that can be used to promote understanding of the genetic and molecular mechanisms that mediate social stress-induced neuropsychiatric disorders as well as a host of other important biomedical questions for which hamsters represent an excellent model.

References

Abbott CM, Proud CG (2004) Translation factors: in sickness and in health. Trends in biochemical sciences 29:25-31.

Agid O, Kohn Y, Lerer B (2000) Environmental stress and psychiatric illness. Biomedicine & pharmacotherapy = Biomedecine & pharmacotherapie 54:135-141.

Agranoff BW, Davis RE, Casola L, Lim R (1967) Actinomycin D blocks formation of memory of shock-avoidance in goldfish. Science 158:1600-1601.

Albers HE, Ferris CF (1984) Neuropeptide Y: role in light-dark cycle entrainment of hamster circadian rhythms. Neuroscience letters 50:163-168.

Albers HE, Prishkolnik J (1992) Sex differences in odor-stimulated flank marking in the golden hamster (Mesocricetus auratus). Hormones and behavior 26:229-239.

Albers HE, Huhman KL, Meisel RL (2002) Hormonal basis of social conflict and communication. Hormones, brain and behavior 1:393-433.

Albertin CB, Simakov O, Mitros T, Wang ZY, Pungor JR, Edsinger-Gonzales E, Brenner S, Ragsdale CW, Rokhsar DS (2015) The octopus genome and the evolution of cephalopod neural and morphological novelties. Nature 524:220-224.

Altemus M (2006) Sex differences in depression and anxiety disorders: potential biological determinants. Hormones and behavior 50:534-538.

Altschul SF, Gish W, Miller W, Myers EW, Lipman DJ (1990) Basic local alignment search tool. J Mol Biol 215:403-410.

Antle MC, Mistlberger RE (2000) Circadian clock resetting by sleep deprivation without exercise in the Syrian hamster. The Journal of neuroscience : the official journal of the Society for Neuroscience 20:9326-9332.

Antoine-Bertrand J, Duquette PM, Alchini R, Kennedy TE, Fournier AE, Lamarche-Vane N (2016) p120RasGAP Protein Mediates Netrin-1 Protein-induced Cortical Axon Outgrowth and Guidance. The Journal of biological chemistry 291:4589-4602.

Arent CO, Valvassori SS, Fries GR, Stertz L, Ferreira CL, Lopes-Borges J, Mariot E, Varela RB, Ornell F, Kapczinski F, Andersen ML, Quevedo J (2011) Neuroanatomical profile of antimaniac effects of histone deacetylases inhibitors. Molecular neurobiology 43:207-214.

Aruga J, Mikoshiba K (2003) Identification and characterization of Slitrk, a novel neuronal transmembrane protein family controlling neurite outgrowth. Molecular and cellular neurosciences 24:117-129.

Ashburner M, Ball CA, Blake JA, Botstein D, Butler H, Cherry JM, Davis AP, Dolinski K, Dwight SS, Eppig JT, Harris MA, Hill DP, Issel-Tarver L, Kasarskis A, Lewis S, Matese JC, Richardson JE, Ringwald M, Rubin GM, Sherlock G (2000) Gene ontology: tool for the unification of biology. The Gene Ontology Consortium. Nat Genet 25:25-29.

Balasubramanyam K, Varier RA, Altaf M, Swaminathan V, Siddappa NB, Ranga U, Kundu TK (2004) Curcumin, a novel p300/CREB-binding protein-specific inhibitor of acetyltransferase, represses the acetylation of histone/nonhistone proteins and histone acetyltransferase-dependent chromatin transcription. The Journal of biological chemistry 279:51163-51171.

Bannon M, Kapatos G, Albertson D (2005) Gene expression profiling in the brains of human cocaine abusers. Addiction biology 10:119-126.

Barber RD, Harmer DW, Coleman RA, Clark BJ (2005) GAPDH as a housekeeping gene: analysis of GAPDH mRNA expression in a panel of 72 human tissues. Physiological genomics 21:389-395.

Beery AK, Zucker I (2011) Sex bias in neuroscience and biomedical research. Neuroscience & Biobehavioral Reviews 35:565-572.

Bell MR, Sisk CL (2013) Dopamine mediates testosterone-induced social reward in male Syrian hamsters. Endocrinology 154:1225-1234.

Bernstein HG, Dobrowolny H, Schott BH, Gorny X, Becker V, Steiner J, Seidenbecher CI, Bogerts B (2013) Increased density of AKAP5-expressing neurons in the anterior cingulate cortex of subjects with bipolar disorder. J Psychiatr Res 47:699-705.

Berton O, McClung CA, Dileone RJ, Krishnan V, Renthal W, Russo SJ, Graham D, Tsankova NM, Bolanos CA, Rios M, Monteggia LM, Self DW, Nestler EJ (2006) Essential role of BDNF in the mesolimbic dopamine pathway in social defeat stress. Science 311:864-868.

Bjorkqvist K (2001) Social defeat as a stressor in humans. Physiology & behavior 73:435-442.

Blanchard DC, Spencer RL, Weiss SM, Blanchard RJ, McEwen B, Sakai RR (1995) Visible burrow system as a model of chronic social stress: behavioral and neuroendocrine correlates. Psychoneuroendocrinology 20:117-134.

Blank M, Dornelles AS, Werenicz A, Velho LA, Pinto DF, Fedi AC, Schroder N, Roesler R (2014) Basolateral amygdala activity is required for enhancement of memory consolidation produced by histone deacetylase inhibition in the hippocampus. Neurobiology of learning and memory 111:1-8.

Borghans B, Homberg JR (2015) Animal models for posttraumatic stress disorder: An overview of what is used in research. World J Psychiatry 5:387-396.

Bowers G, Cullinan WE, Herman JP (1998) Region-specific regulation of glutamic acid decarboxylase (GAD) mRNA expression in central stress circuits. The Journal of neuroscience 18:5938-5947.

Bredy TW, Barad M (2008) The histone deacetylase inhibitor valproic acid enhances acquisition, extinction, and reconsolidation of conditioned fear. Learning & memory 15:39-45.

Bredy TW, Wu H, Crego C, Zellhoefer J, Sun YE, Barad M (2007) Histone modifications around individual BDNF gene promoters in prefrontal cortex are associated with extinction of conditioned fear. Learning & memory 14:268-276.

Breslau N, Davis GC, Andreski P, Peterson EL, Schultz LR (1997) Sex differences in posttraumatic stress disorder. Arch Gen Psychiatry 54:1044-1048.

Broide RS, Redwine JM, Aftahi N, Young W, Bloom FE, Winrow CJ (2007) Distribution of histone deacetylases 1-11 in the rat brain. Journal of molecular neuroscience : MN 31:47-58.

Carninci P, Kasukawa T, Katayama S, Gough J, Frith M, Maeda N, Oyama R, Ravasi T, Lenhard B, Wells C (2005) The transcriptional landscape of the mammalian genome. Science 309:1559-1563.

Cassel S, Carouge D, Gensburger C, Anglard P, Burgun C, Dietrich JB, Aunis D, Zwiller J (2006) Fluoxetine and cocaine induce the epigenetic factors MeCP2 and MBD1 in adult rat brain. Molecular pharmacology 70:487-492.

Catalan A, Hutter S, Parsch J (2012) Population and sex differences in Drosophila melanogaster brain gene expression. BMC Genomics 13:654.

Chano T, Okabe H, Hulette CM (2007) RB1CC1 insufficiency causes neuronal atrophy through mTOR signaling alteration and involved in the pathology of Alzheimer's diseases. Brain research 1168:97-105.

Chaouloff F (2013) Social stress models in depression research: what do they tell us? Cell and tissue research 354:179-190.

Chen B, Piel WH, Gui L, Bruford E, Monteiro A (2005) The HSP90 family of genes in the human genome: insights into their divergence and evolution. Genomics 86:627-637.

Choi M, Wang SE, Ko SY, Kang HJ, Chae SY, Lee SH, Kim YS, Duman RS, Son H (2014) Overexpression of human GATA-1 and GATA-2 interferes with spine formation and produces depressive behavior in rats. PloS one 9:e109253.

Choi M, Lee SH, Wang SE, Ko SY, Song M, Choi JS, Kim YS, Duman RS, Son H (2015) Ketamine produces antidepressant-like effects through phosphorylation-dependent nuclear export of histone deacetylase 5 (HDAC5) in rats. Proceedings of the National Academy of Sciences of the United States of America 112:15755-15760.

Covington HE, 3rd, Maze I, Vialou V, Nestler EJ (2015) Antidepressant action of HDAC inhibition in the prefrontal cortex. Neuroscience 298:329-335.

Covington HE, 3rd, Maze I, LaPlant QC, Vialou VF, Ohnishi YN, Berton O, Fass DM, Renthal W, Rush AJ, 3rd, Wu EY, Ghose S, Krishnan V, Russo SJ, Tamminga C, Haggarty SJ, Nestler EJ (2009) Antidepressant actions of histone deacetylase inhibitors. The Journal of neuroscience : the official journal of the Society for Neuroscience 29:11451-11460.

Crawley JN, Belknap JK, Collins A, Crabbe JC, Frankel W, Henderson N, Hitzemann RJ, Maxson SC, Miner LL, Silva AJ, Wehner JM, Wynshaw-Boris A, Paylor R (1997) Behavioral phenotypes of inbred mouse strains: implications and recommendations for molecular studies. Psychopharmacology 132:107-124.

Daoust A, Bohic S, Saoudi Y, Debacker C, Gory-Faure S, Andrieux A, Barbier EL, Deloulme JC (2014) Neuronal transport defects of the MAP6 KO mouse - a model of schizophrenia - and alleviation by Epothilone D treatment, as observed using MEMRI. Neuroimage 96:133-142.

Davis M (1992) The role of the amygdala in fear and anxiety. Annual review of neuroscience 15:353-375.

De Smaele E, Di Marcotullio L, Moretti M, Pelloni M, Occhione MA, Infante P, Cucchi D, Greco A, Pietrosanti L, Todorovic J, Coni S, Canettieri G, Ferretti E, Bei R, Maroder M, Screpanti I, Gulino A (2011) Identification and characterization of KCASH2 and KCASH3, 2 novel Cullin3 adaptors suppressing histone deacetylase and Hedgehog activity in medulloblastoma. Neoplasia (New York, NY) 13:374-385.

De Vries GJ (2004) Minireview: Sex differences in adult and developing brains: compensation, compensation, compensation. Endocrinology 145:1063-1068.

de Vries GJ, Forger NG (2015) Sex differences in the brain: a whole body perspective. Biology of sex differences 6:15.

Degenhardt F et al. (2013) Duplications in RB1CC1 are associated with schizophrenia; identification in large European sample sets. Transl Psychiatry 3:e326.

Dias C et al. (2014) beta-catenin mediates stress resilience through Dicer1/microRNA regulation. Nature 516:51-55.

Duvarci S, Pare D (2014) Amygdala microcircuits controlling learned fear. Neuron 82:966-980.

Ehlers A, Maercker A, Boos A (2000) Posttraumatic stress disorder following political imprisonment: the role of mental defeat, alienation, and perceived permanent change. Journal of abnormal psychology 109:45-55.

Espallergues J, Teegarden SL, Veerakumar A, Boulden J, Challis C, Jochems J, Chan M, Petersen T, Deneris E, Matthias P, Hahn CG, Lucki I, Beck SG, Berton O (2012) HDAC6 regulates glucocorticoid receptor signaling in serotonin pathways with critical impact on stress resilience. The Journal of neuroscience : the official journal of the Society for Neuroscience 32:4400-4416.

Fanselow MS, Gale GD (2003) The amygdala, fear, and memory. Annals of the New York Academy of Sciences 985:125-134.

Faruzzi AN, Solomon MB, Demas GE, Huhman KL (2005) Gonadal hormones modulate the display of submissive behavior in socially defeated female Syrian hamsters. Hormones and behavior 47:569-575.

Feng NY, Fergus DJ, Bass AH (2015) Neural transcriptome reveals molecular mechanisms for temporal control of vocalization across multiple timescales. BMC Genomics 16:408.

Ferris CF, Axelson JF, Shinto LH, Albers HE (1987) Scent marking and the maintenance of dominant/subordinate status in male golden hamsters. Physiology & behavior 40:661-664.

Finn RD, Clements J, Eddy SR (2011) HMMER web server: interactive sequence similarity searching. Nucleic Acids Res 39:W29-37.

Fitzsimons HL, Schwartz S, Given FM, Scott MJ (2013) The histone deacetylase HDAC4 regulates long-term memory in Drosophila. PloS one 8:e83903.

Foster MT, Solomon MB, Huhman KL, Bartness TJ (2006) Social defeat increases food intake, body mass, and adiposity in Syrian hamsters. American journal of physiology Regulatory, integrative and comparative physiology 290:R1284-1293.

Fraser BA, Weadick CJ, Janowitz I, Rodd FH, Hughes KA (2011) Sequencing and characterization of the guppy (Poecilia reticulata) transcriptome. BMC Genomics 12:202.

Fu AK, Hung KW, Wong HH, Fu WY, Ip NY (2013) Cdk5 phosphorylates a component of the HDAC complex and regulates histone acetylation during neuronal cell death. Neuro-Signals 21:55-60.

Gao M, Zhang B, Liu J, Guo X, Li H, Wang T, Zhang Z, Liao J, Cong N, Wang Y, Yu L, Zhao D, Liu G (2014) Generation of transgenic golden Syrian hamsters. Cell research 24:380-382.

Gao Y, Jiang T, Qu C, Tao H, Cao H, Zhao Y, Wang Y, Qu J, Chen JG (2013) Atlastin-1 regulates dendritic morphogenesis in mouse cerebral cortex. Neurosci Res 77:137-142.

Garner CC, Garner A, Huber G, Kozak C, Matus A (1990) Molecular Cloning of Microtubule-Associated Protein 1 (MAP1A) and Microtubule-Associated Protein 5 (MAP1B): Identification of Distinct Genes and Their Differential Expression in Developing Brain. Journal of neurochemistry 55:146-154.

Gimenez-Conti IB, Slaga TJ (1993) The hamster cheek pouch carcinogenesis model. Journal of cellular biochemistry Supplement 17F:83-90.

Gottlicher M, Minucci S, Zhu P, Kramer OH, Schimpf A, Giavara S, Sleeman JP, Lo Coco F, Nervi C, Pelicci PG, Heinzel T (2001) Valproic acid defines a novel class of HDAC inhibitors inducing differentiation of transformed cells. The EMBO journal 20:6969-6978.

Grabherr MG et al. (2011) Full-length transcriptome assembly from RNA-Seq data without a reference genome. Nature biotechnology 29:644-652.

Gray AL, Hyde TM, Deep-Soboslay A, Kleinman JE, Sodhi MS (2015a) Sex differences in glutamate receptor gene expression in major depression and suicide. Molecular psychiatry 20:1057-1068.

Gray CL, Norvelle A, Larkin T, Huhman KL (2015b) Dopamine in the nucleus accumbens modulates the memory of social defeat in Syrian hamsters (Mesocricetus auratus). Behavioural brain research 286:22-28.

Haas BJ et al. (2013) De novo transcript sequence reconstruction from RNA-seq using the Trinity platform for reference generation and analysis. Nature protocols 8:1494-1512.

Harmon AC, Huhman KL, Moore TO, Albers HE (2002a) Oxytocin inhibits aggression in female Syrian hamsters. Journal of neuroendocrinology 14:963-969.

Harmon AC, Moore TO, Huhman KL, Albers HE (2002b) Social experience and social context alter the behavioral response to centrally administered oxytocin in female Syrian hamsters. Neuroscience 109:767-772.

Hastie ND, Bishop JO (1976) The expression of three abundance classes of messenger RNA in mouse tissues. Cell 9:761-774.

Heim C, Nemeroff CB (2001) The role of childhood trauma in the neurobiology of mood and anxiety disorders: preclinical and clinical studies. Biological psychiatry 49:1023-1039.

Heinrichs SC, Leite-Morris KA, Rasmusson AM, Kaplan GB (2013) Repeated valproate treatment facilitates fear extinction under specific stimulus conditions. Neuroscience letters 552:108-113.

Hendrickx A, Pierrot N, Tasiaux B, Schakman O, Kienlen-Campard P, De Smet C, Octave JN (2014) Epigenetic regulations of immediate early genes expression involved in memory formation by the amyloid precursor protein of Alzheimer disease. PloS one 9:e99467.

Hennessey AC, Huhman KL, Albers HE (1994) Vasopressin and sex differences in hamster flank marking. Physiology & behavior 55:905-911.

Herry C, Ciocchi S, Senn V, Demmou L, Muller C, Luthi A (2008) Switching on and off fear by distinct neuronal circuits. Nature 454:600-606.

Hollis F, Kabbaj M (2014) Social defeat as an animal model for depression. ILAR journal / National Research Council, Institute of Laboratory Animal Resources 55:221-232.

Hollis F, Duclot F, Gunjan A, Kabbaj M (2011) Individual differences in the effect of social defeat on anhedonia and histone acetylation in the rat hippocampus. Hormones and behavior 59:331-337.

Huhman KL (2006) Social conflict models: can they inform us about human psychopathology? Hormones and behavior 50:640-646.

Huhman KL, Moore TO, Ferris CF, Mougey EH, Meyerhoff JL (1991) Acute and repeated exposure to social conflict in male golden hamsters: increases in plasma POMC-peptides and cortisol and decreases in plasma testosterone. Hormones and behavior 25:206-216.

Huhman KL, Solomon MB, Janicki M, Harmon AC, Lin SM, Israel JE, Jasnow AM (2003) Conditioned defeat in male and female Syrian hamsters. Hormones and behavior 44:293-299.

Hui B, Wang W, Li J (2010) Biphasic modulation of cocaine-induced conditioned place preference through inhibition of histone acetyltransferase and histone deacetylase. Saudi medical journal 31:389-393.

Iga J, Ueno S, Yamauchi K, Numata S, Kinouchi S, Tayoshi-Shibuya S, Song H, Ohmori T (2007) Altered HDAC5 and CREB mRNA expressions in the peripheral leukocytes of major depression. Progress in neuro-psychopharmacology & biological psychiatry 31:628-632.

Itzhak Y, Liddie S, Anderson KL (2013) Sodium butyrate-induced histone acetylation strengthens the expression of cocaine-associated contextual memory. Neurobiology of learning and memory 102:34-42.

Itzhak Y, Anderson KL, Kelley JB, Petkov M (2012) Histone acetylation rescues contextual fear conditioning in nNOS KO mice and accelerates extinction of cued fear conditioning in wild type mice. Neurobiology of learning and memory 97:409-417.

Jang S et al. (2016) Synaptic adhesion molecule IgSF11 regulates synaptic transmission and plasticity. Nature neuroscience 19:84-93.

Jasnow AM, Huhman KL (2001) Activation of GABA(A) receptors in the amygdala blocks the acquisition and expression of conditioned defeat in Syrian hamsters. Brain research 920:142-150.

Jasnow AM, Cooper MA, Huhman KL (2004) N-methyl-D-aspartate receptors in the amygdala are necessary for the acquisition and expression of conditioned defeat. Neuroscience 123:625-634.

Jasnow AM, Shi C, Israel JE, Davis M, Huhman KL (2005) Memory of social defeat is facilitated by cAMP response element-binding protein overexpression in the amygdala. Behavioral neuroscience 119:1125-1130.

Jaworski A, Tom I, Tong RK, Gildea HK, Koch AW, Gonzalez LC, Tessier-Lavigne M (2015) Operational redundancy in axon guidance through the multifunctional receptor Robo3 and its ligand NELL2. Science 350:961-965.

Jing L, Luo J, Zhang M, Qin WJ, Li YL, Liu Q, Wang YT, Lawrence AJ, Liang JH (2011) Effect of the histone deacetylase inhibitors on behavioural sensitization to a single morphine exposure in mice. Neuroscience letters 494:169-173.

Joset P, Wacker A, Babey R, Ingold EA, Andermatt I, Stoeckli ET, Gesemann M (2011) Rostral growth of commissural axons requires the cell adhesion molecule MDGA2. Neural development 6:22.

Kaestner KH, Ntambi J, Kelly T, Lane M (1989) Differentiation-induced gene expression in 3T3-L1 preadipocytes. A second differentially expressed gene encoding stearoyl-CoA desaturase. Journal of Biological Chemistry 264:14755-14761.

Kambe Y, Miyata A (2015) Potential involvement of the mitochondrial unfolded protein response in depressive-like symptoms in mice. Neuroscience letters 588:166-171.

Kang J, Chen J, Shi Y, Jia J, Zhang Y (2005) Curcumin-induced histone hypoacetylation: the role of reactive oxygen species. Biochemical pharmacology 69:1205-1213.

Kelleher I, Harley M, Lynch F, Arseneault L, Fitzpatrick C, Cannon M (2008) Associations between childhood trauma, bullying and psychotic symptoms among a school-based adolescent sample. The British journal of psychiatry : the journal of mental science 193:378-382.

Kessler S, Elliott GR, Orenberg EK, Barchas JD (1977) A genetic analysis of aggressive behavior in two strains of mice. Behavior Genetics 7:313-321.

Kilgore M, Miller CA, Fass DM, Hennig KM, Haggarty SJ, Sweatt JD, Rumbaugh G (2010) Inhibitors of class 1 histone deacetylases reverse contextual memory deficits in a mouse model of Alzheimer's disease. Neuropsychopharmacology : official publication of the American College of Neuropsychopharmacology 35:870-880.

Kim MS, Akhtar MW, Adachi M, Mahgoub M, Bassel-Duby R, Kavalali ET, Olson EN, Monteggia LM (2012) An essential role for histone deacetylase 4 in synaptic plasticity and memory formation. The Journal of neuroscience : the official journal of the Society for Neuroscience 32:10879-10886.

Kim WY, Kim S, Kim JH (2008) Chronic microinjection of valproic acid into the nucleus accumbens attenuates amphetamine-induced locomotor activity. Neuroscience letters 432:54-57.

Kollack-Walker S, Newman SW (1995) Mating and agonistic behavior produce different patterns of Fos immunolabeling in the male Syrian hamster brain. Neuroscience 66:721-736.

Kollack-Walker S, Watson SJ, Akil H (1997) Social stress in hamsters: defeat activates specific neurocircuits within the brain. The Journal of neuroscience : the official journal of the Society for Neuroscience 17:8842-8855.

Koppel I, Timmusk T (2013) Differential regulation of Bdnf expression in cortical neurons by class-selective histone deacetylase inhibitors. Neuropharmacology 75:106-115.

Krishnan V (2014) Defeating the fear: new insights into the neurobiology of stress susceptibility. Exp Neurol 261:412-416.

Krogh A, Larsson B, von Heijne G, Sonnhammer EL (2001) Predicting transmembrane protein topology with a hidden Markov model: application to complete genomes. J Mol Biol 305:567-580.

Kudryavtseva NN, Bakshtanovskaya IV, Koryakina LA (1991) Social model of depression in mice of C57BL/6J strain. Pharmacology, biochemistry, and behavior 38:315-320.

Lagesen K, Hallin P, Rodland EA, Staerfeldt HH, Rognes T, Ussery DW (2007) RNAmmer: consistent and rapid annotation of ribosomal RNA genes. Nucleic Acids Res 35:3100-3108.

Langfelder P, Horvath S (2008) WGCNA: an R package for weighted correlation network analysis. BMC Bioinformatics 9:1-13.

Lanktree M, Squassina A, Krinsky M, Strauss J, Jain U, Macciardi F, Kennedy JL, Muglia P (2008) Association study of brain-derived neurotrophic factor (BDNF) and LIN-7 homolog (LIN-7) genes with adult attention-deficit/hyperactivity disorder. Am J Med Genet B Neuropsychiatr Genet 147B:945-951.

LaRocca CJ, Han J, Gavrikova T, Armstrong L, Oliveira AR, Shanley R, Vickers SM, Yamamoto M, Davydova J (2015) Oncolytic adenovirus expressing interferon alpha in a syngeneic Syrian hamster model for the treatment of pancreatic cancer. Surgery 157:888-898.

Larson ET, Winberg S, Mayer I, Lepage O, Summers CH, Overli O (2004) Social stress affects circulating melatonin levels in rainbow trout. Gen Comp Endocrinol 136:322-327.

Lattal KM, Barrett RM, Wood MA (2007) Systemic or intrahippocampal delivery of histone deacetylase inhibitors facilitates fear extinction. Behavioral neuroscience 121:1125-1131.

Lebow M, Neufeld-Cohen A, Kuperman Y, Tsoory M, Gil S, Chen A (2012) Susceptibility to PTSD-like behavior is mediated by corticotropin-releasing factor receptor type 2 levels in the bed nucleus of the stria terminalis. The Journal of neuroscience : the official journal of the Society for Neuroscience 32:6906-6916.

Lee JY, Kwak M, Lee PC (2015) Impairment of social behavior and communication in mice lacking the Uba6-dependent ubiquitin activation system. Behavioural brain research 281:78-85.

Levy RJ, Kvajo M, Li Y, Tsvetkov E, Dong W, Yoshikawa Y, Kataoka T, Bolshakov VY, Karayiorgou M, Gogos JA (2015) Deletion of Rapgef6, a candidate schizophrenia susceptibility gene, disrupts amygdala function in mice. Transl Psychiatry 5:e577.

Li B, Dewey CN (2011) RSEM: accurate transcript quantification from RNA-Seq data with or without a reference genome. BMC Bioinformatics 12:1-16.

Li JJ, Li SA (1984) Estrogen-induced tumorigenesis in hamsters: roles for hormonal and carcinogenic activities. Archives of toxicology 55:110-118.

Li X, Rubio FJ, Zeric T, Bossert JM, Kambhampati S, Cates HM, Kennedy PJ, Liu QR, Cimbro R, Hope BT, Nestler EJ, Shaham Y (2015) Incubation of methamphetamine craving is associated with selective increases in expression of Bdnf and trkb, glutamate receptors, and epigenetic enzymes in cue-activated fos-

expressing dorsal striatal neurons. The Journal of neuroscience : the official journal of the Society for Neuroscience 35:8232-8244.

MacManes MD, Lacey EA (2012) The social brain: transcriptome assembly and characterization of the hippocampus from a social subterranean rodent, the colonial tuco-tuco (Ctenomys sociabilis). PloS one 7:e45524.

Maddox SA, Watts CS, Schafe GE (2013a) p300/CBP histone acetyltransferase activity is required for newly acquired and reactivated fear memories in the lateral amygdala. Learning & memory 20:109-119.

Maddox SA, Watts CS, Doyere V, Schafe GE (2013b) A naturally-occurring histone acetyltransferase inhibitor derived from Garcinia indica impairs newly acquired and reactivated fear memories. PloS one 8:e54463.

Mahan AL, Mou L, Shah N, Hu JH, Worley PF, Ressler KJ (2012) Epigenetic modulation of Homer1a transcription regulation in amygdala and hippocampus with pavlovian fear conditioning. The Journal of neuroscience : the official journal of the Society for Neuroscience 32:4651-4659.

Majdazari A, Stubbusch J, Muller CM, Hennchen M, Weber M, Deng CX, Mishina Y, Schutz G, Deller T, Rohrer H (2013) Dendrite complexity of sympathetic neurons is controlled during postnatal development by BMP signaling. The Journal of neuroscience : the official journal of the Society for Neuroscience 33:15132-15144.

Manzardo AM, McGuire A, Butler MG (2015) Clinically relevant genetic biomarkers from the brain in alcoholism with representation on high resolution chromosome ideograms. Gene 560:184-194.

Markham CM, Huhman KL (2008) Is the medial amygdala part of the neural circuit modulating conditioned defeat in Syrian hamsters? Learning & memory 15:6-12.

Markham CM, Taylor SL, Huhman KL (2010) Role of amygdala and hippocampus in the neural circuit subserving conditioned defeat in Syrian hamsters. Learning & memory 17:109-116.

Markham CM, Luckett CA, Huhman KL (2012) The medial prefrontal cortex is both necessary and sufficient for the acquisition of conditioned defeat. Neuropharmacology 62:933-939.

Maruyama E, Ogawa K, Endo S, Tsujimoto M, Hashikawa T, Nabetani T, Tsugita A (2007) Brain-derived neurotrophic factor induces cell surface expression of short-form tenascin R complex in hippocampal postsynapses. The international journal of biochemistry & cell biology 39:1930-1942.

McCann KE, Huhman KL (2012) The effect of escapable versus inescapable social defeat on conditioned defeat and social recognition in Syrian hamsters. Physiology & behavior 105:493-497.

McCann KE, Bicknese CN, Norvelle A, Huhman KL (2014) Effects of inescapable versus escapable social stress in Syrian hamsters: the importance of stressor duration versus escapability. Physiology & behavior 129:25-29.

McGaugh JL (2004) The amygdala modulates the consolidation of memories of emotionally arousing experiences. Annual review of neuroscience 27:1-28.

Mead AN, Stephens DN (2003) Involvement of AMPA receptor GluR2 subunits in stimulus-reward learning: evidence from glutamate receptor gria2 knock-out mice. The Journal of neuroscience 23:9500-9507.

Menna E, Disanza A, Cagnoli C, Schenk U, Gelsomino G, Frittoli E, Hertzog M, Offenhauser N, Sawallisch C, Kreienkamp HJ, Gertler FB, Di Fiore PP, Scita G, Matteoli M (2009) Eps8 regulates axonal filopodia in hippocampal neurons in response to brain-derived neurotrophic factor (BDNF). PLoS biology 7:e1000138.

Menna E, Zambetti S, Morini R, Donzelli A, Disanza A, Calvigioni D, Braida D, Nicolini C, Orlando M, Fossati G, Cristina Regondi M, Pattini L, Frassoni C, Francolini M, Scita G, Sala M, Fahnestock M, Matteoli M (2013) Eps8 controls dendritic spine density and synaptic plasticity through its actin-capping activity. The EMBO journal 32:1730-1744.

Merenlender-Wagner A, Shemer Z, Touloumi O, Lagoudaki R, Giladi E, Andrieux A, Grigoriadis NC, Gozes I (2014) New horizons in schizophrenia treatment: autophagy protection is coupled with behavioral improvements in a mouse model of schizophrenia. Autophagy 10:2324-2332.

Mi H, Thomas P (2009) PANTHER pathway: an ontology-based pathway database coupled with data analysis tools. Methods Mol Biol 563:123-140.

Mi H, Muruganujan A, Casagrande JT, Thomas PD (2013) Large-scale gene function analysis with the PANTHER classification system. Nature protocols 8:1551-1566.

Mi H, Poudel S, Muruganujan A, Casagrande JT, Thomas PD (2016) PANTHER version 10: expanded protein families and functions, and analysis tools. Nucleic Acids Res 44:D336-342.

Mizuno M, Matsumoto A, Hamada N, Ito H, Miyauchi A, Jimbo EF, Momoi MY, Tabata H, Yamagata T, Nagata K (2015) Role of an adaptor protein Lin-7B in brain development: possible involvement in autism spectrum disorders. J Neurochem 132:61-69.

Monsey MS, Gerhard DM, Boyle LM, Briones MA, Seligsohn M, Schafe GE (2015) A diet enriched with curcumin impairs newly acquired and reactivated fear memories. Neuropsychopharmacology : official publication of the American College of Neuropsychopharmacology 40:1278-1288.

Moy SS, Nadler JJ, Young NB, Perez A, Holloway LP, Barbaro RP, Barbaro JR, Wilson LM, Threadgill DW, Lauder JM (2007) Mouse behavioral tasks relevant to autism: phenotypes of 10 inbred strains. Behavioural brain research 176:4-20.

Murray EK, Hien A, de Vries GJ, Forger NG (2009) Epigenetic control of sexual differentiation of the bed nucleus of the stria terminalis. Endocrinology 150:4241-4247.

Narayan S, Tang B, Head SR, Gilmartin TJ, Sutcliffe JG, Dean B, Thomas EA (2008) Molecular profiles of schizophrenia in the CNS at different stages of illness. Brain research 1239:235-248.

Nau H, Loscher W (1982) Valproic acid: brain and plasma levels of the drug and its metabolites, anticonvulsant effects and gamma-aminobutyric acid (GABA) metabolism in the mouse. The Journal of pharmacology and experimental therapeutics 220:654-659.

Nemeroff CB (1998) The neurobiology of depression. Scientific American 278:42-49.

Nolen-Hoeksema S (1987) Sex differences in unipolar depression: evidence and theory. Psychological bulletin 101:259.

Nor C, Sassi FA, de Farias CB, Schwartsmann G, Abujamra AL, Lenz G, Brunetto AL, Roesler R (2013) The histone deacetylase inhibitor sodium butyrate promotes cell death and differentiation and reduces neurosphere formation in human medulloblastoma cells. Molecular neurobiology 48:533-543.

Pan ZZ (2012) Transcriptional control of Gad2. Transcription 3:68-72.

Panja D, Kenney JW, D'Andrea L, Zalfa F, Vedeler A, Wibrand K, Fukunaga R, Bagni C, Proud CG, Bramham CR (2014) Two-stage translational control of dentate gyrus LTP consolidation is mediated by sustained BDNF-TrkB signaling to MNK. Cell Rep 9:1430-1445.

Parsons RG, Ressler KJ (2013) Implications of memory modulation for post-traumatic stress and fear disorders. Nature neuroscience 16:146-153.

Pascual M, Do Couto BR, Alfonso-Loeches S, Aguilar MA, Rodriguez-Arias M, Guerri C (2012) Changes in histone acetylation in the prefrontal cortex of ethanol-exposed adolescent rats are associated with ethanol-induced place conditioning. Neuropharmacology 62:2309-2319.

Petersen TN, Brunak S, von Heijne G, Nielsen H (2011) SignalP 4.0: discriminating signal peptides from transmembrane regions. Nat Methods 8:785-786.

Phiel CJ, Zhang F, Huang EY, Guenther MG, Lazar MA, Klein PS (2001) Histone deacetylase is a direct target of valproic acid, a potent anticonvulsant, mood stabilizer, and teratogen. The Journal of biological chemistry 276:36734-36741.

Ploense KL, Kerstetter KA, Wade MA, Woodward NC, Maliniak D, Reyes M, Uchizono RS, Bredy TW, Kippin TE (2013) Exposure to histone deacetylase inhibitors during Pavlovian conditioning enhances subsequent cue-induced reinstatement of operant behavior. Behavioural pharmacology 24:164-171.

Potegal M, Huhman K, Moore T, Meyerhoff J (1993) Conditioned defeat in the Syrian golden hamster (Mesocricetus auratus). Behavioral and neural biology 60:93-102.

Prescott J, Falzarano D, Feldmann H (2015) Natural Immunity to Ebola Virus in the Syrian Hamster Requires Antibody Responses. The Journal of infectious diseases 212 Suppl 2:S271-276.

Pulliam JV, Dawaghreh AM, Alema-Mensah E, Plotsky PM (2010) Social defeat stress produces prolonged alterations in acoustic startle and body weight gain in male Long Evans rats. J Psychiatr Res 44:106-111.

Punta M, Coggill PC, Eberhardt RY, Mistry J, Tate J, Boursnell C, Pang N, Forslund K, Ceric G, Clements J, Heger A, Holm L, Sonnhammer EL, Eddy SR, Bateman A, Finn RD (2012) The Pfam protein families database. Nucleic Acids Res 40:D290-301.

Qi XR, Zhao J, Liu J, Fang H, Swaab DF, Zhou JN (2015) Abnormal retinoid and TrkB signaling in the prefrontal cortex in mood disorders. Cerebral cortex (New York, NY : 1991) 25:75-83.

Reolon GK, Maurmann N, Werenicz A, Garcia VA, Schroder N, Wood MA, Roesler R (2011) Posttraining systemic administration of the histone deacetylase inhibitor sodium butyrate ameliorates aging-related memory decline in rats. Behavioural brain research 221:329-332.

Robinson MD, McCarthy DJ, Smyth GK (2010) edgeR: a Bioconductor package for differential expression analysis of digital gene expression data. Bioinformatics 26:139-140.

Sailaja BS, Cohen-Carmon D, Zimmerman G, Soreq H, Meshorer E (2012) Stress-induced epigenetic transcriptional memory of acetylcholinesterase by HDAC4. Proceedings of the National Academy of Sciences of the United States of America 109:E3687-3695.

Sapolsky RM (1990) A. E. Bennett Award paper. Adrenocortical function, social rank, and personality among wild baboons. Biological psychiatry 28:862-878.

Schoenfeld T, McKerracher L, Obar R, Vallee R (1989) MAP 1A and MAP 1B are structurally related microtubule associated proteins with distinct developmental patterns in the CNS. The Journal of Neuroscience 9:1712-1730.

Selenica ML, Benner L, Housley SB, Manchec B, Lee DC, Nash KR, Kalin J, Bergman JA, Kozikowski A, Gordon MN, Morgan D (2014) Histone deacetylase 6 inhibition improves memory and reduces total tau levels in a mouse model of tau deposition. Alzheimer's research & therapy 6:12.

Senatore A, Edirisinghe N, Katz PS (2015) Deep mRNA sequencing of the Tritonia diomedea brain transcriptome provides access to gene homologues for neuronal excitability, synaptic transmission and peptidergic signalling. PloS one 10:e0118321.

Sharma E, Kunstner A, Fraser BA, Zipprich G, Kottler VA, Henz SR, Weigel D, Dreyer C (2014) Transcriptome assemblies for studying sex-biased gene expression in the guppy, Poecilia reticulata. BMC Genomics 15:400.

Shively CA (1998) Social subordination stress, behavior, and central monoaminergic function in female cynomolgus monkeys. Biological psychiatry 44:882-891.

Simao FA, Waterhouse RM, Ioannidis P, Kriventseva EV, Zdobnov EM (2015) BUSCO: assessing genome assembly and annotation completeness with single-copy orthologs. Bioinformatics 31:3210-3212.

Simon-O'Brien E, Alaux-Cantin S, Warnault V, Buttolo R, Naassila M, Vilpoux C (2015) The histone deacetylase inhibitor sodium butyrate decreases excessive ethanol intake in dependent animals. Addiction biology 20:676-689.

Singh J, Khan M, Singh I (2011) HDAC inhibitor SAHA normalizes the levels of VLCFAs in human skin fibroblasts from X-ALD patients and downregulates the expression of proinflammatory cytokines in Abcd1/2-silenced mouse astrocytes. Journal of lipid research 52:2056-2069.

Sinning A, Liebmann L, Hubner CA (2015) Disruption of Slc4a10 augments neuronal excitability and modulates synaptic short-term plasticity. Frontiers in cellular neuroscience 9:223.

Soleimani L, Roder JC, Dennis JW, Lipina T (2008) Beta N-acetylglucosaminyltransferase V (Mgat5) deficiency reduces the depression-like phenotype in mice. Genes Brain Behav 7:334-343.

Solomon MB, Karom MC, Huhman KL (2007a) Sex and estrous cycle differences in the display of conditioned defeat in Syrian hamsters. Hormones and behavior 52:211-219.

Solomon MB, Foster MT, Bartness TJ, Huhman KL (2007b) Social defeat and footshock increase body mass and adiposity in male Syrian hamsters. American journal of physiology Regulatory, integrative and comparative physiology 292:R283-290.

Solomon MB, Karom MC, Norvelle A, Markham CA, Erwin WD, Huhman KL (2009) Gonadal hormones modulate the display of conditioned defeat in male Syrian hamsters. Hormones and behavior 56:423-428.

St John RD, Corning PA (1973) Maternal aggression in mice. Behavioral biology 9:635-639.

Stafford JM, Raybuck JD, Ryabinin AE, Lattal KM (2012) Increasing histone acetylation in the hippocampus-infralimbic network enhances fear extinction. Biological psychiatry 72:25-33.

Su AI, Wiltshire T, Batalov S, Lapp H, Ching KA, Block D, Zhang J, Soden R, Hayakawa M, Kreiman G (2004) A gene atlas of the mouse and human protein-encoding transcriptomes. Proceedings of the National Academy of Sciences of the United States of America 101:6062-6067.

Takahashi M, Ishida M, Saito T, Ohshima T, Hisanaga S (2014) Valproic acid downregulates Cdk5 activity via the transcription of the p35 mRNA. Biochemical and biophysical research communications 447:678-682.

Tamashiro KL, Nguyen MM, Sakai RR (2005) Social stress: from rodents to primates. Front Neuroendocrinol 26:27-40.

Tamura G, Olson D, Miron J, Clark TG (2005) Tolloid-like 1 is negatively regulated by stress and glucocorticoids. Brain Res Mol Brain Res 142:81-90.

Tao W, Chen Q, Wang L, Zhou W, Wang Y, Zhang Z (2015) Brainstem brain-derived neurotrophic factor signaling is required for histone deacetylase inhibitor-induced pain relief. Molecular pharmacology 87:1035-1041.

Taravosh-Lahn K, Delville Y (2004) Aggressive behavior in female golden hamsters: development and the effect of repeated social stress. Hormones and behavior 46:428-435.

Taylor SL, Stanek LM, Ressler KJ, Huhman KL (2011) Differential brain-derived neurotrophic factor expression in limbic brain regions following social defeat or territorial aggression. Behavioral neuroscience 125:911-920.

Team RC (2014) R: A language and environment for statistical computing. R Foundation for Statistical Computing, Vienna, Austria. 2013. In: ISBN 3-900051-07-0.

Theissinger K, Falckenhayn C, Blande D, Toljamo A, Gutekunst J, Makkonen J, Jussila J, Lyko F, Schrimpf A, Schulz R, Kokko H (2016) De Novo assembly and annotation of the freshwater crayfish Astacus astacus transcriptome. Marine Genomics.

Tian F, Hu XZ, Wu X, Jiang H, Pan H, Marini AM, Lipsky RH (2009) Dynamic chromatin remodeling events in hippocampal neurons are associated with NMDA receptor-mediated activation of Bdnf gene promoter 1. J Neurochem 109:1375-1388.

Toth I, Neumann ID (2013) Animal models of social avoidance and social fear. Cell and tissue research 354:107-118.

Trabzuni D, Ramasamy A, Imran S, Walker R, Smith C, Weale ME, Hardy J, Ryten M, North American Brain Expression C (2013) Widespread sex differences in gene expression and splicing in the adult human brain. Nat Commun 4:2771.

Tremolizzo L, Carboni G, Ruzicka WB, Mitchell CP, Sugaya I, Tueting P, Sharma R, Grayson DR, Costa E, Guidotti A (2002) An epigenetic mouse model for molecular and behavioral neuropathologies related to schizophrenia vulnerability. Proceedings of the National Academy of Sciences of the United States of America 99:17095-17100.

Tripp A, Oh H, Guilloux JP, Martinowich K, Lewis DA, Sibille E (2012) Brain-derived neurotrophic factor signaling and subgenual anterior cingulate cortex dysfunction in major depressive disorder. The American journal of psychiatry 169:1194-1202.

Tsai H-W, Grant PA, Rissman EF (2009) Sex differences in histone modifications in the neonatal mouse brain. Epigenetics 4:47-53.

Tunnicliff G (1999) Actions of sodium valproate on the central nervous system. Journal of physiology and pharmacology : an official journal of the Polish Physiological Society 50:347-365.

UniProt C (2015) UniProt: a hub for protein information. Nucleic Acids Res 43:D204-212.

Vairaktaris E, Spyridonidou S, Papakosta V, Vylliotis A, Lazaris A, Perrea D, Yapijakis C, Patsouris E (2008) The hamster model of sequential oral oncogenesis. Oral oncology 44:315-324.

Van Loo PL, Van Zutphen LF, Baumans V (2003) Male management: Coping with aggression problems in male laboratory mice. Lab Anim 37:300-313.

Van Maldergem L, Hou Q, Kalscheuer VM, Rio M, Doco-Fenzy M, Medeira A, de Brouwer AP, Cabrol C, Haas SA, Cacciagli P, Moutton S, Landais E, Motte J, Colleaux L, Bonnet C, Villard L, Dupont J, Man HY (2013) Loss of function of KIAA2022 causes mild to severe intellectual disability with an autism spectrum disorder and impairs neurite outgrowth. Human molecular genetics 22:3306-3314.

Venter JC, Adams MD, Myers EW, Li PW, Mural RJ, Sutton GG, Smith HO, Yandell M, Evans CA, Holt RA (2001) The sequence of the human genome. Science 291:1304-1351.

Virgin CE, Jr., Sapolsky RM (1997) Styles of male social behavior and their endocrine correlates among low-ranking baboons. Am J Primatol 42:25-39.

Wahl-Jensen V, Bollinger L, Safronetz D, de Kok-Mercado F, Scott DP, Ebihara H (2012) Use of the Syrian hamster as a new model of ebola virus disease and other viral hemorrhagic fevers. Viruses 4:3754-3784.

Wang Y, Lai J, Cui H, Zhu Y, Zhao B, Wang W, Wei S (2015) Inhibition of histone deacetylase in the basolateral amygdala facilitates morphine context-associated memory formation in rats. Journal of molecular neuroscience : MN 55:269-278.

Watanabe SY, Iga J, Ishii K, Numata S, Shimodera S, Fujita H, Ohmori T (2015) Biological tests for major depressive disorder that involve leukocyte gene expression assays. J Psychiatr Res 66-67:1-6.

Weissman MM, Klerman GL (1977) Sex differences and the epidemiology of depression. Archives of general psychiatry 34:98.

Weng J, Symons MN, Singh SM (2009) Ethanol-responsive genes (Crtam, Zbtb16, and Mobp) located in the alcohol-QTL region of chromosome 9 are associated with alcohol preference in mice. Alcoholism, clinical and experimental research 33:1409-1416.

White AO, Wood MA (2014) Does stress remove the HDAC brakes for the formation and persistence of long-term memory? Neurobiology of learning and memory 112:61-67.

Whittle N, Singewald N (2014) HDAC inhibitors as cognitive enhancers in fear, anxiety and trauma therapy: where do we stand? Biochemical Society transactions 42:569-581.

Wille A, Maurer V, Piatti P, Whittle N, Rieder D, Singewald N, Lusser A (2015) Impaired Contextual Fear Extinction Learning is Associated with Aberrant Regulation of CHD-Type Chromatin Remodeling Factors. Front Behav Neurosci 9:313.

Wilson CB, McLaughlin LD, Ebenezer PJ, Nair AR, Francis J (2014) Valproic acid effects in the hippocampus and prefrontal cortex in an animal model of post-traumatic stress disorder. Behavioural brain research 268:72-80.

Wingo AP, Almli LM, Stevens JJ, Klengel T, Uddin M, Li Y, Bustamante AC, Lori A, Koen N, Stein DJ, Smith AK, Aiello AE, Koenen KC, Wildman DE, Galea S, Bradley B, Binder EB, Jin P, Gibson G, Ressler KJ (2015) DICER1 and microRNA regulation in post-traumatic stress disorder with comorbid depression. Nat Commun 6:10106.

Wommack JC, Delville Y (2003) Repeated social stress and the development of agonistic behavior: individual differences in coping responses in male golden hamsters. Physiology & behavior 80:303-308.

Xia Y, Luo C, Dai S, Yao D (2013) Increased EphA/ephrinA expression in hippocampus of pilocarpine treated mouse. Epilepsy research 105:20-29.

Xing B, Zhao Y, Zhang H, Dang Y, Chen T, Huang J, Luo Q (2011) Microinjection of valproic acid into the ventrolateral orbital cortex exerts an antidepressant-like effect in the rat forced swim test. Brain research bulletin 85:153-157.

Xu K, Wu Z, Renier N, Antipenko A, Tzvetkova-Robev D, Xu Y, Minchenko M, Nardi-Dei V, Rajashankar KR, Himanen J, Tessier-Lavigne M, Nikolov DB (2014) Neural migration. Structures of netrin-1 bound to two receptors provide insight into its axon guidance mechanism. Science 344:1275-1279.

Xu Q, Yang GY, Liu N, Xu P, Chen YL, Zhou Z, Luo ZG, Ding X (2012) P4-ATPase ATP8A2 acts in synergy with CDC50A to enhance neurite outgrowth. FEBS letters 586:1803-1812.

Yamamoto A, Uchiyama K, Nara T, Nishimura N, Hayasaka M, Hanaoka K, Yamamoto T (2014) Structural abnormalities of corpus callosum and cortical axonal tracts accompanied by decreased anxiety-like behavior and lowered sociability in spock3- mutant mice. Developmental neuroscience 36:381-395.

Zhang DF, Li J, Wu H, Cui Y, Bi R, Zhou HJ, Wang HZ, Zhang C, Wang D, Kong QP, Li T, Fang Y, Jiang T, Yao YG (2016) CFH Variants Affect Structural and Functional Brain Changes and Genetic Risk of Alzheimer's Disease. Neuropsychopharmacology : official publication of the American College of Neuropsychopharmacology 41:1034-1045.

Zhang S, Yanzhu Y, Yuguang S (2005) Characterization of human SCD2, an oligomeric desaturase with improved stability and enzyme activity by cross-linking in intact cells. Biochemical Journal 388:135-142.

Zhong T, Qing QJ, Yang Y, Zou WY, Ye Z, Yan JQ, Guo QL (2014) Repression of contexual fear memory induced by isoflurane is accompanied by reduction in histone acetylation and rescued by sodium butyrate. Br J Anaesth 113:634-643.

Zhou L, Talebian A, Meakin SO (2015) The signaling adapter, FRS2, facilitates neuronal branching in primary cortical neurons via both Grb2- and Shp2-dependent mechanisms. Journal of molecular neuroscience : MN 55:663-677.

Zhou R, Niwa S, Guillaud L, Tong Y, Hirokawa N (2013) A molecular motor, KIF13A, controls anxiety by transporting the serotonin type 1A receptor. Cell Rep 3:509-519.

Zunino G, Messina A, Sgado P, Baj G, Casarosa S, Bozzi Y (2016) Brain-derived neurotrophic factor signaling is altered in the forebrain of Engrailed-2 knockout mice. Neuroscience 324:252-261.

Appendices

Appendix A Supplemental Figures

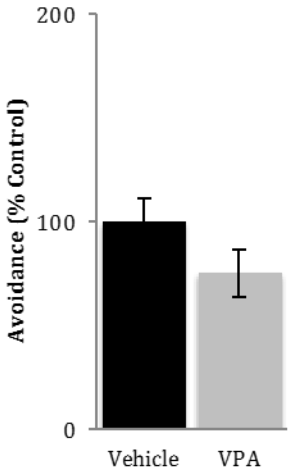

Supplemental Figure 1 Effects of VPA are temporally specific
VPA (200mg/kg (n=13)) did not alter social avoidance during testing when given 1hr before social defeat when compared with saline animals (n=12) ($t(23)=1.593$, $p=0.125$).

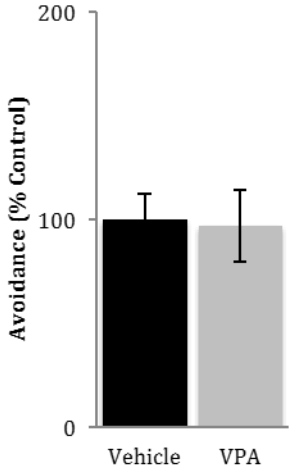

Supplemental Figure 2 Effects of VPA are specific to acquisition
VPA did not have an effect on the expression of conditioned defeat. Animals given VPA (200mg/kg (n=6)) 2hr before social avoidance testing exhibited the same amount of avoidance as animals given saline (n=6) ($t(10)=0.15$, $p=0.883$).

Appendix B Transcriptome Tables

Appendix B.1 Tables for whole brain transcriptome

Supplemental Table 1 Most highly expressed genes
Top 20 genes that are the most highly expressed in Syrian hamster brain (both males and females).

Gene ID	Gene	Uniprot ID
Nlrc3	Protein NLRC3	NLRC3_MOUSE
Plp1	Myelin proteolipid protein	MYPR_RAT
Scd2	Acyl-CoA desaturase 2	ACOD2_RAT
Hspa8	Heatshock cognate 71 kDa	HSP7C_RAT
Mbp	Myelin basic protein	MBP_MOUSE
Eef1a1	Elongation factor 1-alpha-1	EF1A1_RAT
Gapdh	Glyceraldehyde-3-phosphate dehydrogenase	G3P_CRIGR
Ywhag	14-3-3 protein gamma	1433G_RAT
Hsp90aa1	Heat shock protein HSP 90-alpha	HS90A_MOUSE
Sptbn1	Spectrin beta chain, non-erythrocytic 1	SPTB2_MOUSE
Atp5b	ATP synthase subunit beta, mitochondrial	ATPB_RAT
Glul	Glutamine synthase	GLNA_ACOCA
Aldoa	Fructose-bisphosphate aldolase A	ALDOA_RAT
Camk2n1	Calcium/calmodulin-dependent protein kinase II inhibitor 1	CK2N1_RAT
Atp2a2	Sarcoplasmic/endoplasmic reticulum calcium ATPase 2	AT2A2_MOUSE
Snrpn	Small nuclear ribonucleoprotein-associated protein N	RSMN_RAT
Psap	Prosaposin	SAP_RAT
Map1a	Microtubule-associated protein 1A	MAP1A_MOUSE
Serinc1	Serine incorporator 1	SERC1_RAT
Gpm6a	Neuronal membrane glycoprotein M6-a	GPM6A_RAT

Supplemental Table 2 Differential expression in male and female whole brain
A comprehensive list of the genes that were differentially regulated in whole brain of male and female hamsters. Regulation indicates in which sex the gene was more highly expressed. If both sexes are indicated, different isoforms of the same gene were differentially regulated in males and females.

Gene ID	Gene	Uniprot ID	Regulation
Abcb7	ATP-binding cassette sub-family B member 7, mitochondrial	ABCB7_RAT	FEMALE
Abcb10	ATP-binding cassette sub-family B member 10, mitochondrial	ABCBA_MOUSE	FEMALE
Adgra1	Adhesion G protein-coupled receptor A1	AGRA1_MOUSE	FEMALE
Anapc1	Anaphase-promoting complex subunit 1	APC1_MOUSE	MALE
Apex1	DNA-(apurinic or apyrimidinic site) lyase	APEX1_MOUSE	FEMALE
Asap3	Arf-GAP with SH3 domain, ANK repeat and PH domain-containing protein 3	ASAP3_MOUSE	MALE
Atp13a3	Probable cation-transporting ATPase 13A3	AT133_MOUSE	FEMALE
Atp2b1	Plasma membrane calcium-transporting ATPase 1	AT2B1_RAT	MALE
Atp2c1	Calcium-transporting ATPase type 2c member 1	AT2C1_RAT	MALE
Bcor	BCL-6 corepressor	BCOR_MOUSE	MALE
Bmpr1b	Bone morphogenetic protein receptor type-1B	BMR1B_MOUSE	MALE
Brd8	Bromodomain-containing protein 8	BRD8_MOUSE	MALE
Btf3l4	Transcription factor BTF3 homolog 4	BT3L4_MOUSE	FEMALE
C1ql3	Complement C1q-like protein 3	C1QL3_MOUSE	FEMALE
Ccdc186	Coiled-coil domain-containing protein 186	CC186_MOUSE	MALE
Ccm2	Cerebral cavernous malformations protein 2 homolog	CCM2_MOUSE	MALE
Ccnt1	Cyclin-T1	CCNT1_MOUSE	FEMALE
Ccs	Copper chaperone for superoxide dismutase	CCS_RAT	FEMALE
Cdr2l	Cerebellar degeneration-related protein 2-like	CDR2L_MOUSE	FEMALE
Cep68	Centrosomal protein of 68 kDa	CEP68_MOUSE	FEMALE
Cfh	Complement factor H	CFAH_MOUSE	MALE
Csgalnact1	Chondroitin sulfate N-acetylgalactosaminyltransferase 1	CGAT1_MOUSE	MALE
Chd1	Chromodomain-helicase-DNA-binding protein 1	CHD1_MOUSE	MALE
Chd5	Chromodomain-helicase-DNA-binding protein 5	CHD5_MOUSE	FEMALE MALE
Cherp	Calcium homeostasis endoplasmic reticulum protein	CHERP_MOUSE	MALE

Gene ID	Gene	Uniprot ID	Regulation
Cldnd1	Claudin domain-containing protein 1	CLDN1_MOUSE	FEMALE
Cluh	Clustered mitochondria protein homolog	CLU_MOUSE	MALE
Cnot3	CCR4-NOT transcription complex subunit 3	CNOT3_MOUSE	MALE
Col11a1	Collagen alpha-1(XI) chain	COBA1_RAT	FEMALE
Cog3	Conserved oligomeric Golgi complex subunit 3	COG3_MOUSE	FEMALE MALE
Col23a1	Collagen alpha-1(XXIII) chain	CONA1_RAT	MALE
Cpne2	Copine-2	CPNE2_MOUSE	FEMALE
Crym	Ketimine reductase mu-crystallin	CRYM_MOUSE	MALE
Ctnnal1	Alpha-catulin	CTNL1_MOUSE	FEMALE
Cit	Citron Rho-interacting kinase	CTRO_MOUSE	MALE
Ddx3y	ATP-dependent RNA helicase DDX3Y	DDX3Y_MOUSE	MALE
Dlk2	Protein delta homolog 2	DLK2_MOUSE	MALE
Dmxl2	DmX-like protein 2	DMXL2_MOUSE	FEMALE
Dync2h1	Cytoplasmic dynein 2 heavy chain 1	DYHC2_RAT	MALE
Edc4	Enhancer of mRNA-decapping protein 4	EDC4_MOUSE	MALE
Ahctf1	Protein ELYS	ELYS_MOUSE	FEMALE
Eno1	Alpha-enolase	ENOA_RAT	FEMALE
Eps15	Epidermal growth factor receptor substrate 15	EPS15_MOUSE	FEMALE
Erap1	Endoplasmic reticulum aminopeptidase 1	ERAP1_RAT	MALE
Etfdh	Electron transfer flavoprotein-ubiquinone oxidoreductase, mitochondrial	ETFD_MOUSE	FEMALE
Ezh1	Histone-lysine N-methyltransferase EZH1	EZH1_MOUSE	MALE
Fam126b	Protein FAM126B	F126B_MOUSE	MALE
Fam83h	Protein FAM83H	FA83H_MOUSE	MALE
Fastkd1	FAST kinase domain-containing protein 1	FAKD1_MOUSE	FEMALE
Fhl1	Four and a half LIM domains protein 1	FHL1_RAT	FEMALE
Flii	Protein flightless-1 homolog	FLII_MOUSE	FEMALE
Fuz	Protein fuzzy homology	FUZZY_MOUSE	FEMALE

Gene ID	Gene	Uniprot ID	Regulation
Fzr1	Fizzy-related protein homolog	FZR_MOUSE	MALE
Gata2	Endothelial transcription factor GATA-2	GATA2_RAT	MALE
Slc25a22	Mitochondrial glutamate carrier 1	GHC1_MOUSE	MALE
Gria3	Glutamate receptor 3	GRIA3_MOUSE	MALE
Slc2a8	Solute carrier family 2, facilitated glucose transporter member 8	GTR8_RAT	FEMALE
Hcfc2	Host cell factor 2	HCFC2_RAT	FEMALE
Hdac5	Histone deacetylase 5	HDAC5_CRIGR	MALE
Hepacam	Hepatocyte cell adhesion molecule	HECAM_MOUSE	MALE
Hes5	Transcription factor HES-5	HES5_RAT	MALE
Hipk2	Homeodomain-interacting protein kinase 2	HIPK2_MESAU	FEMALE
Hsp90ab1	Heat shock protein HSP 90-beta	HS90B_RAT	FEMALE
Ift172	Intraflagellar transport protein 172 homolog	IF172_MOUSE	MALE
Eif5	Eukaryotic translation initiation factor 5	IF5_MOUSE	FEMALE
Ppa2	Inorganic pyrophosphatase 2, mitochondrial	IPYR2_MOUSE	MALE
Kiaa0556	Uncharacterized protein KIAA0556	K0556_MOUSE	FEMALE
Kansl1l	KAT8 regulatory NSL complex subunit 1-like protein	KAL1L_MOUSE	MALE
Kctd15	BTB/POZ domain-containing protein KCTD15	KCD15_MOUSE	MALE
Kcng4	Potassium voltage-gated channel subfamily G member 4	KCNG4_MOUSE	MALE
Kdm1b	Lysine-specific histone demethylase 1B	KDM1B_MOUSE	FEMALE
Kdm5c	Lysine-specific demethylase 5C	KDM5C_MOUSE	MALE
Kdm5d	Lysine-specific demethylase 5D	KDM5D_MOUSE	MALE
Kdm6a	Lysine-specific demethylase 6A	KDM6A_MOUSE	FEMALE MALE
Kif9	Kinesin-like protein KIF9	KIF9_MOUSE	MALE
Krcc1	Lysine-rich coiled-coil protein 1	KRCC1_MOUSE	FEMALE
Rps6ka2	Ribosomal protein S6 kinase alpha-2	KS6A2_MOUSE	MALE
Faim2	Protein lifeguard 2	LFG2_RAT	FEMALE
Lin7b	Protein lin-7 homolog B	LIN7B_RAT	FEMALE

Gene ID	Gene	Uniprot ID	Regulation
L3mbtl3	Lethal(3)malignant brain tumor-like protein 3	LMBL3_MOUSE	MALE
Aatk	Serine/threonine-protein kinase LMTK1	LMTK1_MOUSE	MALE
Lrig2	Leucine-rich repeats and immunoglobulin-like domains protein 2	LRIG2_MOUSE	MALE
Lrp3	Low-density lipoprotein receptor-related protein 3	LRP3_RAT	MALE
Tmem57	Macoilin	MACOI_MOUSE	MALE
Mamld1	Mastermind-like domain-containing protein 1	MAMD1_MOUSE	MALE
Map6	Microtubule-associated protein 6	MAP6_MOUSE	FEMALE
Matk	Megakaryocyte-associated tyrosine-protein kinase	MATK_MOUSE	FEMALE
Mga	MAX gene-associated protein	MGAP_MOUSE	MALE
Mgat5	Alpha-1,6-mannosylglycoprotein 6-beta-N-acetylglucosaminyltransferase A	MGT5A_CRIGR	FEMALE
Mink1	Misshapen-like kinase 1	MINK1_MOUSE	FEMALE
Mapk13	Mitogen-activated protein kinase 13	MK13_MOUSE	MALE
Mobp	Myelin-associated oligodendrocyte basic protein	MOBP_MOUSE	MALE
Mpeg1	Macrophage-expressed gene 1 protein	MPEG1_MOUSE	FEMALE
Cdc42bpb	Serine/threonine-protein kinase MRCK beta	MRCKB_MOUSE	MALE
Mreg	Melanoregulin	MREG_MOUSE	FEMALE
Msl3	Male-specific lethal 3 homolog	MS3L1_MOUSE	MALE
N4bp2l1	NEDD4-binding protein 2-like 1	N42L1_MOUSE	MALE
Neurl4	Neuralized-like protein 4	NEUL4_MOUSE	FEMALE
Nfyc	Nuclear transcription factor Y subunit gamma	NFYC_RAT	FEMALE
Olfm2	Noelin-2	NOE2_RAT	FEMALE
Nrdc	Nardilysin	NRDC_MOUSE	MALE
Nsun5	Probable 28S rRNA (cytosine-C(5))-methyltransferase	NSUN5_MOUSE	MALE
Nudcd3	NudC domain-containing protein 3	NUDC3_MOUSE	MALE
Oma1	Metalloendopeptidase OMA1, mitochondrial	OMA1_MOUSE	FEMALE
Otof	Otoferlin	OTOF_RAT	MALE
Pawr	PRKC apoptosis WT1 regulator protein	PAWR_MOUSE	FEMALE

Gene ID	Gene	Uniprot ID	Regulation
Pcdhb14	Protocadherin beta-14	PCDBE_MOUSE	FEMALE
Pcnx	Pecanex-like protein 1	PCX1_MOUSE	MALE
Per3	Period circadian protein homolog 3	PER3_RAT	FEMALE
Rabggta	Geranylgeranyl transferase type-2 subunit alpha	PGTA_RAT	MALE
Phyhip	Phytanoyl-CoA hydroxylase-interacting protein	PHYIP_RAT	FEMALE
Pitpna	Phosphatidylinositol transfer protein alpha isoform	PIPNA_MOUSE	FEMALE MALE
Plec	Plectin	PLEC_CRIGR	MALE
Plod3	Procollagen-lysine,2-oxoglutarate 5-dioxygenase 3	PLOD3_MOUSE	MALE
Plxnb2	Plexin-B2	PLXB2_MOUSE	MALE
Ppp1r3e	Protein phosphatase 1 regulatory subunit 3E	PPR3E_MOUSE	MALE
Prex2	Phosphatidylinositol 3,4,5-triphosphate-dependent Rac exchanger 2 protein	PREX2_MOUSE	MALE
Primpol	DNA-directed primase/polymerase protein	PRIPO_MOUSE	MALE
Prkra	Interferon-inducible double-stranded RNA-dependent protein kinase activator A	PRKRA_RAT	MALE
Ptprn	Receptor-type tyrosine-protein phosphatase-like N	PTPRN_RAT	MALE
Ptpro	Receptor-type tyrosine-protein phosphatase O	PTPRO_MOUSE	MALE
Pus7l	Pseudouridylate synthase 7 homolog-like protein	PUS7L_MOUSE	FEMALE
Rb1cc1	RB1-inducible coiled-coil protein 1	RBCC1_MOUSE	MALE
Rbm45	RNA-binding protein 45	RBM45_RAT	FEMALE
Rexo1	RNA exonuclease 1 homolog	REXO1_MOUSE	MALE
Rfx5	DNA-binding protein Rfx5	RFX5_MOUSE	FEMALE MALE
Rgs8	Regulator of G-protein signaling 8	RGS8_RAT	MALE
Riok1	Serine/threonine-protein kinase RIO1	RIOK1_MOUSE	MALE
Rnf212	Probable E3 SUMO-protein ligase RNF212	RN212_MOUSE	MALE
Rapgef2	Rap guanine nucleotide exchange factor 2	RPGF2_MOUSE	MALE
Rreb1	Ras-responsive element-binding protein 1	RREB1_MOUSE	MALE
Rtf1	RNA polymerase-associated protein RTF1 homolog	RTF1_MOUSE	FEMALE
Rubcn	Run domain Beclin-1-interacting and cysteine-rich domain containing protein	RUBIC_MOUSE	FEMALE

Gene ID	Gene	Uniprot ID	Regulation
Slc12a6	Solute carrier family 12 member 6	S12A6_MOUSE	FEMALE
Sec61a1	Protein transport protein Sec61 subunit alpha isoform 1	S61A1_RAT	MALE
Sec22c	Vesicle-trafficking protein SEC22c	SC22C_MOUSE	FEMALE
Sdccag3	Serologically defined colon cancer antigen 3 homolog	SDCG3_MOUSE	MALE
Setd5	SET domain-containing protein 5	SETD5_MOUSE	MALE
St6galnac4	Alpha-N-acetyl-neuraminyl-2,3-beta-galactosyl-1,3-N-acetyl-galactosaminide alpha-2,6-sialyltransferase	SIA7D_MOUSE	MALE
Snx24	Sorting nexin-24	SNX24_RAT	FEMALE
Spata7	Spermatogenesis-associated protein 7 homolog	SPAT7_MOUSE	MALE
Stra6	Stimulated by retinoic acid gene 6 protein homolog	STRA6_RAT	FEMALE
Suco	SUN domain-containing ossification factor	SUCO_MOUSE	MALE
Sympk	Symplekin	SYMPK_MOUSE	MALE
Rars	Arginine--tRNA ligase, cytoplasmic	SYRC_CRIGR	FEMALE
Tll1	Tolloid-like protein 1	TLL1_MOUSE	FEMALE MALE
Tmem18	Transmembrane protein 18	TMM18_RAT	FEMALE
Txnrd3	Thioredoxin reductase 3	TRXR3_MOUSE	FEMALE
Txndc11	Thioredoxin domain-containing protein 11	TXD11_MOUSE	FEMALE
Tyk2	Non-receptor tyrosine-protein kinase TYK2	TYK2_MOUSE	FEMALE
Usp14	Ubiquitin carboxyl-terminal hydrolase 14	UBP14_MOUSE	MALE
Usp16	Ubiquitin carboxyl-terminal hydrolase 16	UBP16_RAT	MALE
Unc13a	Protein unc-13 homolog A	UN13A_MOUSE	MALE
Usp9x	Probable ubiquitin carboxyl-terminal hydrolase FAF-X	USP9X_MOUSE	MALE
Uty	Histone demethylase UTY	UTY_MOUSE	MALE
Vmn2r116	Vomeronasal type-2 receptor 116	V2116_MOUSE	FEMALE
Vasp	Vasodilator-stimulated phosphoprotein	VASP_MOUSE	FEMALE
Hdlbp	Vigilin	VIGLN_MOUSE	MALE
Vps13c	Vacuolar protein sorting-associated protein	VP13C_MOUSE	MALE
Wdfy3	WD repeat and FYVE domain-containing protein 3	WDFY3_MOUSE	MALE

Gene ID	Gene	Uniprot ID	Regulation
Wiz	Protein Wiz	WIZ_MOUSE	FEMALE
Wnk2	Serine/threonine-protein kinase WNK2	WNK2_MOUSE	MALE
Xpo4	Exportin-4	XPO4_MOUSE	FEMALE
Yme1l1	ATP-dependent zinc metalloprotease YME1L1	YMEL1_MOUSE	MALE
Zbtb46	Zinc finger and BTB domain-containing protein 46	ZBT46_MOUSE	MALE
Zfyve16	Zinc finger FYVE domain-containing protein 16	ZFY16_MOUSE	FEMALE
Znf569	Zinc finger protein 569	ZN569_MOUSE	FEMALE
Znf18	Zinc finger protein 18	ZNF18_RAT	FEMALE MALE
Zswim6	Zinc finger SWIM domain-containing protein 6	ZSWM6_MOUSE	MALE

Appendix B.2 Tables for amygdala transcriptome

Supplemental Table 3 Most highly expressed genes in amygdala of male and female hamsters
The top 20 genes that are most highly expressed in the amygdala of home cage controls.
* Indicates gene is also among the top 20 genes expressed in the whole brain

Gene ID	Gene	Uniprot ID
MT-CO2	Cytochrome c oxidase subunit 2	COX2_MICNA
Mtnd2	NADH-ubiquinone oxidoreductase chain 2	NU2M_MOUSE
Eef1a1*	Elongation factor 1-alpha 1	EF1A1_RAT
Scd2*	Acyl-CoA desaturase 2	ACOD2_MOUSE
Cpe	Carboxypeptidase E	CBPE_MOUSE
Map1a*	Microtubule-associated protein 1A	MAP1A_MOUSE
GNAS	Guanine nucleotide-binding protein G(s) subunit alpha	GNAS_MESAU
Calm1	Calmodulin	CALM_RAT
Atp1b1	Sodium/potassium-transporting ATPase subunit beta-1	AT1B1_RAT
Hsp90aa1*	Heat shock protein HSP 90-alpha	HS90A_MOUSE
NSF	Vesicle-fusing ATPase	NSF_CRIGR
Gapdh*	Glyceraldehyde-3-phosphate dehydrogenase	G3P_CRIGR
Actg1	Actin, cytoplasmic 2	ACTG_RAT
Camk2a	Calcium/calmodulin-dependent protein kinase type II subunit alpha	KCC2A_RAT
Sparcl1	SPARC-like protein 1	SPRL1_RAT
Slc1a3	Excitatory amino acid transporter 1	EAA1_RAT
Ywhaz	14-3-3 protein zeta/delta	1433Z_RAT
Prickle3	Prickle-like protein 3	PRIC3_MOUSE
Gpm6b	Neuronal membrane glycoprotein M6-b	GPM6B_RAT
Tspan7	Tetraspanin-7	TSN7_MOUSE

Supplemental Table 4 Differentially expressed genes in males of different social status
A comprehensive list of the genes that were differentially regulated in dominant and subordinate males compared with home-cage controls.

Gene ID	Gene	Uniprot ID	Regulation
Eif4ebp2	Eukaryotic translation initiation factor 4E-binding protein 2	4EBP2_MOUSE	↓ Dominant
Abcd3	ATP-binding cassette sub-family D member 3	ABCD3_MOUSE	↑ Subordinate
Acsm5	Acyl-coenzyme A synthetase ACSM5, mitochondrial	ACSM5_MOUSE	↑ Dominant
Acyp2	Acylphosphatase-2	ACYP2_MOUSE	↑ Dominant ↑ Subordinate
Adcy3	Adenylate cyclase type 3	ADCY3_RAT	↓ Dominant
Akap5	A-kinase anchor protein 5	AKAP5_MOUSE	↓ Subordinate
Aldh1a1	Retinal dehydrogenase 1	AL1A1_MESAU	↓ Dominant
Ankrd6	Ankyrin repeat domain-containing protein 6	ANKR6_MOUSE	↓ Dominant
Api5	Apoptosis inhibitor 5	API5_MOUSE	↓ Dominant
Arhgef4	Rho guanine nucleotide exchange factor 4	ARHG4_MOUSE	↑ Subordinate
Arhgef11	Rho guanine nucleotide exchange factor 11	ARHGB_RAT	↑ Dominant
Aga	N(4)-(Beta-N-acetylglucosaminyl)-L-asparaginase	ASPG_RAT	↓ Dominant ↓ Subordinate
Asxl3	Putative Polycomb group protein ASXL3	ASXL3_MOUSE	↑ Subordinate
Atp8a2	Phospholipid-transporting ATPase IB	AT8A2_MOUSE	↑ Dominant
Atl1	Atlastin-1	ATLA1_RAT	↑ Dominant ↑ Subordinate
Atr	Serine/threonine-protein kinase ATR	ATR_MOUSE	↑ Dominant
Bmpr1b	Bone morphogenetic protein receptor type-1B	BMR1B_MOUSE	↑ Dominant
Cacna1e	Voltage-dependent R-type calcium channel subunit alpha-1E	CAC1E_RAT	↓ Dominant ↓ Subordinate
Cacna1h	Voltage-dependent T-type calcium channel subunit alpha-1H	CAC1H_RAT	↑ Subordinate
Cacnb4	Voltage-dependent L-type calcium channel subunit beta-4	CACB4_MOUSE	↓ Subordinate
Casc4	Protein CASC4	CASC4_MOUSE	↓ Dominant
Cblb	E3 ubiquitin-protein ligase CBL-B	CBLB_RAT	↑ Dominant
Ccser2	Serine-rich coiled-coil domain-containing protein 2	CCSE2_MOUSE	↑ Dominant
N/a	Bombesin receptor-activated protein C6orf89 homolog	CF089_RAT	↓ Dominant
Cntn1	Contactin-1	CNTN1_MOUSE	↓ Subordinate
Col16a1	Collagen alpha-1(XVI) chain	COGA1_MOUSE	↓ Dominant

Gene ID	Gene	Uniprot ID	Regulation
Cul3	Cullin-3	CUL3_RAT	↓ Dominant
N/a	UPF0428 protein CXorf56 homolog	CX056_MOUSE	↑ Dominant
Cyyr1	Cysteine and tyrosine-rich protein 1	CYYR1_MOUSE	↓ Dominant
Dcc	Netrin receptor DCC	DCC_RAT	↑ Dominant
Gad2	Glutamate decarboxylase 2	DCE2_RAT	↑ Dominant
Dgkb	Diacylglycerol kinase beta	DGKB_RAT	↓ Dominant
Dhdds	Dehydrodolichyl diphosphate synthase complex subunit Dhdds	DHDDS_MOUSE	↑ Dominant
Dicer1	Endoribonuclease Dicer	DICER_CRIGR	↑ Dominant
Dnai1	Dynein intermediate chain 1, axonemal	DNAI1_MOUSE	↑ Subordinate
Dnajc5	DnaJ homolog subfamily C member 5	DNJC5_RAT	↑ Dominant
Epb41l4b	Band 4.1-like protein 4B	E41LB_RAT	↑ Dominant
Efcab14	EF-hand calcium-binding domain-containing protein 14	EFC14_MOUSE	↑ Dominant
Eme2	Probable crossover junction endonuclease EME2	EME2_MOUSE	↑ Subordinate
Epha10	Ephrin type-A receptor 10	EPHAA_MOUSE	↑ Dominant
Ept	Ethanolaminephosphotransferase 1	EPT1_MOUSE	↓ Subordinate
Fam102a	Protein FAM102A	F102A_MOUSE	↓ Dominant
Fam179b	Protein FAM179B	F179B_MOUSE	↓ Dominant
Fam169b	Protein FAM169B	F196B_MOUSE	↑ Dominant
Fam57a	Protein FAM57A	FA57A_MOUSE	↑ Dominant
Fasn	Fatty acid synthase	FAS_RAT	↓ Dominant
Fbxw11	F-box/WD repeat-containing protein 11	FBW1B_MOUSE	↑ Dominant ↑ Subordinate
Fbxl2	F-box/LRR-repeat protein 2	FBXL2_MOUSE	↑ Dominant
Fbxl5	F-box/LRR-repeat protein 5	FBXL5_MOUSE	↓ Subordinate
Fchsd2	F-BAR and double SH3 domains protein 2	FCSD2_MOUSE	↑ Dominant
G6pd	Glucose-6-phosphate 1-deydrogenase	G6PD_CRIGR	↑ Dominant ↑ Subordinate
Gpcpd1	Glycerophosphocholine phosphodiesterase	GPCP1_MOUSE	↓ Dominant
Gpr45	Probable G-protein coupled receptor 45	GPR45_MOUSE	↑ Dominant

Gene ID	Gene	Uniprot ID	Regulation
Gpsm1	G-protein-signaling modulator 1	GPSM1_RAT	↓ Dominant
Ccdc88a	Girdin	GRDN_MOUSE	↑ Subordinate
Gria2	Glutamate receptor 2	GRIA2_MOUSE	↑ Dominant ↑ Subordinate
Gtf2ird1	General transcription factor II-I repeat domain-containing protein 1	GT2D1_MOUSE	↑ Subordinate
Gtf2ird2	General transcription factor II-I repeat domain-containing protein 2	GT2D2_MOUSE	↑ Dominant
Hecw1	E3 ubiquitin-protein ligase HECW1	HECW1_MOUSE	↑ Dominant
Hmmr	Hyaluronan-mediated motility receptor	HMMR_RAT	↑ Dominant
Heatr5a	HEAT repeat-containing protein 5A	HTR5A_MOUSE	↑ Dominant
Igsf11	Immunoglobin superfamily member 11	IGS11_MOUSE	↓ Dominant
Ikzf4	Zinc finger protein Eos	IKZF4_MOUSE	↑ Subordinate
Ipo9	Importin-9	IPO9_MOUSE	↑ Subordinate
Itm2c	Integral membrane protein 2c	ITM2C_RAT	↑ Dominant ↑ Subordinate
Kiaa2022	Protein KIAA2022	K2022_MOUSE	↑ Subordinate
Kbtbd4	Kelch repeat and BTB domain-containing protein 4	KBTB4_MOUSE	↓ Dominant
Kcnh3	Potassium voltage-gated channel subfamily H member 3	KCNH3_RAT	↓ Subordinate
Kctd7	BTB/POZ domain-containing protein KCTD7	KCTD7_MOUSE	↑ Dominant ↑ Subordinate
Kdm6b	Lysine-specific demethylase 6B	KDM6B_MOUSE	↑ Subordinate
Pkm	Pyruvate kinase PKM	KPYM_RAT	↑ Dominant
Krcc1	Lysine-rich coiled-coil protein 1	KRCC1_MOUSE	↑ Subordinate
Lama1	Laminin subunit alpha-1	LAMA1_MOUSE	↑ Subordinate
Ldlr	Low-density lipoprotein receptor	LDLR_CRIGR	↓ Dominant
Lpl	Lipoprotein lipase	LIPL_RAT	↑ Subordinate
Plppr4	Phospholipid phosphatase-related protein type 4	LPPR4_MOUSE	↓ Dominant
Lrch1	Leucine-rich repeat and calponin homology domain-containing protein 1	LRCH1_MOUSE	↑ Subordinate
Lsm8	U6 snRNA-associated Sm-like protein LSm8	LSM8_MOUSE	↓ Dominant
Map3k6	Mitogen-activated protein kinase kinase kinase 6	M3K6_MOUSE	↑ Dominant
Map1s	Microtubule-associated protein 1S	MAP1S_MOUSE	↓ Subordinate

Gene ID	Gene	Uniprot ID	Regulation
Map6	Microtubule-associated protein 6	MAP6_MOUSE	↑ Subordinate
Mbnl2	Muscleblind-like protein 2	MBNL2_RAT	↓ Dominant
Mdga2	MAM domain-containing glycosylphosphatidylinositol anchor protein 2	MDGA2_RAT	↓ Subordinate
Mep1a	Meprin A subunit alpha	MEP1A_RAT	↑ Subordinate
Mfhas1	Malignant fibrous histiocytoma-amplified sequence 1 homolog	MFHA1_MOUSE	↑ Subordinate
Mios	WD repeat-containing protein mio	MIO_MOUSE	↑ Subordinate
Mkl1	MKL/myocardin-like protein 1	MKL1_MOUSE	↑ Dominant
N4bp2l1	NEDD4-binding protein 2-like 1	N42L1_MOUSE	↑ Dominant
Neurl4	Neuralized-like protein 4	NEUL4_MOUSE	↑ Dominant
Neu1	Sialidase-1	NEUR1_MOUSE	↓ Dominant
Nmt2	Glycylpeptide N-tetradecanoyltransferase 2	NMT2_MOUSE	↓ Subordinate
Nos3	Nitric oxide synthase, endothelial	NOS3_MOUSE	↑ Dominant
Smpd2	Sphingomyelin phosphodiesterase 2	NSMA_RAT	↑ Subordinate
Nup50	Nuclear pore complex protein Nup50	NUP50_RAT	↓ Subordinate
Ogfod2	2-oxoglutarate and iron-dependent oxygenase domain-containing protein 2	OGFD2_MOUSE	↑ Dominant
Dchs1	Protocadherin-16	PCD16_MOUSE	↑ Dominant
Pcnxl3	Pecanex-like protein 3	PCX3_MOUSE	↑ Dominant
Pfkm	ATP-dependent 6-phosphofructokinase, muscle type	PFKAM_MOUSE	↑ Subordinate
Phf2	Lysine-specific demethylase PHF2	PHF2_MOUSE	↑ Dominant
Plec	Plectin	PLEC_CRIGR	↑ Dominant ↑ Subordinate
Pnpla8	Calcium-independent phospholipase A2-gamma	PLPL8_MOUSE	↑ Subordinate
Ppp3ca	Serine/threonine-protein phosphatase 2B catalytic subunit alpha isoform	PP2BA_RAT	↑ Dominant
Ppme1	Protein phosphatase methylesterase 1	PPME1_RAT	↑ Dominant
Prpf40a	Pre-mRNA-processing factor 40 homolog A	PR40A_MOUSE	↑ Dominant
Prpf4b	Serine/threonine-protein kinase PRP4 homolog	PRP4B_RAT	↓ Dominant
Ptchd2	Patched domain-containing protein 2	PTHD2_MOUSE	↑ Subordinate
Ctps1	CTP synthase 1	PYRG1_MOUSE	↓ Dominant ↓ □□□□□ □□□□□□

Gene ID	Gene	Uniprot ID	Regulation
R3hdm2	R3H domain-containing protein 2	R3HD2_MOUSE	↓ Dominant ↓ Subordinate
Rad51d	DNA repair protein RAD51 homolog 4	RA51D_MOUSE	↑ Dominant
Rab43	Ras-related protein Rab-43	RAB43_MOUSE	↑ Dominant
Rap1a	Ras-related protein Rap-1A	RAP1A_RAT	↑ Subordinate
Rabgap1	Rab GTPase-activating protein 1	RBGP1_MOUSE	↑ Dominant
Rere	Arginine-glutamic acid dipeptide repeats protein	RERE_RAT	↑ Dominant ↑ Subordinate
Rab11fip3	Rab11 family-interacting protein 3	RFIP3_MOUSE	↑ Subordinate
Rpl3	60S ribosomal protein L3	RL3_MOUSE	↑ Dominant
Rnf121	RING finger protein 121	RN121_MOUSE	↑ Subordinate
Rps6kl1	Ribosomal protein S6 kinase-like 1	RPKL1_MOUSE	↓ Dominant ↓ Subordinate
Rubcn	Run domain Beclin-1-interacting and cysteine-rich domain-containing protein	RUBIC_MOUSE	↑ Dominant ↑ Subordinate
Slc15a2	Solute carrier family 15 member 2	S15A2_MOUSE	↑ Subordinate
Sdccag3	Serologically defined colon cancer antigen 3 homolog	SDCG3_MOUSE	↑ Subordinate
Senp6	Sentrin-specific protease 6	SENP6_MOUSE	↑ Subordinate
Sgip1	SH3-containing GRB2-like protein 3-interacting protein 1	SGIP1_MOUSE	↓ Dominant
Sipa1l2	Signal-induced proliferation-associated 1-like protein 2	SI1L2_MOUSE	↑ Subordinate
Slco3a1	Solute carrier organic anion transporter family member 3A1	SO3A1_MOUSE	↑ Dominant ↑ Subordinate
Supt16h	FACT complex subunit SPT16	SP16H_MOUSE	↑ Subordinate
Sspn	SCO-spondin	SSPO_RAT	↑ Dominant
St5	Suppression of tumorigenicity 5 protein	ST5_MOUSE	↑ Subordinate
Strn3	Striatin-3	STRN3_MOUSE	↓ Subordinate
Stxbp4	Syntaxin-binding protein 4	STXB4_MOUSE	↑ Subordinate
Stxbp6	Syntaxin-binding protein 6	STXB6_MOUSE	↑ Dominant
Tuba1b	Tubulin alpha-1B chain	TBA1B_RAT	↑ Dominant
Tbc1d24	TBC1 domain family member 24	TBC24_MOUSE	↑ Dominant
Tjap1	Tight junction-associated protein 1	TJAP1_MOUSE	↑ Dominant
Tm2d1	TM2 domain-containing protein 1	TM2D1_MOUSE	↓ Dominant

Gene ID	Gene	Uniprot ID	Regulation
Trim33	E3 ubiquitin-protein ligase TRIM33	TRI33_MOUSE	↓ Dominant
Trim9	E3 ubiquitin-protein ligase TRIM9	TRIM9_MOUSE	↑ Dominant
Tspan9	Tetraspanin-9	TSN9_MOUSE	↑ Dominant ↑ Subordinate
Ttc33	Tetratricopeptide repeat protein 33	TTC33_MOUSE	↓ Dominant
Ttr	Transthyretin	TTHY_MOUSE	↓ Dominant
Tulp4	Tubby-related protein 4	TULP4_MOUSE	↓ Subordinate
N/a	Putative UPF0730 protein encoded by LINC00643 homolog	U730_MOUSE	↑ Subordinate ↓ Subordinate
Uap1	UDP-N-acteylhexosamine pyrophosphorylase	UAP1_MOUSE	↑ Dominant
Uba6	Ubiquitin-like modifier-activating enzyme 6	UBA6_MOUSE	↓ Subordinate
Usp53	Inactive ubiquitin carboxyl-terminal hydrolase 53	UBP53_MOUSE	↑ Subordinate
Vps13c	Vacuolar protein sorting associated protein 13C	VP13C_MOUSE	↑ Dominant ↑ Subordinate
Atp6v0a2	V-type proton ATPase 116 kDa subunit a isoform 2	VPP2_MOUSE	↑ Dominant ↑ Subordinate
Wdr35	WD repeat-containing protein 35	WDR35_MOUSE	↑ Subordinate
Wnk4	Serine/threonine-protein kinase WNK4	WNK4_RAT	↑ Dominant
Slc7a11	Cystine/glutamate transporter	XCT_MOUSE	↑ Dominant
Cse1l	Exportin-2	XPO2_MOUSE	↑ Dominant
Xpo4	Exportin-4	XPO4_MOUSE	↑ Dominant
Zdhhc17	Palmitoyltransferase ZDHHC17	ZDH17_RAT	↑ Subordinate
Hivep2	Human immunodeficiency virus type I enhancer-binding protein 2 homolog	ZEP2_RAT	↑ Dominant ↑ Subordinate
Hivep3	Transcription factor HIVEP3	ZEP3_MOUSE	↑ Dominant
Znf106	Zinc finger protein 106	ZN106_MOUSE	↓ Dominant
Znf532	Zinc finger protein 532	ZN532_MOUSE	↑ Dominant ↑ Subordinate

Supplemental Table 5 Differentially expressed genes in females of different social status
A comprehensive list of the genes that were differentially regulated in dominant and subordinate females compared with home cage controls.

Gene ID	Gene	Uniprot ID	Regulation
Ppp2r5c	Serine/threonine-protein phosphatase 2A 56 kDa regulatory subunit gamma isoform	2A5G_MOUSE	↓ Subordinate
App	Amyloid beta A4 protein	A4_RAT	↑ Dominant
Abhd6	Monoacylglycerol lipase ABHD6	ABHD6_RAT	↑ Dominant
Chrm2	Muscarinic acetylcholine receptor M2	ACM2_RAT	↓ Subordinate
Adam12	Disintegrin and metalloproteinase domain-containing protein 12	ADA12_MOUSE	↑ Dominant
Ank3	Ankyrin-3	ANK3_RAT	↓ Subordinate
Prmt7	Protein arginine N-methyltransferase 7	ANM7_CRILO	↑ Dominant
Ap1b1	AP-1 complex subunit beta-1	AP1B1_MOUSE	↓ Subordinate
Ap1s2	AP-1 complex subunit sigma-2	AP1S2_MOUSE	↑ Subordinate
Apbb1	Amyloid beta A4 precursor protein-binding family B member 1	APBB1_MOUSE	↓ Subordinate
Apc2	Adenomatous polyposis coli protein 2	APC2_MOUSE	↑ Dominant ↑ Subordinate
Arid5b	AT-rich interactive domain-containing protein 5B	ARI5B_MOUSE	↑ Dominant
Adamtsl1	ADAMTS-like protein 1	ATL1_MOUSE	↓ Subordinate
Bard1	BRCA1-associated RING domain protein 1	BARD1_MOUSE	↑ Subordinate
Bard1	BRCA1-associated RING domain protein 1	BARD1_RAT	↓ Subordinate
Bcorl1	BCL-6 corepressor-like protein 1	BCORL_MOUSE	↓ Subordinate ↑ Subordinate
Bmpr1a	Bone morphogenetic protein receptor type-1A	BMR1A_MOUSE	↓ Subordinate
Cacna2d2	Voltage-dependent calcium channel subunit alpha-2/delta-2	CA2D2_MOUSE	↑ Dominant ↑ Subordinate
Sdf4	45 kDa calcium-binding protein	CAB45_MOUSE	↓ Dominant
Cacna1e	Voltage-dependent R-type calcium channel subunit alpha-1E	CAC1E_RAT	↓ Dominant
Capn15	Calpain-15	CAN15_MOUSE	↓ Subordinate
Ccdc92	Coiled-coil domain-containing protein 92	CCD92_MOUSE	↓ Subordinate
Ccm2	Cerebral cavernous malformations protein 2 homolog	CCM2_MOUSE	↑ Dominant
Ccnl1	Cyclin-L1	CCNL1_MOUSE	↑ Dominant ↑ Subordinate
Cdk5	Cyclin-dependent-like kinase 5	CDK5_MOUSE	↑ Dominant ↑ Subordinate
Cenpc	Centromere protein C	CENPC_MOUSE	↑ Subordinate

Gene ID	Gene	Uniprot ID	Regulation
D17wsu92e	Uncharacterized protein C6orf106 homolog	CF106_MOUSE	↑ Subordinate
Csgalnact1	Chondroitin sulfate N-acetylgalactosaminyltransferase 1	CGAT1_MOUSE	↑ Subordinate
N/a	UPF0488 protein C8orf33 homolog	CH033_MOUSE	↑ Dominant
Chsy3	Chondroitin sulfate synthase 3	CHSS3_MOUSE	↓ Dominant
Kiaa1524	Protein CIP2A	CIP2A_MOUSE	↑ Dominant
Cep250	Centrosome-associated protein CEP250	CP250_MOUSE	↓ Dominant ↓ Subordinate
N/a	Uncharacterized protein C20orf194 homolog	CT194_MOUSE	↓ Subordinate
Cul3	Cullin-3	CUL3_RAT	↓ Dominant
Cul9	Cullin-9	CUL9_MOUSE	↓ Subordinate
Cxadr	Coxsackievirus and adenovirus receptor homolog	CXAR_MOUSE	↓ Dominant
Dapk3	Death-associated protein kinase 3	DAPK3_MOUSE	↓ Subordinate
Dcc	Netrin receptor DCC	DCC_RAT	↑ Dominant ↑ Subordinate
Ddx58	Probable ATP-dependent RNA helicase DDX58	DDX58_MOUSE	↑ Subordinate
Dhx9	ATP-dependent RNA helicase A	DHX9_MOUSE	↓ Dominant
Dnah17	Dynein heavy chain 17, axonemal	DYH17_MOUSE	↑ Dominant
Dzip3	E3 ubiquitin-protein ligase DZIP3	DZIP3_MOUSE	↓ Dominant
Epb41l1	Band 4.1-like protein 1	E41L1_RAT	↑ Subordinate
Epb41l1	Band 4.1-like protein 1	E41L2_MOUSE	↑ Subordinate
Ehd4	EH domain-containing protein 4	EHD4_MOUSE	↑ Dominant
Eps8	Epidermal growth factor receptor kinase substrate 8	EPS8_MOUSE	↑ Dominant
Evi5	Ecotropic viral integration site 5 protein	EVI5_MOUSE	↑ Dominant ↑ Subordinate
Fam117b	Protein FAM117B	F117B_MOUSE	↑ Subordinate
Fam76b	Protein FAM76B	FA76B_MOUSE	↑ Subordinate
Fbxo41	F-box only protein 41	FBX41_MOUSE	↓ Subordinate
Fgd1	FYVE, RhoGEF and PH domain-containing protein 1	FGD1_MOUSE	↓ Dominant ↑ Dominant
Flnb	Filamin-B	FLNB_MOUSE	↑ Dominant ↑ Subordinate
Fndc3a	Fibronectin type-III domain-containing protein 3A	FND3A_MOUSE	↑ Subordinate

Gene ID	Gene	Uniprot ID	Regulation
Frs2	Fibroblast growth factor receptor substrate 2	FRS2_MOUSE	↑ Dominant
Fbxl17	F-box/LRR-repeat protein 17	FXL17_MOUSE	↑ Dominant ↑ Subordinate
Ggact	Gamma-glutamylaminecyclotransferase	GGACT_RAT	↓ Subordinate ↑ Subordinate
Ghr	Growth hormone receptor	GHR_RAT	↓ Subordinate
Gpbp1l1	Vasculin-like protein 1	GPBL1_RAT	↑ Subordinate
H2-l	H-2 class I histocompatibility antigen, L-D alpha chain	HA1L_MOUSE	↑ Dominant
Hebp1	Heme-binding protein 1	HEBP1_MOUSE	↓ Dominant ↓ Subordinate
Helz2	Helicase with zinc finger domain 2	HELZ2_MOUSE	↓ Subordinate
Hnrnpdl	Heterogeneous nuclear ribonucleoprotein D-like	HNRDL_MOUSE	↑ Dominant
Hpca	Neuron-specific calcium-binding protein hippocalcin	HPCA_RAT	↑ Subordinate
Heatr5b	HEAT repeat-containing protein 5B	HTR5B_MOUSE	↑ Subordinate
Tor1aip2	Torsin-1A-interacting protein 2, isoform IFRG15	IFG15_MOUSE	↑ Subordinate
Impdh2	Inosine-5'-monophosphate dehydrogenase 2	IMDH2_MOUSE	↓ Subordinate
Ip6k2	Inositol hexakisphosphate kinase 2	IP6K2_MOUSE	↓ Subordinate
Itm2c	Integral membrane protein 2C	ITM2C_RAT	↑ Dominant ↓ Subordinate
Itsn2	Intersectin-2	ITSN2_MOUSE	↓ Dominant
Jph1	Junctophilin-1	JPH1_MOUSE	↓ Subordinate
Kiaa2022	Protein KIAA2022	K2022_MOUSE	↑ Dominant
Ak4	Adenylate kinase 4, mitochondrial	KAD4_RAT	↓ Subordinate
Kbtbd4	Kelch repeat and BTB domain-containing protein 4	KBTB4_MOUSE	↑ Dominant ↑ Subordinate
Kdm3a	Lysine-specific demethylase 3A	KDM3A_MOUSE	↓ Dominant
Kdm6b	Lysine-specific demethylase 6B	KDM6B_MOUSE	↑ Subordinate
Kif13a	Kinesin-like protein KIF13A	KI13A_MOUSE	↓ Subordinate
Kifc3	Kinesin-like protein KIFC3	KIFC3_MOUSE	↑ Dominant
Pkm	Pyruvate kinase PKM	KPYM_RAT	↑ Dominant
Lama1	Laminin subunit alpha-1	LAMA1_MOUSE	↓ Subordinate
Lama2	Laminin subunit alpha-2	LAMA2_MOUSE	↓ Dominant

Gene ID	Gene	Uniprot ID	Regulation
Lonrf3	LON peptidase N-terminal domain and RING finger protein 3	LONF3_MOUSE	↓ Subordinate
Lrch4	Leucine-rich repeat and calponin homology domain-containing protein 4	LRCH4_MOUSE	↑ Dominant
Lrfn5	Leucine-rich repeat and fibronectin type-III domain-containing protein 5	LRFN5_MOUSE	↑ Dominant
Magi2	Membrane-associated guanylate kinase, WW and PDZ domain-containing protein 2	MAGI2_MOUSE	↑ Subordinate
Map4	Microtubule-associated protein 4	MAP4_MOUSE	↓ Subordinate
Mapre3	Microtubule-associated protein RP/EB family member 3	MARE3_RAT	↓ Subordinate
March1	E3 ubiquitin-protein ligase MARCH1	MARH1_MOUSE	↓ Subordinate
Mbd1	Methyl-CpG-binding domain protein 1	MBD1_MOUSE	↓ Dominant
Mdga2	MAM domain-containing glycosylphosphatidylinositol anchor protein 2	MDGA2_RAT	↑ Dominant
Med12	Mediator of RNA polymerase II transcription subunit 12	MED12_MOUSE	↑ Subordinate
Megf8	Multiple epidermal growth factor-like domains protein 8	MEGF8_MOUSE	↑ Subordinate
Mep1a	Meprin A subunit alpha	MEP1A_RAT	↓ Dominant
Mfsd6	Major facilitator superfamily domain-containing protein 6	MFSD6_MOUSE	↑ Dominant
Mgat5	Alpha-1,6-mannosylglycoprotein 6-beta-N-acetylglucosaminyltransferase A	MGT5A_CRIGR	↓ Subordinate
Mapk4	Mitogen-activated protein kinase 4	MK04_MOUSE	↑ Subordinate
Morf4l2	Mortality factor 4-like protein 2	MO4L2_RAT	↓ Subordinate
Mtmr12	Myotubularin-related protein 12	MTMRC_MOUSE	↓ Subordinate
Mxi1	Max-interacting protein 1	MXI1_RAT	↓ Subordinate
Nab1	NGFI-A-binding protein 1	NAB1_MESAU	↓ Subordinate
Nab2	NGFI-A-binding protein 2	NAB2_MOUSE	↑ Dominant
Nell2	Protein kinase C-binding protein NELL2	NELL2_RAT	↓ Dominant
Nfat5	Nuclear factor of activated T-cells 5	NFAT5_RAT	↑ Dominant
Nfyb	Nuclear transcription factor Y subunit beta	NFYB_RAT	↓ Subordinate
Nipa1	Magnesium transporter NIPA1	NIPA1_MOUSE	↓ Subordinate
Nktr	NK-tumor recognition protein	NKTR_MOUSE	↓ Subordinate
Olfm3	Noelin-3	NOE3_RAT	↑ Dominant ↑ Subordinate
Nop14	Nucleolar protein 14	NOP14_MOUSE	↑ Dominant

Gene ID	Gene	Uniprot ID	Regulation
Nphp1	Nephrocystin-1	NPHP1_MOUSE	↑ Subordinate
Nup214	Nuclear pore complex protein Nup214	NU214_MOUSE	↑ Subordinate
Nwd2	NACHT and WD repeat domain-containing protein 2	NWD2_MOUSE	↑ Dominant
Ogdh	2-oxoglutarate dehydrogenase, mitochondrial	ODO1_RAT	↓ Subordinate
Osbpl6	Oxysterol-binding protein-related protein 6	OSBL6_MOUSE	↑ Dominant
Pak2	Serine/threonine-protein kinase PAK 2	PAK2_RAT	↑ Subordinate ↓ Subordinate
Papolg	Poly(A) polymerase gamma	PAPOG_MOUSE	↓ Subordinate
Pcyt1b	Choline-phosphate cytidylyltransferase B	PCY1B_RAT	↑ Dominant
Pde1b	Calcium/calmodulin-dependent 3',5'-cyclic nucleotide phosphodiesterase 1B	PDE1B_RAT	↑ Subordinate
Phf21a	PHD finger protein 21A	PF21A_MOUSE	↓ Dominant
Pfkm	ATP-dependent 6-phosphofructokinase, muscle type	PFKAM_MOUSE	↓ Subordinate
Plaa	Phospholipase A-2-activating protein	PLAP_RAT	↑ Subordinate
Plcb1	1-phosphatidylinositol 4,5-bisphosphate phosphodiesterase beta-1	PLCB1_RAT	↓ Subordinate
Ppp3cb	Serine/threonine-protein phosphatase 2B catalytic subunit beta isoform	PP2BB_MOUSE	↑ Subordinate
Prpf6	Pre-mRNA-processing factor 6	PRP6_MOUSE	↑ Subordinate
Prpf8	Pre-mRNA-processing-splicing factor 8	PRP8_MOUSE	↑ Subordinate
Psma2	Proteasome subunit alpha type-2	PSA2_RAT	↑ Dominant
Ptbp2	Polypyrimidine tract-binding protein 2	PTBP2_RAT	↑ Dominant
Ptpn2	Tyrosine-protein phosphatase non-receptor type 2	PTN2_RAT	↑ Dominant
Ptpra	Receptor-type tyrosine-protein phosphatase alpha	PTPRA_RAT	↓ Subordinate
Ptprd	Receptor-type tyrosine-protein phosphatase delta	PTPRD_MOUSE	↑ Subordinate ↓ Dominant
Rbm12b1	RNA-binding protein 12B-A	R12BA_MOUSE	↑ Subordinate
Rad50	DNA repair protein RAD50	RAD50_RAT	↑ Dominant
Ran	GTP-binding nuclear protein Ran	RAN_RAT	↓ Dominant ↓ Subordinate
Rbm14	RNA-binding protein 14	RBM14_MOUSE	↑ Subordinate
Rfx4	Transcription factor RFX4	RFX4_MOUSE	↓ Subordinate
Rims1	Regulating synaptic membrane exocytosis protein 1	RIMS1_MOUSE	↑ Subordinate

Gene ID	Gene	Uniprot ID	Regulation
Rnf213	E3 ubiquitin-protein ligase RNF213	RN213_MOUSE	↓ Subordinate
Rogdi	Protein rogdi homolog	ROGDI_RAT	↓ Dominant
Rpn2	Dolichyl-diphosphooligosaccharide--protein glycosyltransferase subunit 2	RPN2_RAT	↓ Subordinate
Mrps15	28S ribosomal protein S15, mitochondrial	RT15_RAT	↑ Subordinate
Rufy1	RUN and FYVE domain-containing protein 1	RUFY1_MOUSE	↓ Subordinate
Slc4a10	Sodium-driven chloride bicarbonate exchanger	S4A10_MOUSE	↓ Dominant
Sardh	Sarcosine dehydrogenase, mitochondrial	SARDH_MOUSE	↓ Dominant
Sec24a	Protein transport protein Sec24A	SC24A_MOUSE	↓ Subordinate
Sema3c	Semaphorin-3c	SEM3C_MOUSE	↑ Subordinate
Sh3bp4	SH3 domain-binding protein 4	SH3B4_MOUSE	↓ Dominant
Slitrk2	SLIT and NTRK-like protein 2	SLIK2_MOUSE	↓ Dominant
Sgms1	Phosphatidylcholine:ceramide cholinephosphotransferase 1	SMS1_RAT	↑ Subordinate
Slco3a1	Solute carrier organic anion transporter family member 3A1	SO3A1_MOUSE	↑ Subordinate
Ftsj3	Pre-rRNA processing protein FTSJ3	SPB1_MOUSE	↑ Dominant ↑ Subordinate
Sult4a1	Sulfotransferase 4A1	ST4A1_RAT	↑ Subordinate
Stxbp4	Syntaxin-binding protein 4	STXB4_MOUSE	↓ Dominant ↑ Dominant
Sv2b	Synaptic vesicle glycoprotein 2B	SV2B_RAT	↑ Subordinate
Hars2	Probable histidine-tRNA ligase, mitochondrial	SYHM_MOUSE	↓ Subordinate
Szt2	Protein SZT2	SZT2_MOUSE	↑ Subordinate ↓ Dominant
Tsc22d4	TSC22 domain family protein 4	T22D4_MOUSE	↓ Subordinate
Gtf2e1	General transcription factor IIE subunit 1	T2EA_MOUSE	↓ Subordinate
Tenm1	Teneurin-1	TEN1_MOUSE	↑ Dominant
Tnr	Tenascin-R	TENR_MOUSE	↓ Subordinate
Tns3	Tensin-3	TENS3_MOUSE	↑ Dominant
Spock3	Testican-3	TICN3_MOUSE	↑ Subordinate
Tm2d1	TM2 domain-containing protein 1	TM2D1_MOUSE	↑ Subordinate
Ttc14	Tetraicopeptide repeat protein 14	TTC14_MOUSE	↓ Dominant

Gene ID	Gene	Uniprot ID	Regulation
Igsf9	Protein turtle homolog A	TUTLA_RAT	↓ Subordinate
Usp53	Inactive ubiquitin carboxyl-terminal hydrolase 53	UBP53_MOUSE	↓ Dominant
Use1	Vesicle transport protein USE1	USE1_MOUSE	↓ Subordinate
Wnk3	Serine/threonine-protein kinase WNK3	WNK3_MOUSE	↓ Dominant ↓ Subordinate
Wnt5a	Protein Wnt-5a	WNT5A_MOUSE	↑ Subordinate
Wscd1	WSC domain-containing protein 1	WSCD1_MOUSE	↓ Dominant ↓ Subordinate
Yeats2	YEATS domain-containing protein 2	YETS2_MOUSE	↓ Subordinate
Yif1b	Protein YIF1B	YIF1B_MOUSE	↑ Dominant
Ythdf3	YTH domain-containing family protein 3	YTHD3_MOUSE	↓ Subordinate
Hivep3	Transcription factor HIVEP3	ZEP3_MOUSE	↓ Subordinate
Zfp62	Zinc finger protein 62	ZFP62_MOUSE	↑ Dominant
Znf281	Zinc finger protein 281	ZN281_MOUSE	↑ Subordinate
Znf775	Zinc finger protein 775	ZN775_MOUSE	↑ Subordinate
Tjp1	Tight junction protein ZO-1	ZO1_MOUSE	↑ Dominant